Joana Batista Nunes Fernandes
B.Sc. in Biology

Liquid Effluent Bioremediation Resorting to Microalgae Cultivation

Dissertation for the obtention of the academic master's degree
in biotechnology for sustainability

Supervisors:
Dr.ª Sara Badenes, Head of the Innovation Centre at A4F-Algae for Future

Prof.ª Dr.ª Lígia Oliveira Martins, Principal Investigator, Instituto de Tecnologia Química e Biológica António Xavier/Universidade Nova de Lisboa

Co-supervisor:
Pedro Cardoso, RD&I Pilot Unit Manager at A4F-Algae for Future

February 2023

Joana Batista Nunes Fernandes
B.Sc. in Biology

Liquid Effluent Bioremediation Resorting to Microalgae Cultivation

Dissertation for the obtention of the academic master's degree
in biotechnology for sustainability

Supervisors:
Dr. ª Sara Badenes, Head of the Innovation Centre at A4F-Algae for Future

Prof.ª Dr. ª Lígia Oliveira Martins, Principal Investigator, Instituto de Tecnologia Química e Biológica António Xavier/Universidade Nova de Lisboa

Co-supervisor:
Pedro Cardoso, RD&I Pilot Unit Manager at A4F-Algae for Future

Jury:
President:
Opponent:

February 2023

Liquid Effluent Bioremediation Resorting to Microalgae Cultivation

Acknowledgements

This dissertation marks the crowning of my academic journey, one characterized by hard work and perseverance, throughout which I learnt important life lessons and was fortunate to meet amazing people who were unwaveringly supportive, helping me reach this milestone. To them, I would like to express my sincerest gratitude.

I would like to thank ITQB and A4F for providing me with the opportunity to develop my master's dissertation outside academia, allowing me to explore the potential of scientific knowledge and development in a more practical setting, which had always been a goal.

A huge thank you to all the members of A4F's RD&I team, and in particular to those with whom I spent the majority of the past two years – **Pedro Cardoso**, **Pedro Coelho**, **Diana Gomes**, **João Alexandre**, **Hasti Calá**, **Mariana Oliveira**, **Daniela Silva**. I want to thank you for both the skills and knowledge you provided me with, but also for the support, companionship, joy and laughter shared throughout. A special thanks to my two greatest teachers along this journey, **Pedro Cardoso** and **Diana Gomes**, for the time, support, encouragement, and guidance, for all the conversations which inspired me to think outside the box, and for the shared passion for science and development of thorough scientific knowledge and practices. It has been an absolute pleasure working with you.

To **Dr.ª Sara Badenes** for allowing me to explore different research and experimental paths within this project, believing in my ability to conduct this work and foreseeing my potential to integrate this spectacular team.

To **Sofia Santos,** the most consistent presence throughout this journey, and with whom I now share a beautiful friendship potentiated by the shared adversity brought about by this experience.

To **Maria Martins** for accompanying me at the start of the writing process and pushing me towards achieving this goal, and to **Rita Moura** for reassuring me in the latter stages of this process.

To my friends **Di**, **Mariachi**, **Inêsita**, and **Xaroquita**, for always being present, with a special thanks to **Catjó**, for the hands-on help. To **Kizomba** for all the kindness and support, and **Sú** for being my role model and always cheering me along.

To my family, **Parents**, **Aunt** & **Uncle**, and **Siblings**, particularly **Filipe** and **Nara**, thank you so much for all the love, care, support, patience and understanding, for always being there for me cheering every step of the way whilst accepting my absence. *À minha* ***Sapinha***, who has brought me so much joy, by always greeting me with hugs, kisses and giggles. I love you all dearly.

To **Tunassa** – *Tuna Feminina do Instituto Superior de Agronomia*, for allowing me to further develop my passion for music, but most importantly for providing me with amazing people who brought me infinite moments of true happiness.

Lastly, I would like to leave a last heart-felt thank-you to my four-legged companion – **Bony**, who carried me through the best and hardest of times over the last 15 years. Although your favourite chair now sits empty, the memories of our happy times, are forever mine to keep.

Thank you all for believing in my abilities, especially during the times in which I was unable to.

Abstract

Agricultural and industrial activities require extensive use of raw materials and generate large amounts of nutrient-rich waste streams. These have been linked to a drastic and widespread increase in the pollution of aquatic systems, and incidence of eutrophication events. The need to reduce nutrient run-offs and preserve the presently available water resources is a major concern and a great opportunity to develop nutrient removal and recovery processes for waste streams.

Microalgae have been exploited for the treatment of different industrial wastewaters, coupling microalgal biomass production with resource recovery and waste valorisation, demonstrating the potential of microalgal-based systems to integrate a circular economy model.

Outdoor microalgae production systems are susceptible to seasonal variations in radiation intensity, photoperiod, and temperature, which impact the annual productivity and economic feasibility of large-scale operations. As these parameters are unique to every location, it is important to study their patterns within the geographical area of interest before the implementation of any production unit. In this sense, this work aims to assess the performance of a naturally established endogenous microalgal assemblage for the bioremediation of a nitrogen-rich effluent derived from an industrial fertilizer production plant. The experiments were carried out by operating a 700 L pilot-scale raceway pond in semi-continuous mode from 2020 to 2021. Data acquired in 2019 were integrated into this analysis to allow the assessment of the system's long-term performance accounting for year-round variations. Nitrogen removal efficiency, biomass productivity, and the ecosystem's species evolution were the parameters evaluated.

Additionally, several production cycles were performed under different pH values (6.5, 8.0 and 9.5), to promote alterations in the microalgal assemblage and, consequently, in the biomass batches obtained. The biomass was processed into three extracts which were tested as biostimulant priming treatment products in rice (*Oryza sativa* L. Japonica) under optimal and salinity stress conditions (80 and 160 mM) to assess their impacts on germination.

Keywords: Microalgae, Open raceways, Nutrient recycling, Wastewater bioremediation, Circular economy, Plant biostimulants.

Resumo

Atividades agrícolas e industriais requerem a utilização de grandes quantidades de matérias-primas, gerando também grandes quantidades de resíduos ricos em nutrientes. Estes resíduos estão associados a um aumento drástico e generalizado da poluição de sistemas aquáticos e incidência de eventos de eutrofização. A necessidade de redução da introdução excessiva de nutrientes no ambiente, e de preservação dos recursos hídricos ainda disponíveis, é preocupante; no entanto, compõe uma oportunidade para o desenvolvimento de processos de remoção e recuperação de nutrientes de águas residuais.

As microalgas têm sido exploradas para o tratamento de diferentes efluentes industriais, acoplando a produção de biomassa à recuperação de recursos e valorização de resíduos, demonstrando o potencial de sistemas de produção de microalgas para integrar um modelo de economia circular.

Sistemas de produção abertos são suscetíveis a variações sazonais na intensidade de radiação, fotoperíodo e temperatura, que impactam a produtividade anual e a viabilidade económica de operações em grande escala. Uma vez que estes parâmetros são específicos para cada localidade, é importante estudar os seus padrões dentro da área geográfica de interesse, antes da implementação de qualquer unidade de produção. Este trabalho, apresenta uma avaliação do desempenho de um consórcio de microalgas endógenas, naturalmente estabelecido, na biorremediação de um efluente rico em azoto proveniente de uma indústria de produção de fertilizantes. Foi utilizado um *raceway* convencional à escala piloto (700 L), que foi operado em modo semi-contínuo entre 2020 e 2021. Dados adquiridos em 2019 foram incluídos nesta análise, para possibilitar a avaliação do desempenho do sistema a longo prazo, considerando a sazonalidade. Efetuou-se o acompanhamento da eficácia de remoção de azoto, produtividade de biomassa e da evolução das espécies do ecossistema.

Foram ainda realizados vários ciclos de produção a diferentes valores de pH (6,5, 8,0 e 9,5), para promover alterações ao nível do consórcio e, consequentemente, dos lotes de biomassa obtidos. A biomassa foi processada em três extratos que foram avaliados como biostimulantes agrícolas, para o tratamento de *priming* em sementes de arroz (*Oryza sativa* L. Japónica). Os extratos foram testados sob condições ótimas e de stresse salino (80 e 160 mM), para avaliar os seus impactos na germinação.

Palavras-Chave: Microalgas, *Raceways* abertos, Reciclagem de nutrientes, Biorremediação de efluentes, Economia circular, Bioestimulantes vegetais.

Table of Contents

List of Figures

List of Tables

List of Abbreviations

A4F	Algae for Future
ANOVA	Analysis of Variance
ATP	Adenosine Triphosphate
BNR	Biological Nutrient Removal System
BOD	Biochemical Oxygen Demand
CO_2	Carbon Dioxide
COD	Chemical Oxygen Demand
DI	Deionized Water
DO	Dissolved Oxygen
DW	Dry Weight
FGP	Final Germination Percentage
GI	Germination Index
GI_c	Corrected Germination Index
IFPP	Industrial Fertilizer Production Plant
MBS	Microalgae-based Biostimulant
MGT	Mean Germination Time
N	Nitrogen
N_2	Dinitrogen
NaCl	Sodium Chloride
NH_4^+	Ammonium
$N–NH_4^+$	Nitrogen in Ammonium Form
$N–NO_3^-$	Nitrogen in Nitrate Form
NO_3^-	Nitrate
O_2	Molecular Oxygen
p	Pearson Product-Moment Correlation
P	Phosphorous
PAOs	Phosphorous Accumulating Bacteria
PAR	Photosynthetic Active Radiation
PBs	Planetary Boundaries
pH	Potential of Hydrogen
Photo-BNRs	Phototrophic Biological Nutrient Removal Systems
r_s	Spearman Rank Correlation Coefficient
RWP	Raceway Pond
SD	Standard Deviation
SVI	Seedling Vigour Index

1. Motivation

Economic development, populational growth and industrial expansion are coupled with increased reliance on natural resources. Aquatic ecosystems have been greatly compromised by decades of continued resource overexploitation, poor ecosystem management and pollution. Agricultural runoffs and discharge of untreated wastewaters are major contributors towards water quality degradation, through the introduction of pathogenic organisms, heavy metals, organic pollutants, and high amounts of nutrients – particularly of nitrogen (N) and phosphorous (P), which cause the increased occurrence of eutrophication events.[1–3] From 2008 to 2019, the global number of dead zones nearly doubled, seriously threatening global public health, food security, and biodiversity.[1] Meeting the targets established by the United Nations, to ensure the preservation of water resources, drinking water, hygiene and sanitation by 2030, requires the pace of progress to quadruple.[1] Therefore, extending scientific knowledge and technical expertise on sustainable management of natural resources is crucial for the development of water conservation and reuse systems.[1,4]

Over recent years, the environmental risks of the current economic model have been increasingly considered, with political and societal pressure pushing industries to reduce the generation of waste and its unregulated discharge. Additionally, due to climate warming and water scarcity, farmers have been considering non-conventional sources of water, looking at wastewater as a potential resource for nutrient recovery and water reclaim. The recycling of wastewaters after appropriate treatment can provide environmental and financial benefits, incorporating the concept of a circular economy.[5,6]

In this sense, the company Algae for Future (A4F) developed a collaborative project with a chemical fertilizer production company to evaluate the viability and effectiveness of microalgae-based open systems for the bioremediation and valorisation of the nitrogen-rich effluent derived from their production process.

1.1. Bioremediation of a N-rich Effluent Derived from Industrial Fertilizer Production – Overview and Background of the Assay

The industrial production of chemical fertilizers comprises different processing steps and numerous types of equipment, which must be washed and maintained after each production cycle, generating large amounts of aqueous effluents that hold a high concentration of the fertilizers' constituents, most notably in this particular case, nitrogen compounds.

As nitrogen is at the base of plant and algal nutrition, microalgae-based bioremediation systems might be interesting from an environmental perspective, while simultaneously providing an alternative source of income for the fertilizer production companies; since microalgal biomass might hold potential to be transformed into new and 'greener' agronomic products. Additionally, reducing the volume of effluent discharges into the sewage system will decrease expenses associated with the payment of legal fees that come with the introduction of high amounts of nutrients into wastewater treatment facilities.

In March of 2018, A4F installed a pilot-scale conventional raceway pond in an industrial fertilizer production plant (IFPP), which has since been operated in semi-continuous mode. Effluent bioremediation is achieved by a naturally established assemblage of endogenous microalgal species.

This work presents an analysis of the data acquired from January 2019 onwards; seeking to evaluate the system's performance, considering the impact of year-round environmental variations on biomass productivity, nitrogen removal efficiency and the evolution of the ecosystem's microalgal species.

Additionally, to test the agronomic potential of the biomass derived from the bioremediation process, several production cycles were performed at different pH values, to promote changes in the microalgal assemblage. Different biomass batches were harvested and processed into extracts which were tested as seed biostimulant priming products in rice (*Oryza sativa* L. Japonica), under both optimal and salinity stress conditions.

2. Literature Review

2.1. The Earth's Planetary Boundaries

The Earth's environment has undergone many periods of significant change; however, it has been stable for the past 11,700 years – period termed the Holocene.[7] During this geological era, environmental changes were subtle and naturally occurring, remaining favourable to human development. Temperature, freshwater availability, and biogeochemical flows, all stayed within relatively narrow variation ranges; yet this equilibrium has been disturbed since the 1800s Industrial Revolution. Thereafter, human reliance on fossil fuels, and industrialized forms of agriculture among other actions, have been pushing the Earth system's stability, triggering rapid and global environmental changes, with potentially catastrophic and worldwide consequences, such as extreme weather events; turning the Earth into a less conducive setting to human development.[3,7]

To guide the preservation of the Holocene state, Rockström, Steffen, and Noone et al.[3,8,9] developed a scientific proposal, based on the current understanding of the functioning and resilience of the Earth system; intended to quantify safe operating limits to guide social-economic development, as to reduce its detrimental environmental impacts and preserve the Earth's intrinsic biophysical processes – *The planetary boundaries framework.*[3] It introduces boundaries for nine areas identified as fundamental for the maintenance of the Earth system equilibrium and states that their transgression will severely change the Earth system, with dangerous consequences for humanity.[3] The current status of the Earth's Planetary Boundaries (PBs) is represented in Figure 2.1.

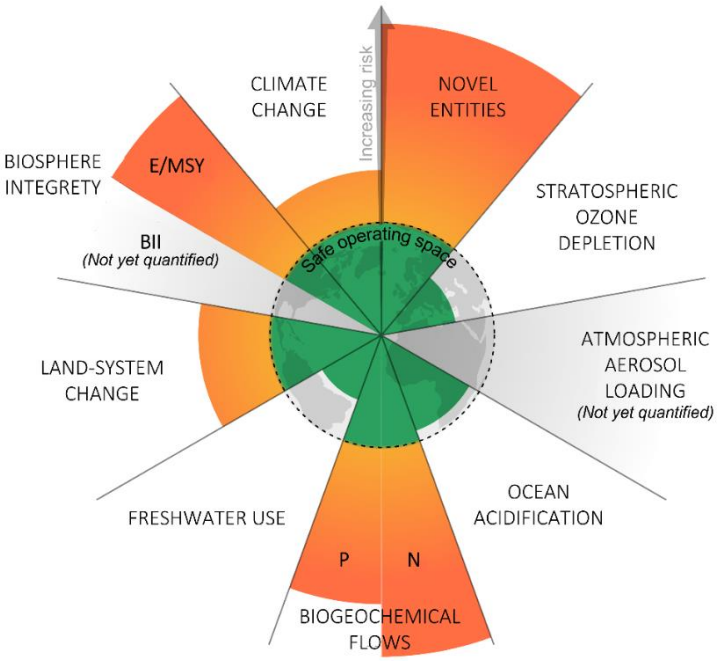

Figure 2.1 – Global status (2022) of the control variables for the nine areas which regulate the Earth System equilibrium. The green section represents the safe operating space (below the planetary boundary – represented by the dashed circle), and the orange scale represents the zone of uncertainty and the high-risk zone. Processes for which global-level boundaries are not yet quantifiable are represented in grey. Designed by Azote for Stockholm Resilience Centre based on the analysis of Persson, and Steffen.[3,10]

The conceptual framework for the PB approach, describes the safe operating space, uncertainty range, and danger level for the core areas identified.[3,9] The established boundaries are not equivalent to a global tipping point, but rather to a value upstream of each parameter's threshold (Figure 2.2).[3]

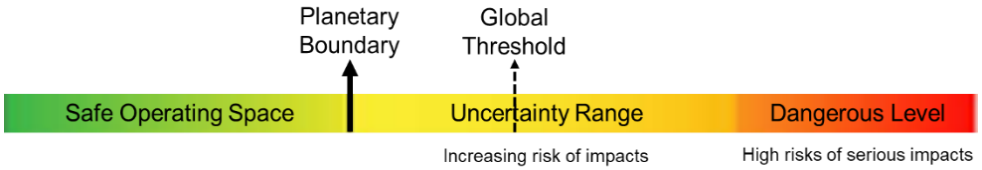

Figure 2.2 – Representation of the conceptual framework for the planetary boundary approach. Adapted from Steffen et al.[3]

2.1.1. Biogeochemical Flows – Nitrogen and Phosphorus

The present work is included in the thematic of the Earth's Planetary Boundaries, addressing the issues related to the Earth's biogeochemical flows; particularly the nitrogen (N) cycle and N recovery. The PBs established for this core area, have been set to eliminate the risk of widespread eutrophication of aquatic ecosystems.[3]

Eutrophication is the natural ageing process of aquatic ecosystems, typically of somewhat confined and slow-flowing waterbodies, such as lakes, reservoirs, rivers, and freshwater wetlands.[3,11] It occurs over a geological timescale, and results from the progression of the ecosystems' nutrient profile, whereby changes in the relative proportion and accumulation of chemical forms of N and phosphorous (P), stimulate aquatic plant growth, causing the production and build-up of organic material. This build-up limits light penetration throughout the water column, eventually causing algal death, and enhancing bacterial aerobic oxidative decomposition of the gathered biomass. The decomposition process causes the depletion of dissolved oxygen (DO), leading to hypoxia or anoxia[1], and ultimately acidification of the waterbody; resulting in the deterioration of water quality and death of the existing fauna, disrupting the system's overall ecology.[12,13]

Despite it being a naturally occurring phenomenon, anthropogenic activities have caused a drastic and widespread increase in eutrophication events.[2,12,14] The intensified use of chemical fertilizers and manure in agricultural production, has significantly improved crop yields and food security for the growing human population. However, the improper or inadvertent discharge or run-off of large amounts of nutrient-rich waters, has had a major impact on N and P cycling in global continental waters, leading to the rise of anthropogenically-driven eutrophication events (cultural eutrophication, Figure 2.3).[3,12] As a result, the evaluation of the Earth's biogeochemical flows is currently achieved through the quantification of the N and P inputs to croplands, through fertilizer application. The established boundary values are indicated in Table 2.1.

[1]Water systems with DO concentrations under 2 mg L^{-1} are termed hypoxic. Once oxygen is depleted, the system becomes anoxic usually being referred to as a 'dead zone'.[123]

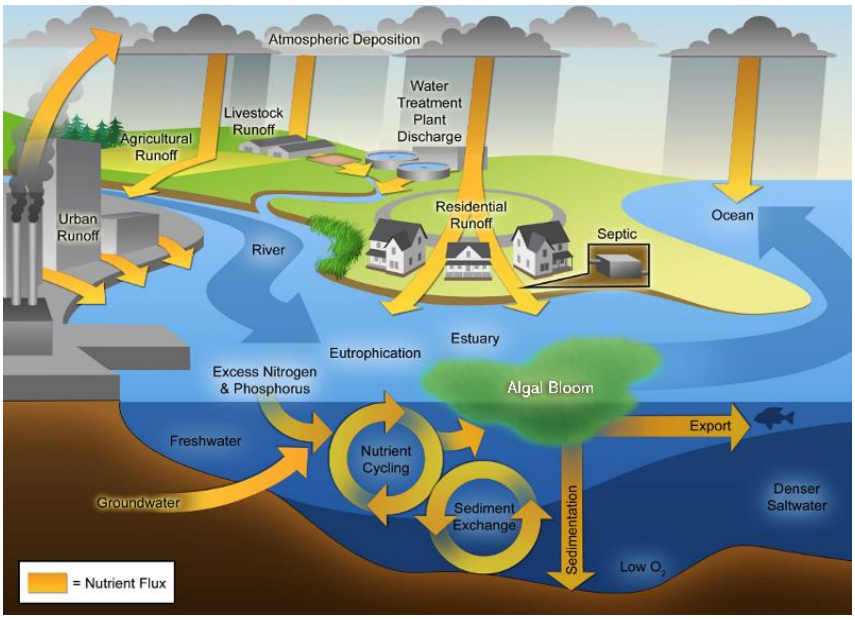

Figure 2.3 – Functional linkages between hydrology, anthropogenic nutrient inputs, eutrophication (phytoplankton blooms), and hypoxia/anoxia in estuarine and coastal aquatic ecosystems. Sourced from Paerl.[15]

It would be most appropriate to use the N and P flows from soil to freshwater systems, as the control parameters for the establishment of PBs for biogeochemical flows, due to their direct relationship to the risk of eutrophication.[3] However, as fertilizer application is the main form of anthropogenic perturbation of both the N and P cycles, and it is known that around a third of the N applied to agricultural lands is not removed with crop harvest[16]; the application rate of fertilizers containing N fixed by the Harber-Bosch process and mined P, were the variables selected for the establishment of these boundaries. This was an important decision, as it is an easier parameter to measure and track, simplifying policy regulation and management.[3]

Table 2.1 – Control variables used to assess the state of Earth's biogeochemical flows, proposed Planetary Boundaries and safe operating limits at a global scale (uncertainty ranges); and current values globally expressed. Adapted from Steffen et al.[3]

Control Variable	Planetary Boundaries & Uncertainty Range	Current Global Value
Fertilizer-N addition to croplands	**62–82 Tg N year^{-1}** *****Equivalent to the addition of 41–55 kg N ha^{-1} year^{-1}	**≈ 150 Tg year^{-1}** (82% beyond uncertainty range)
Fertilizer-P addition to croplands	**6.2–11.2 Tg P year^{-1}** *****Equivalent to the addition of 4.1–7.5 kg P ha^{-1} year^{-1}	**≈ 14 Tg year^{-1}** (25% beyond uncertainty range)

*Assuming the total global cropland area determined by Bouwman et al.[17] – 1494 x 10^6 ha.

The current global N and P application rates (150 Tg N year^{-1} and 14 Tg P year^{-1} – Table 2.1) exceed the environmental limits by 82 and 25% for N and P, respectively; transgressing the proposed PBs for this core area (Table 2.1). The same has been verified for most of the critical areas established (Figure 2.1). Additionally, after downscaling the PBs through an equal-per-capita allocation approach, it was

verified that not only does the European Union significantly exceed its 'fair share' of the global safe operating space for biogeochemical flows, but that it also surpasses the global P and N consumption average by a factor of two and three, respectively.[18]

Despite fertilizer-derived nutrient inputs being the most significant towards cultural eutrophication, the introduction of these nutrients to waterbodies, through direct or indirect discharges of poorly treated industrial and urban effluents, is also an important contributor to this phenomenon, due to their high N and P contents.[19] Therefore, it is important to address this thematic, since with the expected increase in the global population and development of the industrial sector, its implications on the Earth's biogeochemical flows, will inevitably increase; and countermeasures need to be timely established.

2.2. Wastewater Treatment and The Circular Economy

The Circular Economy action plan is included in the European Green Deal[2] and seeks to accelerate the transition towards a sustainable and regenerative growth model, decoupled from resource exploitation, respecting the Earth's PBs.[20,21] This transition can deliver substantial material savings, through the development of strategies to extend overall products' lifespan, increasing the use of renewable resources and repurposing waste streams; ultimately slowing, closing, and narrowing material and energy loops (Figure 2.4**Erro! A origem da referência não foi encontrada.**), maximizing resource value, while meeting the goals set for both sustainability and economic competitiveness.[20,22]

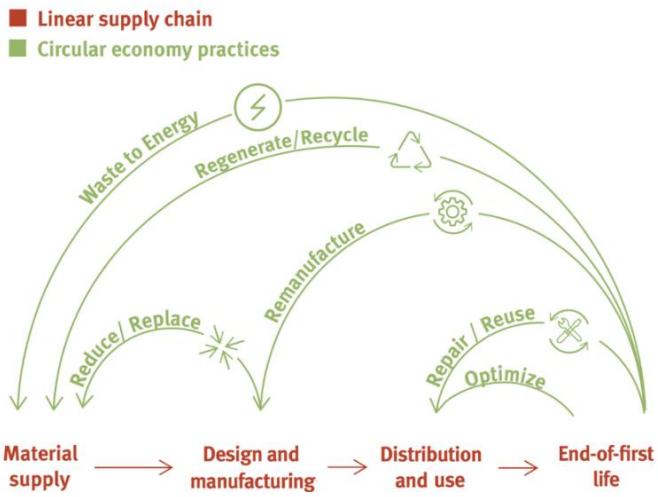

Figure 2.4 – Linear *versus* circular economy practices. Sourced from UNIDO, 2019.

Sewage treatment is essential for the protection of human and environmental health. Despite their high cost, current wastewater treatment techniques are effective in N and P removal, but not in their recovery for reuse; mainly focusing on cleaning wastewater to allow its safe reintroduction to the environment.[5,23]

[2]Package of policy initiatives, intended to set the path for the European Union's green transition, with the goal of achieving climate neutrality by 2050; while supporting its transformation towards a fair and prosperous society with a modern and competitive economy.[124]

Circularity can be supported by transitioning Urban Wastewater Treatment Plants, recently re-named Water Resource Recovery Facilities (WRRF), from the role of costly 'pollutant removal units' to profit-generating 'resource factories' for waste valorisation and nutrient recovery. To improve the sustainability of wastewater treatment processes, efforts must be put into achieving greater water recovery, lowering energy and chemical consumption, and resource extraction; creating a variety of useful end products, through the implementation of various extraction stages.[5,23,24]

Nutrient recycling is important to avoid the depletion of non-renewable resources and reduce the environmental impacts linked to their extraction, manufacture, and use; despite it being an underexplored approach.[23] In theory, if it were possible to recover the total amount of N and P present in global food, animal and human waste streams; the amount of nutrients attained would be 2.7 times higher than that contained in the total volume of chemical fertilizers currently used.[23] However, agricultural nutrient requirements are still met through the overapplication of mineral fertilizers.[6] Therefore, as nutrient recovery technologies are not yet fully mature, it is important to expand research on this topic, for process development and optimization, towards the enhancement of their full-scale commercial applicability.[6]

2.2.1. Conventional Wastewater Treatment – an Overview

Composition of Wastewaters

Agro-industrial production generates large volumes of effluents, containing high concentrations of nutrients, organic matter, and microorganisms.[19,25] Large industries, such as those from the pulp and paper, metals, energy, and chemical sectors, often have on-site treatment facilities. In contrast, small-scale manufacturers, typically discharge their effluents into the sewage system.[5] Consequently, WRRFs receive water from several sources, in varying strength and volume according to the lifestyle and activities practised in each considered location. The sewage system may receive domestic wastewaters, surface rainwaters, effluents derived from manufacturing industrial plants, run-off from agricultural lands and leachates from solid waste disposal sites.[19,26] This causes the composition of the raw sewage to be complex and variable, generally comprising mixtures of both natural organic and inorganic materials, pathogenic and non-pathogenic microorganisms, as well as synthetic compounds such as pharmaceuticals.[19,25,26]

Conventional Wastewater Treatment Process

Wastewater treatment primarily aims at the degradation and removal of organic matter, so that effluent discharge does not compromise public health or extensively damage the environment.[19,26] The degree of treatment required, depends on the effluent characteristics and susceptibility of the disposal site.[25] Complete sewage treatment comprises a combination of physical, chemical, and biological steps, which fall into four major categories – Preliminary, primary, secondary, and tertiary or advanced treatment[19,25], as is represented in Figure 2.5.

As advanced effluent treatment, usually follows secondary treatment processes, it is often referred to as tertiary treatment; however, these steps are not necessarily independent, and only primary and secondary treatment processes are widely applied.[19,26]

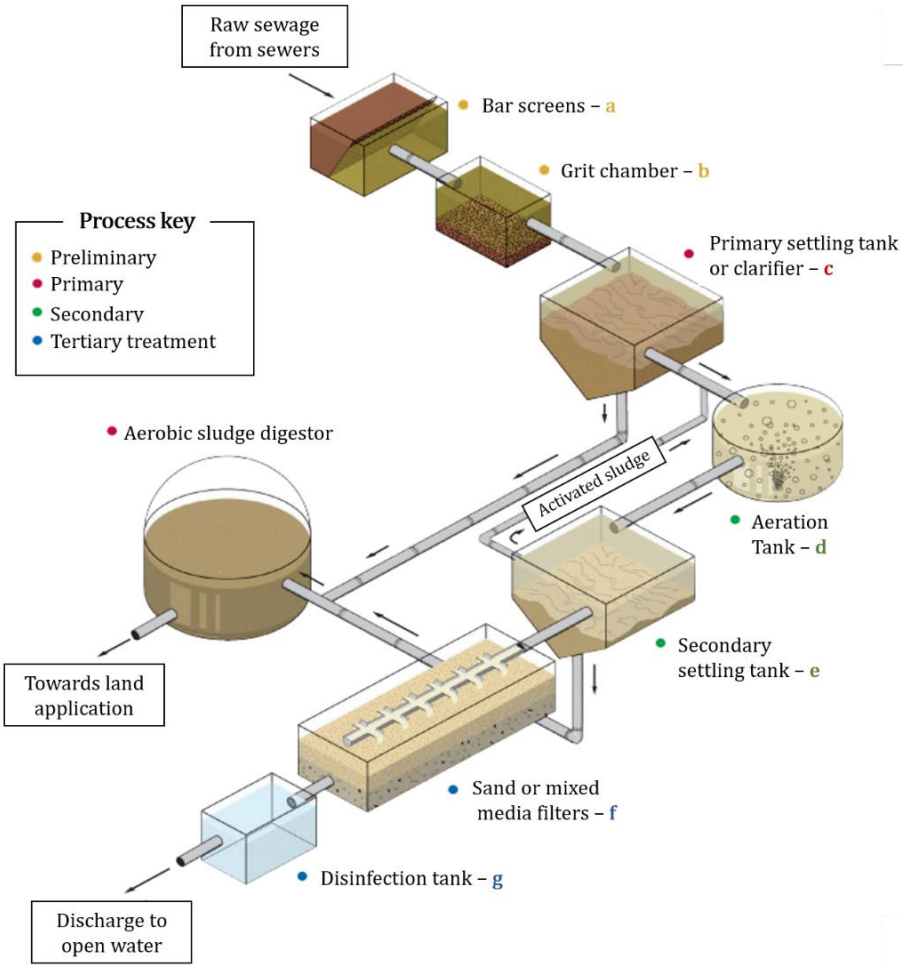

Figure 2.5 – Standard wastewater treatment process of modern WRRFs. Only the steps relevant to this chapter are specified. Adapted from Gerba & Pepper.[19]

I. Preliminary and Primary Treatment

Consists of the physical separation of large materials.[19,26] During preliminary treatment, the sewage water passes through a metal grating, which blocks the passage of large solids. A moving screen (Figure 2.5a) then filters out smaller objects, and the wastewater flows through a grit chamber (Figure 2.5b), where sand and gravel settle out of the waste stream. Primary treatment begins once the wastewater is pumped into a primary sedimentation tank (Figure 2.5c), where approximately half of the suspended organic solids settle to the bottom of the tank forming the primary sludge.[19,26] The liquid effluent derived from primary treatment often contains large amounts of suspended organic material and high biochemical and chemical oxygen demand (BOD and COD)[3].[25]

[3]BOD measures the amount of DO required by microorganisms during biochemical oxidation of organic matter; while COD measures the DO consumed during chemical oxidation of organic matter.[19]

II. Secondary Treatment

Presently, activated sludge treatment processes, are the most widely applied forms of biological secondary treatment, due to their efficiency, simplicity, and cost-efficiency. These accomplish the reduction of the wastewater's BOD, through the biochemical oxidation of suspended solids; for the protection of the receiving water body's DO balance.[15,22] Air is diffused into an aeration tank (Figure 2.5d), homogenizing the mixture and providing the necessary oxygen, for heterotrophic bacteria to decompose up to 90% of the effluent's organic matter.[19,25] The waste stream then flows into a secondary settling tank (Figure 2.5e), for decantation of the activated sludge; generating a clear and apparently clean effluent which is at this stage, generally discharged into natural water bodies. However, it is still loaded with inorganic forms of N and P (mainly nitrate, ammoniacal nitrogen and phosphate), which contribute to the disturbance of both its biogeochemical flows. The sludge derived from water cleaning is often incinerated, with the heat being converted into power which is applied to the treatment process[19,25]

Despite secondary treatment achieving the elimination of up to 90% of pathogenic microorganisms, when no further treatment is applied, the effluent is disinfected before discharge (Figure 2.5g).[21,27]

III. Tertiary or Advanced Treatment

Advanced effluent treatment is applied when further reduction of suspended solids, BOD/COD, turbidity, N and P, metals, or pathogens is required; with its main target often being the removal of inorganic N and P.[19,25] Currently, N removal is primarily achieved through bacterial nitrification-denitrification processes, while P compounds are removed through chemical precipitation using metal salts.[6,19,25,26] Many physicochemical methods have been developed for nutrient removal; yet, biological nutrient removal methods (BNRs) are more advantageous from an environmental and financial standpoint and are thus the most widely implemented.[26–28]

2.2.1.1. Biological Nutrient Removal Methods

BNRs methods vary according to the sequence of conditions contained in the multistage bioreactors' sections. Some are designed to achieve simultaneous N and P removal, fusing secondary and advanced effluent treatment, and replacing the fourth step of conventional treatment (e.g., the modified five-step Bardenpho process – Figure 2.6).[19,27]

In the Bardenpho process, the effluent derived from primary clarifiers flows into a five-section multistage bioreactor, with each division providing the appropriate conditions for the development of the microorganisms responsible for nutrient removal: an anaerobic fermentation zone (Figure 2.6a), characterized by very low DO levels and absence of nitrate (NO_3^-), where BOD and COD are reduced and the population of phosphorus accumulating bacteria (PAOs) increases; an anoxic zone (Figure 2.6b), with low DO levels, where heterotrophic bacteria conduct denitrification of NO_3^- to nitrogen gas (N_2); an aerobic zone (Figure 2.6c), where the mechanical addition of oxygen allows aerobic bacteria to

transform ammonium (NH_4^+) to NO_3^- through nitrification, and PAOs to uptake orthophosphate; a second anoxic zone (Figure 2.6d); and a final aeration zone (Figure 2.6e).[19,27]

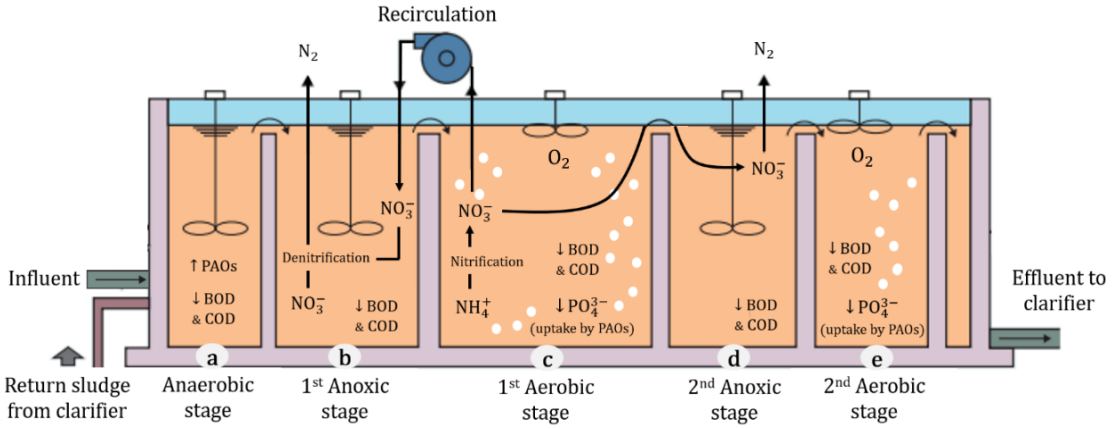

Figure 2.6 – Five-section multistage Bardenpho bioreactor. PAOs – Phosphorous accumulating bacteria; BOD – Biological oxygen demand; COD – Chemical oxygen demand; PO_4^{3-} – Orthophosphate; O_2 – Molecular oxygen; NO_3^- – Nitrate; NH_4^+ – Ammonium; N_2 – Nitrogen gas; ↑ – increase; ↓ – decrease; bold arrows – flow direction. Adapted from Gerba & Pepper.[19]

Nitrogen is released as N_2 and nitrous oxide into the atmosphere, or incorporated into bacterial biomass, and P is incorporated by PAOs. Nitrogen and phosphorous are then removed from the waste stream through the separation of the aqueous phase from the produced sludge.

BNR methods generate fewer secondary waste streams compared to chemical methods. However, these are highly dependent on aeration for O_2 supply and require spatial and or temporal separation of its different steps, resulting in a significant increase in energetic requirements, investment expenses and the need for stricter monitorization and maintenance of the involved equipment.[6,19,25,26]

It is estimated that 0.6 to 3.0% of the total electricity generated in developed nations is expended on the treatment of wastewater, with approximately 60%, being used on aeration.[29–31] Therefore, reducing aeration requirements of conventional BNRs might be a key factor to reduce the processes' environmental impacts and energy requirements.[32]

2.2.1.2. Phototrophic Enhanced Biological Nutrient Removal Systems (Photo-BNRs)

Photo-BNRs have been proposed as sustainable and cost-efficient alternatives to conventional BNRs, due to their low oxygenation requirements and improved nutrient recovery compared to anaerobic digestion technologies of WRRFs.[6,33,34] These rely on the spontaneous development of microalgae-bacterial consortia, where microalgae produce the oxygen required for heterotrophic bacteria to biodegrade carbonaceous material, leading to the release of CO_2, which is fixated by microalgae with simultaneous use of inorganic nutrients for growth (simplified representation in Figure 2.7).[26,32,34,35] Microalgal-bacterial interactions play an important role in nutrient removal due to their synergistic

relationship. Previous studies have demonstrated that wastewater treatment with microalgal-bacterial consortia achieves better nutrient removal efficiencies than strictly bacterial or algal systems.[36,37]

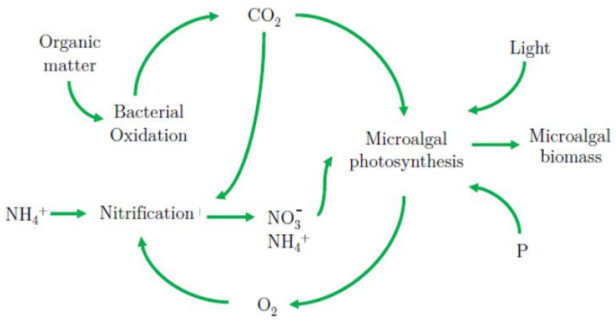

Figure 2.7 – Microalgal-bacterial interactions during photosynthetic oxygenation in BNR systems. Adapted from Muñoz and Guieysse.[34]

The environmental and economic benefits of photo-BNRs lay in the ability to recover nutrient resources in the form of microalgal/bacterial biomass, which can be used as feedstock for the development of a wide array of different products such as biostimulants and biofertilizers, fuels or bioplastics. Coupling wastewater treatment with microalgal biomass recovery and transformation supports the creation of a circular bio-economic model, where waste is economically re-used.[23,38] Therefore, microalgal biomass derived from bioremediation processes, has been gaining increasing attention due to its potential to be used as feedstock in different sectors.[39,40]

2.3. Open Microalgal Cultivation – Raceway Pond Systems

There are several bioreactor designs available to enhance growth and facilitate biomass recovery. These include suspended and non-suspended systems, being sub-categorised into open or closed systems. Suspended cultures enable the microalgae cells to move freely within the medium and are most used in microalgal wastewater treatment.[41]

Open raceway ponds (RWPs) are open, shallow (0.12-1.00 m) lagoon-based systems, composed of a closed loop, where a paddlewheel continuously circulates the medium, with an average velocity range of 0.15 to 0.40 m s^{-1} (Figure 2.8).[42,43]

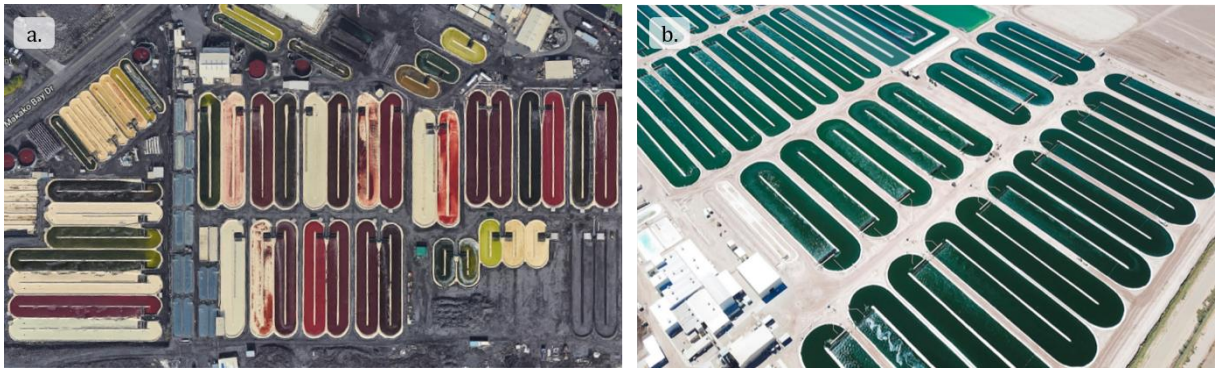

Figure 2.8 – Industrial microalgae production farms. Cyanotech in Hawaii (a.) and Earthrise in California (b.).

These have been widely considered for biological wastewater treatment, as their design creates optimal conditions for microalgal growth and oxygen production; promoting acceptable nutrient removal within a shorter time-frame and less area, compared to other lagoon-based systems.[44–46]

Commercial Microalgae Production

Currently, RWPs are among the most widely used bioreactor designs for industrial microalgae culture. One of their main advantages is that they are easier and cheaper to construct and operate and present lower energy requirements compared to most closed systems. As CO_2 diffusion between the atmosphere and water cannot satisfy the carbon requirements of high-yielding autotrophic microalgal production, industrial-scale systems require the injection of gaseous CO_2 into the culture; acting both as a source of carbon for microalgal growth and as a method for pH regulation.[26,41,42]

Open production systems also present significant drawbacks, such as high evaporative water loss, CO_2 diffusion to the atmosphere, large spatial requirements and poor light utilization by the cells.[13,47,48] These are also highly susceptible to microbial contamination, making it difficult to maintain year-round dominance of the desired microalgal species. Hence, these are mostly used for the cultivation of microalgae which are tolerant to extreme conditions, such as alkaline or acidic pH and high salinity, which discourages the growth of other species.[13,48]

Nonetheless, their cost-efficiency compensates for their low biomass productivity and operational constrains.[13,46]

2.3.1. Factors to Consider for Open Microalgal Cultivation

Environmental Parameters

Microalgae are sensitive to their living environment, with factors such as light, temperature, pH, nutrient concentrations, and optical density (turbidity) influencing their performance.[6] Open systems are more susceptible to changes in environmental conditions, which fluctuate within two different timescales – the diurnal cycle, where radiation, photoperiod, and temperature vary throughout the day; and the seasonal cycle, accounting for the year-round variation of these parameters, which depend on the climatic characteristics of the geographical location of the habitat in which the algae are being produced.[13]

Light availability is one of the main regulators of microalgal performance.[26,43,46–48] Culture depth has a direct influence on both medium temperature and light availability, impacting the systems' microalgal species diversity, photosynthetic performance, and operation costs. Deeper ponds present increased temperature variations and decreased light availability through the water column, potentially limiting microalgal growth, and increasing harvesting costs due to the high water content of the culture.[43,46,47] Opposingly, decreasing pond depth leads to an increase in the bioreactor's required surface-to-volume ratio, intensifying water evaporation losses. Thus, increasing pond depth decreases land footprint, capital and operational costs required for treating a given volume of wastewater, thereby improving the economic viability of RWPs.[38]

The biomass concentration within the culture medium also impacts light availability, with high concentrations causing an increase in turbidity and self-shading, reducing the photosynthetic potential of the system. Efficient culture homogenization is important to avoid biomass sedimentation and to promote efficient light utilization.[41,42,45,46]

Maintaining the dominance of any desired species during the cultivation of microalgal assemblages in open systems would require the control of specific environmental conditions that allow its dominance in the first place. Changes in the structure of these communities are often triggered by fluctuations in one or more environmental parameters, or in biological interactions such as competition for resources and selective predation by zooplankton grazers.[49] However, the influence of these parameters in the composition of microalgal assemblages is still poorly understood.[45]

By increasing the knowledge around this subject, it may be possible to manipulate and favour the growth of desirable species in open production systems.[45,50]

2.4. Microalgae – General Introduction

The emergence of the term 'Algae' as a classifier derived from the need to distinguish plants from other taxonomically unrelated photosynthetic organisms, that due to their physiological traits, cannot be included in this same group. This classification includes organisms, which do not forcibly share a common evolutionary origin, and even derive from different kingdoms of life (Bacteria, Plantae, Chromista, and Protozoa – Figure 2.9).[51,52] These present very distinct cellular structures, shapes, colours, and organization levels; comprising distinct metabolic and ecological requirements.[53,54]

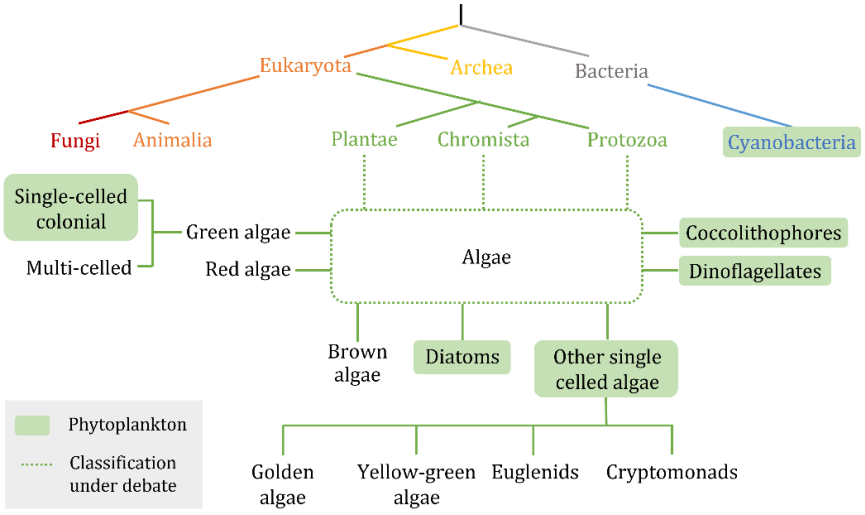

Figure 2.9 – Simplified taxonomical classification of phytoplankton. Adapted from Kosek et al.[55]

'Microalgae' is an equally generic subdivision of the 'Algae' group, which includes all prokaryotic (cyanobacteria) or eukaryotic microbial scale photosynthetic organisms.[52] Most microalgae species are unicellular, despite the existence of some multicellular, filamentous, and colonial forms. They are ubiquitous to most ecosystems and habitats and can grow attached to solid substrates, in soil, and in

symbiosis with plants. However, microalgae are mostly found in fresh and marine aquatic systems, as well as in wastewater streams from varied sources, some presenting motility, while others simply exist in suspension.[13,52,54]

2.4.1. Prokaryotic and Eukaryotic Microalgae

Despite the broadness of the microalgae classification, a defined difference between microalgal species occurs at the cellular level, between prokaryotic cyanobacteria and eukaryotes.

Cyanobacteria belong to the bacterial domain, implying their strictly prokaryotic nature. Prokaryotic cells lack internal compartmentalisation and membrane-bound organelles; presenting no separation between the cytoplasm, DNA and the machinery involved in photosynthesis and cellular respiration. Instead, these cells contain elongated thylakoid membranes which are arranged to hold the light-absorbing pigments and the biochemical components necessary for the photosynthetic process (Figure 2.10).

Eukaryotic cells are significantly more complex, presenting internal compartmentalization of their various organelles. In eukaryotic microalgal and plant cells, thylakoids are enclosed within chloroplasts, organelles which are home to all photosynthetic processes (Figure 2.10).[48,54]

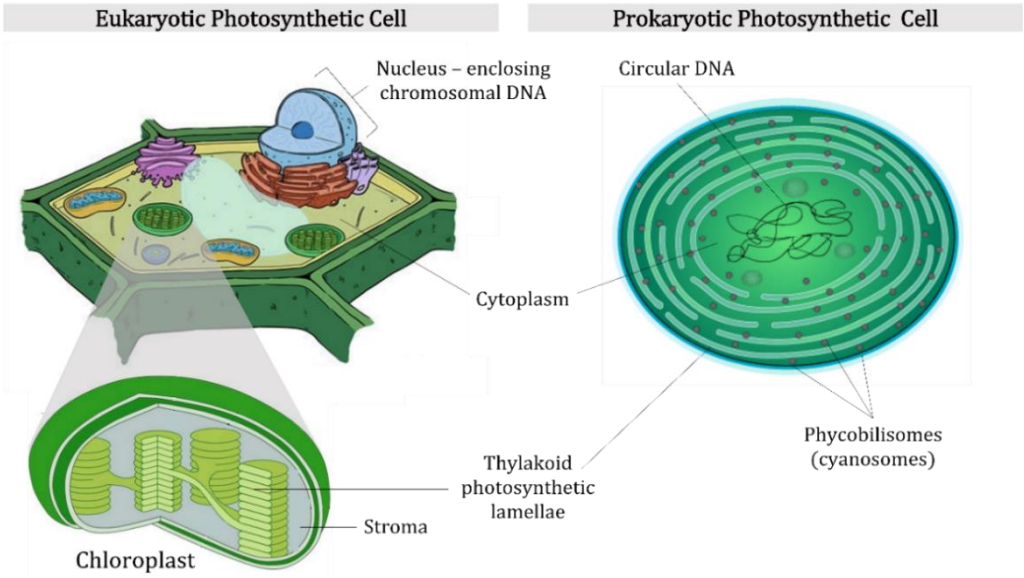

Figure 2.10 – Eukaryotic and prokaryotic photosynthetic cells. Only the organelles relevant to the explanation of the photosynthetic process are indicated.

2.4.2. Photosynthesis

Photosynthesis is the process of sunlight energy conversion, conducted by photoautotrophic organisms, which harvest and utilize the sun's electromagnetic radiation energy to convert inorganic compounds into organic molecules, which are in essence, biocompatible chemical energy forms.[13,54,56]

Virtually all of Earth's organisms are directly or indirectly dependant on photosynthesis, as a source of both organic matter and energy for their metabolism and growth; placing photosynthetic organisms at

the base of most food webs, serving the role of primary producers. Algae, in particular, are responsible for more than 50% of global photosynthetic activity, making them very important primary producers in both freshwater and marine ecosystems.[13,54,57].

The photosynthetic transformation of electromagnetic energy, into organic molecules, is achieved through the conversion of CO_2 and water into carbohydrates (equation (2.1))[56]:

$$nCO_2 + nH_2O + \text{Light} \xrightarrow{\text{Chlorophyll a}} (CH_2O)_n + nO_2 \qquad (2.1)$$

This process is divided into two consecutive and mutually regulatory stages, (I) the light-dependent and (II) light-independent reactions (Figure 2.11).[56,57]

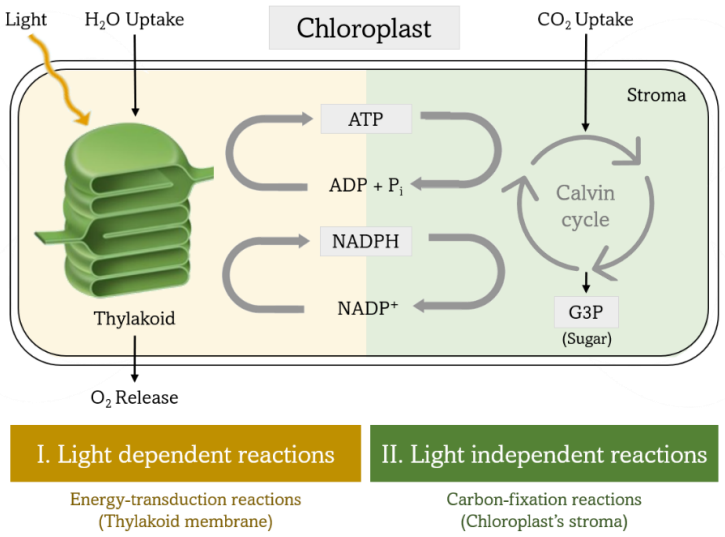

Figure 2.11 – Schematic representation of the photosynthetic reactions in eukaryotic cells. Adapted from Raven.[58]

I. Light-dependent reactions

These take place in the cell's photosynthetic lamellae and involve light-driven electron and proton transfers, that generate high-energy biocompatible molecules. Electrons are transferred from water to nicotine adenine dinucleotide phosphate ($NADP^+$), forming NADPH. This reaction is coupled with the transfer of the water-derived protons, leading to the phosphorylation of adenosine diphosphate (ADP) into adenosine triphosphate (ATP).[56,57]

II. Light-independent reactions

These occur in the stroma or cytoplasm, in eukaryotic and prokaryotic cells, respectively. The NADPH and ATP produced during light reactions, are used as an energy source for the sequential biochemical reduction of CO_2 into G3P via the Calvin cycle; regenerating ADP and $NADP^+$.[56,57] These are later used in a wide range of metabolic pathways, for the synthesis of molecules such as amino acids, lipids, or sugars.[56,57]

2.5. Microalgal Biomass Composition and Potential Applications

Microalgal biomass is manly composed of carbon, oxygen, hydrogen, nitrogen, sulphur, and phosphorus. Calcium, potassium, sodium, chlorine, magnesium, iron, and silicon are present and required in smaller amounts. The former are thus termed macro- and the latter micronutrients. Additional elements occur in trace amounts as they are needed only in catalytic quantities.[54]

The synthesis of organic molecules through photosynthesis and subsequent metabolic pathways greatly depends on nutrient availability and stoichiometry. Therefore, both these parameters need to be considered when analysing the nutritional requirements of microalgae.[59] Due to their prevalence in microalgal biomass, carbon, nitrogen and phosphorus are the most determinant macronutrients for growth[59]; changes in their ratios can affect cellular health causing changes in size, shape, growth and biochemical composition. In natural environments, changes in N and P relative abundance are often responsible for changes in phytoplankton communities.[48,54,60]

The biochemical composition of microalgae has been attracting the interest of several industries, for the production of lower-cost commodities (e.g.; fuels, feeds and foods) and higher-value products (e.g.; β-carotene, polysaccharides).[40,61–65] They are gaining wide acceptance for agricultural applications, as their bioactive compounds, including carbohydrates, minerals, trace elements, and phytohormones have been shown to enhance plant productivity and ability to withstand abiotic stress. Hence, microalgae are being considered for the production of cleaner and more sustainable alternatives to conventional biofertilizers and biostimulants.[40,61–65]

2.5.1. Microalgae in the Agricultural Sector

2.5.1.1. Impacts of Salinity on Rice Development

Nowadays salination is one of the major causes of soil degradation, and the most significant factor behind crop yield reduction, at both a European and global level. It is characterized by the overaccumulation of soluble salts to an electrical conductivity (ECe) value equal to or greater than 4 dS m^{-1} (≈ 40 mM of NaCl)[4]; with sodium chloride (NaCl) being the primary culprit behind this phenomenon.[66–70]

Rice (*Oryza sativa* L.) is a worldwide staple food crop, being the primary source of food for around half of the human population.[68,71,72] It is also the most salt-sensitive cereal crop and is at greater risk of exposure to brackish waters due to sea level rise, especially in delta regions where it is mainly produced.[68,72]

Generally, salination reduces plants' ability to uptake water and nutrients, leading to osmotic stress, ion toxicity, nutrient imbalances, and water deficit. It often causes significant reductions to plant growth and chlorophyll content; with the accumulation of salt ions in plant tissues injuring young photosynthetically

[4]**Soil salinity ranking:** ECe ≤ 2 dS m^{-1} – Non-saline; ECe 2-4 dS m^{-1} – Slightly saline; ECe 4-8 dS m^{-1} – Mildly saline; ECe 8-16 dS m^{-1} – Moderately saline; ECe ≥ 16 dS m^{-1} – Strongly saline.[70]

active leaves, leading to chlorosis and premature leaf senescence. Salt exposure is particularly detrimental during germination and seedling growth stages.[67–69,73,74] In rice, susceptibility to salt varies along the plants' life cycle and depends on its genotype and organs considered; with seedling and reproductive stages being more susceptible compared to the vegetative stage.[68,75,76]

Genetic engineering can provide crops with improved stress tolerance; however, this strategy is still broadly rejected by the public. Identification of salt-tolerant varieties and the development of management strategies are very important to reduce the impacts of salinity and enhance crop yields.[71,76] Biostimulants have been proposed as agronomic tools to counteract the detrimental effects of abiotic stress, as these contain bioactive molecules with the potentially to improve plants' ability to face abiotic stress conditions, by acting on their primary or secondary metabolism.[39]

2.5.2. Microalgae-Based Biostimulants (MBS)

Biofertilizer products typically contain microorganisms and natural substances that can improve the soil's chemical and biological properties, restoring their fertility, and thus potentiating plant growth and development.[39,40,54] Contrastingly, the organic substances and microorganisms contained in biostimulants, interact with plants' metabolic pathways, stimulating growth and development under both optimal and stress conditions; independently of the product's nutrient content.[39,40,54] These often contain mixtures of amino acids and short peptides that are believed to help reduce nutritional deficiencies by increasing root biomass, improving nutrient uptake and translocation, and enhancing enzymatic activity related to nutrient assimilation[39]; thus having the potential to reduce the amount of chemical fertilizers required for crop production, and the agricultural sector's negative impacts on the N and P biogeochemical flows.

Biostimulants are usually applied in small quantities through different methods and at distinct plant developmental stages: as foliar sprays, mixed with soil or as seed priming treatments; at sowing to protect seedlings' early development, during blooming or fruit setting.[39,40,54] The diverse and complex biochemical composition of these products, hinders the identification of the compounds that most impact plant' metabolism, and the mechanisms activated by biostimulant application.[39]

Due to the abundance of microalgal species (approximately 800,000)[52] and the wide range of possible applications, these have been regarded as promising feedstocks for the development of biostimulant and biofertilizer products, to improve the sustainability of agriculture; being considered eco-friendly and cost-effective alternatives to synthetic products.[40] These can be used as substitutes, or in conjunction with synthetic products; enhancing soils' nutrient availability, increasing cellular metabolism and leaf chlorophyll content, improving rooting, crop quality and yields, as well as enhancing tolerance to abiotic stresses.[40,62]

2.5.3. Germination and Seed Priming

Germination and seedling development are determinant for the establishment of plants under both optimal and stress conditions.[77,78] Germination begins with the start of water uptake by the quiescent dry seed and ends once the embryo first emerges from the enclosing tissues (represented in Figure 2.12). It is typically divided into three phases: (I) Seed imbibition – passive hydration of dry tissues; (II) Metabolism activation: activation of cellular repair processes, including DNA repair pathways and antioxidant mechanisms essential for the preservation of genome integrity; (III) Cellular elongation and radicle protrusion (growth).[79] Phases I and III both involve an increase in the water content, which remains stable during metabolic activation. The germinative process is reversible until the end of phase II, as tissue tolerance to desiccation is lost with the initiation of phase III.[79]

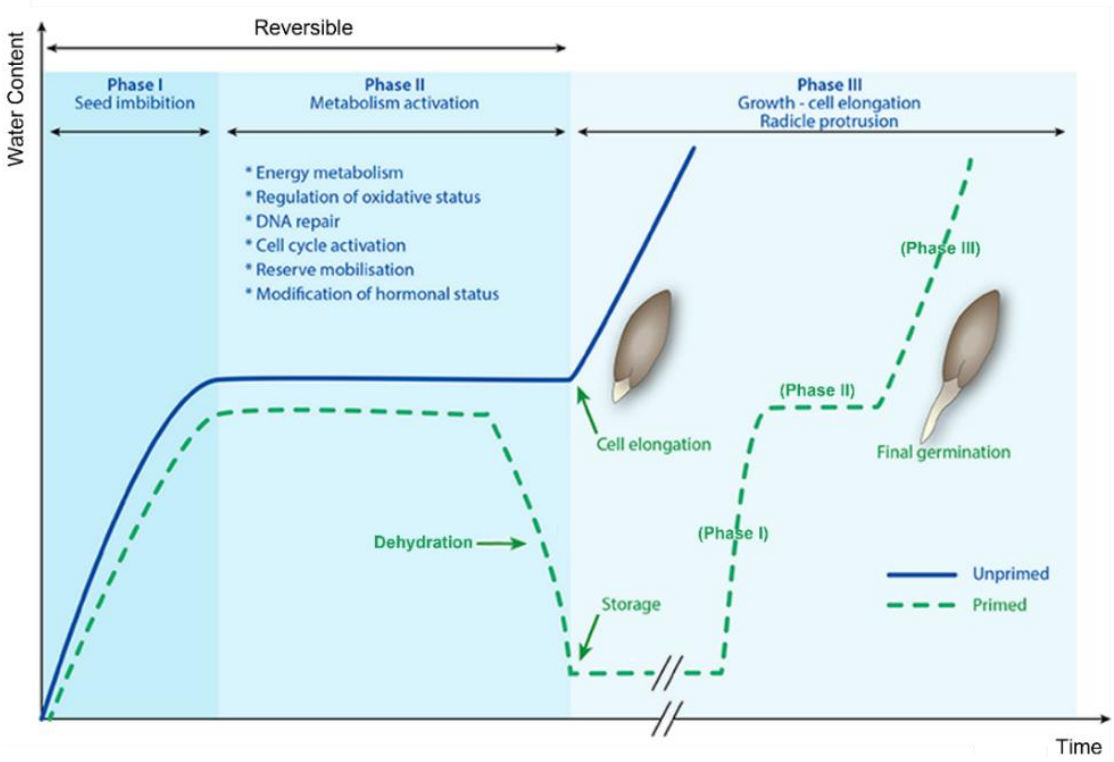

Figure 2.12 – Seed germination phases and hydration curves of both unprimed and primed seeds. Adapted from Lutts et al.[80]

The germinative ability of seeds is not only a genetically controlled character but may also be affected by different external factors. Seed priming techniques take advantage of the metabolism activation achieved during germination phase II, to favour germination and the seeds' ability to withstand exposure to stressful environmental conditions. It consists of the controlled hydration of seeds, which is arrested before the seed transitions into the third germination stage.[79] Different substances can be used as seed priming treatments, including osmotic solutions, mixtures of beneficial live microorganisms, bioactive molecules, plant or microalgal extracts or simply water (hydropriming).[79]

Seeds subjected to priming treatments show faster and more synchronous germination behaviour with plants raised from primed seeds, often showing greater tolerance to abiotic stress and higher yields over

unprimed seeds. Priming treatments concern not only the germinative performance of seeds but the development of the whole plant system, as it provides plants with the ability to react more rapidly and efficiently to abiotic stress conditions. However, the success of seed priming depends on several factors including the chosen priming method, the species and populational genotype, as well as on the viability of the seed lot.[66,79–81]

3. Research Objectives

Under the context of improving the sustainability of our current social-economic model, this thesis was integrated into a collaborative project developed between A4F and a chemical fertilizer production company. The project targets the evaluation of the viability and effectiveness of microalgae-based open systems for the bioremediation and valorisation of the nitrogen-rich effluent derived from their industrial fertilizer production process. The specific goals of this thesis are:

I. To develop an accurate forecast of the annual average biomass productivity and nitrogen removal efficiency, on the location being considered for the implementation of a full-scale production/bioremediation unit; through the analysis of the data acquired from January 2019 to December 2021, considering the impacts of seasonality on the performance of the pilot-scale RWP.

II. To analyse the year-round variations in the microalgal community's genera composition, considering seasonality and identifying the environmental drivers that trigger changes to the community.

III. To evaluate the impact of the ecosystem's dominant microalgal species, on the system's biomass productivity and N removal efficiency;

IV. To preliminarily assess the potential of the microalgal biomass derived from the bioremediation process, for the development of alternative agronomical products; through the elaboration of a seed priming and germination assay, under both optimal and salinity stress incubation conditions.

4. Materials and Methods

4.1. Bioremediation of a N-rich Effluent Derived from Industrial Fertilizer Production

4.1.1. Effluent Characteristics

The IFPP's effluent was sent for elemental analysis in 2019, which revealed a high N concentration in the form of both nitrate and ammonium. The analysis also detected the presence of phosphorous, calcium, magnesium, copper, iron, and zinc, which are essential for microalgal development. However, when present in high amounts, these may be toxic or inhibitory for the growth of some species. This is particularly relevant for copper and zinc, as these elements were detected in higher concentrations than those reported as being toxic for some eutrophic microalgae, such as *Scenedesmus* spp.[82–85]

Table 4.1 – General nitrogen profile of the effluent lots produced in the IFPP from 2019 to 2021 (mean ± SD, *n* = 29) – a.; Nitrogen profile of the effluent lot used throughout the assay (composition determined in 2019) – b.

a. General nitrogen content of the IFPP's effluent		
Nitrate (NO_3^-–N)	Ammonium (NH_4^+–N)	Total Nitrogen
7.70 (± 3.50) g L^{-1} (59%)	5.42 (± 2.75) g L^{-1} (41%)	13.12 (± 5.39) g L^{-1} (100%)
b. Nitrogen content of the effluent lot used from 2019 to 2021		
28.29 g L^{-1} (59%)	19.32 g L^{-1} (41%)	47.61 g L^{-1} (100%)

4.1.2. The Bioreactor – Main Components and Configuration

Figure 4.1 presents the schematic depiction of the RWP installed in the IFPP's industrial, which was used in this assay. It presents a depth of 0.25-0.30 m and a total photosynthetic area of 5 m^2. Its most relevant components and respective importance will be explored bellow.

Paddlewheel

The paddlewheel (Figure 4.1c) is one of the most cost-efficient means of maintaining the continuous circulation and homogenization of the culture.[86] In this case, a single six- bladed paddlewheel, controlled by a Techtop® MS 632-4 B5 motor (Figure 4.1d), homogenises the culture at standard speed to ensure appropriate mixing and recirculation, while minimizing biomass sedimentation and biofilm formation (exact speed undisclosed due to confidentiality).

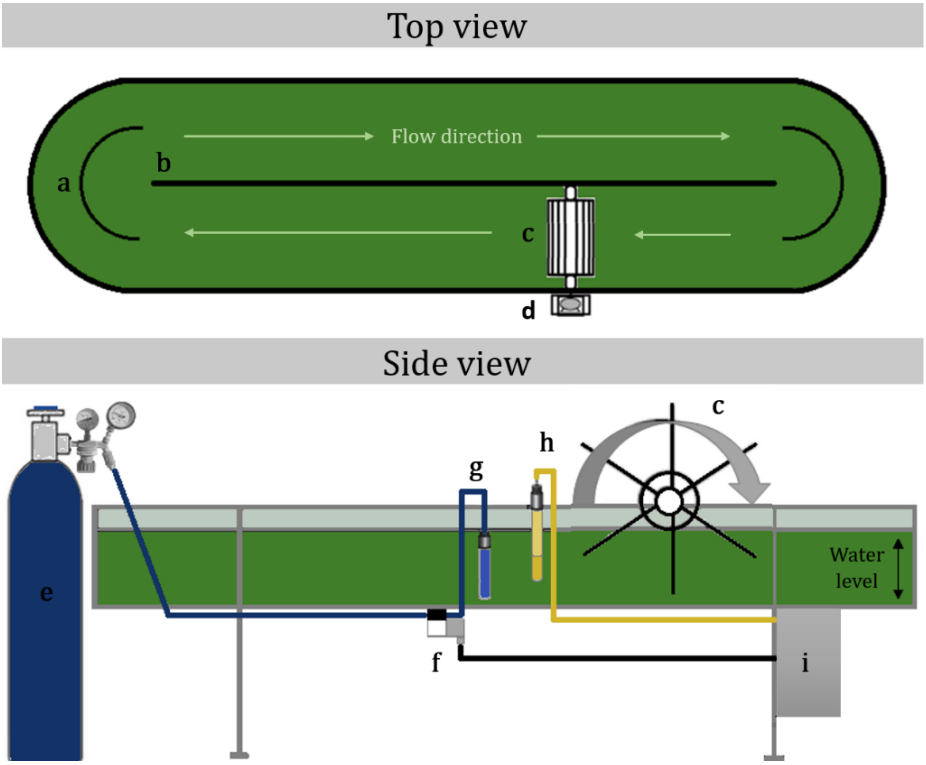

Figure 4.1 – Schematic representation of the RWP installed in the IFPP.

Carbonation Circuit

As CO_2 diffusion between the atmosphere and water cannot satisfy the carbon requirements of high-yielding microalgal production systems[42], and the effluent does not supply the culture with a carbon source, industrial-grade CO_2 is supplemented to the culture media.

The provision of CO_2 is activated in response to the culture's requirements. A sensor (Yokogawa FU20-20-T1-NPT) is submerged into the culture (Figure 4.1h), continuously measuring the system's pH; with the electrovalve (Figure 4.1f) inserted in the carbonation circuit, between the bottle and the diffuser (Figure 4.1g), opening only when the pH exceeds the predetermined setpoint value. As microalgae uptake CO_2 from the system, the culture's pH rises, transgressing the setpoint and activating the overture of the electrovalve, allowing CO_2 to enter the system. Once the culture's pH setpoint is re-established, the electrovalve closes, interrupting CO_2 flux.

Control Panel

The control panel (Figure 4.1i) holds the control apparatuses for the systems installed in the RWP, where the paddlewheel's rotation speed and pH setpoint can be programmed, and the culture's weekly pH and temperature profiles can be examined (Figure 4.2).

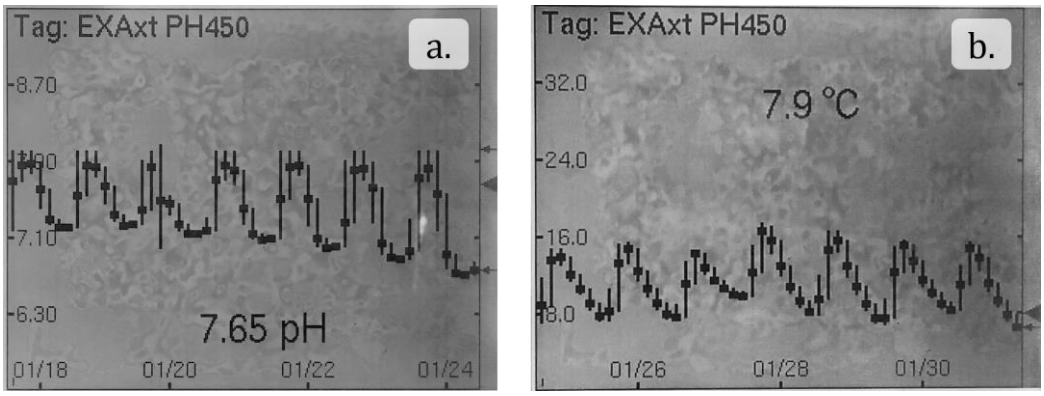

Figure 4.2 – Yokogawa controller's LCD display – (a) pH and (b) temperature graphs.

4.1.3. Overview of the Bioremediation Strategy

The initial process optimization conducted in 2018, revealed that the effluent's high nutrient concentration was unsuitable for microalgae establishment or growth. Freshwater was therefore chosen as the culture medium, with the effluent being used as a nutrient solution, to a final N setpoint concentration of 4.0 (± 1.0) mM.

To ensure the nutritional requirements of microalgae were met, A4F developed a second nutrient solution (NutSupp), to complement the effluent's macro- and micronutrient profile. When combined, the solutions match the composition of the nutrient solution currently used for their industrial-scale microalgae production (composition undisclosed due to confidentiality).

Once the cultivation strategy was outlined, and the spontaneous establishment of a microalgal assortment occurred, the RWP was operated in semi-continuous mode; meaning that after reaching the exponential growth stage, a portion of the culture was discarded to be replaced with freshwater and nutrients (effluent + NutSupp), initiating a new production cycle. The nutrient concentration was controlled through weekly analysis of the medium's N content, and concentrations were re-established in fed-batch mode (further explored in section 4.1.4).

4.1.4. Experimental Design – Standard *In-Situ* Operational Procedures and Culture Maintenance

Being it an outdoor system, exposed to weather fluctuations, some parameters were defined as standard (Table 4.2), being monitored and corrected to maintain culture stability, throughout and among cultivation cycles. The bioreactor was installed in the IFPP, and was monitored one to three times a week, being intervened according to the state of the culture and maintenance requirements. This allowed the assessment of the ecosystem's responses to seasonal environmental fluctuations and its long-term performance.

Table 4.2 – Bioreactor's standard operational parameters.

pH Setpoint	Working Volume	Nitrogen Setpoint
8.0	750 (± 100) L	56.0 (± 14.0) mg L^{-1} (equivalent to 4.0 ± 1.0 mM)

To perform the analysis necessary for the evaluation of the system's performance – state of the microalgal assemblage; biomass growth and nutrient removal efficiency, two samples were collected during each monitorization visit. Before sampling, the culture was homogenized using a scraper, and sampling was conducted in the same area of the RWP, with 0.5 L wide-mouth glass flasks to minimize error. The 1st sample was taken right after culture homogenization, and the 2nd ensuing correction of the working volume and effluent addition.

Analyses were carried out at A4F's laboratory. Operational decisions regarding system renewals and effluent addition were made one week in advance, upon comparison of the analytical results obtained in the two previous weeks (schematic representation in Figure 4.3).

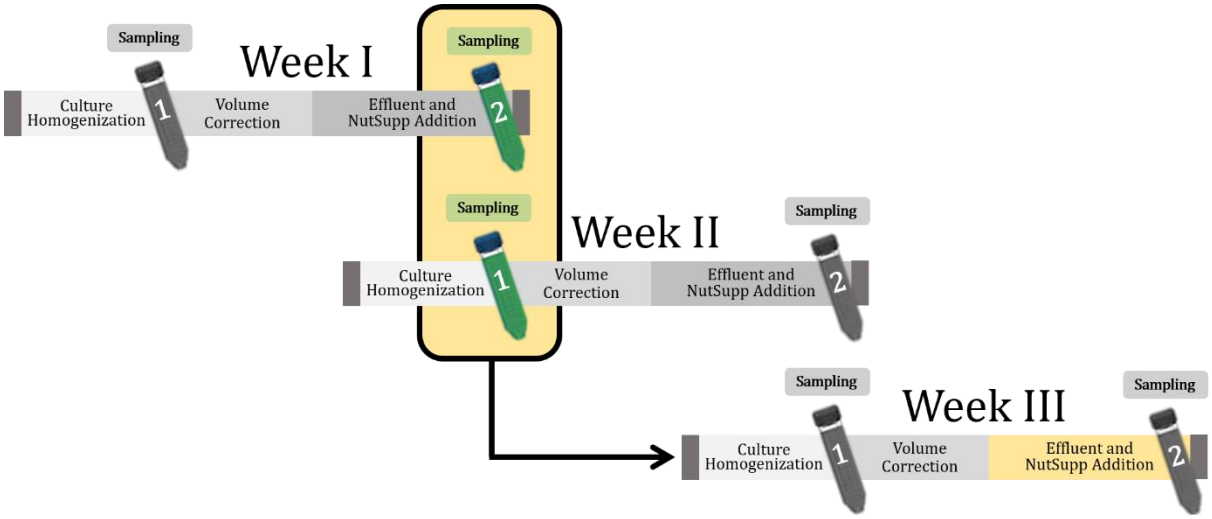

Figure 4.3 – Schematic representation of the strategy behind each week's operational decision-making. The black rectangle marks the samples whose results' comparison determines the amount of NutSupp and effluent that needs to be added in the subsequent week (marked in yellow).

Culture pH and Temperature Monitorization

As described in section 4.1.2, the pH setpoint programmed into the Yokogawa controller was regulated through CO_2 provision according to the system's requirements and was monitored by inspecting the weekly pH profile presented on the Yokogawa's display (Figure 4.2).

Despite 8.0 having been set as the standard pH value for most of this three-year assay, it was sporadically altered according to the assay's objectives' adjustments.

Temperature control followed the same procedure conducted for pH monitorization.

Unexpected deviations, from the predicted pH or temperature profiles, at any given week, were indicative of potential productivity variations; Thus, the importance of monitoring these parameters, for the assessment of the system's behaviour.

Both the pH and temperature profiles were photographed at each monitorization visit, to allow for later analysis.

Culture Volume Management

A volumetric ruler created specifically for this RWP (50 L sensitivity), was used to measure the culture volume. The working volume was seasonally adjusted according to the observed weather conditions. Variations in atmospheric temperature and rainfall, resulted in more or less significant variations in culture volume, having stronger impacts as their significance increased. The culture volume was reset at each visit, through:

I. Freshwater addition – To compensate for water loss derived from evaporation or to re-establish the working volume after system renewals.
II. Culture removal – To counteract water level rise caused by rainfall, or to re-establish the culture volume during renewal procedures.

To conduct these operations, two Ø15 mm hoses (2 and 10 m long); and a flexible impeller pump with a suction lift of 3 m, and a maximum flow of 3000 L h^{-1} were required.

System Renewals

Renewal procedures were conducted before the culture reached the stationary growth stage, as to avoid the decrease in biomass productivity and nutrient removal efficiency, which are characteristic of this stage. These consisted of the removal of a fraction of the culture volume – designated as the renewal rate, which was in this case standardized at 80% of the theoretical working volume (Table 4.2).

As operational decisions were made with a week lag period, upon arrival, the system's actual volume would vary considerably from the theoretical volume, as a result of the weather conditions verified in the week preceding the operation. This meant that the renewal percentage practised, often differed from the standardized 80%; resulting in final biomass and nitrogen concentrations that could slightly vary from the estimated results.

The culture volume and N setpoint were afterwards re-established, through the addition of fresh medium (tap water) and nutrients (effluent + NutSupp). Each renewal intervention dictated the end of the ongoing cultivation cycle and start of the following.

The culture volume removed was occasionally collected for biomass harvesting, although being routinely transferred as waste into an intermediate bulk container that was managed by the IFPP. Despite the removed culture having been discarded throughout this experimental assay, the final goal of the project is to develop an industrial-scale system, in which the produced biomass is harvested to

be further transformed into agronomical products, and the water reintroduced into the production process.

Nitrogen Setpoint

The N-setpoint was adjusted seasonally, considering the culture's final N concentration and its expected N removal rate, which depends on the temperature and radiation conditions verified during each considered month/season. The setpoint was defined at a high enough concentration to sustain microalgae growth amidst visits, but not to cause toxicity or unnecessary effluent disposal during culture volume correction or renewal procedures. Therefore, the effluent volume to be added to the system was determined to offset the N incorporated in the biomass produced within the previous week, considering the theoretic N-content of microalgal biomass (11%)[13], and to re-establish the predetermined setpoint.

4.1.5. Production Cycles Conducted at Different pH Setpoints

To assess the impact of pH on the ecological succession of microalgal species, and their respective productivities, three cultivation cycles were conducted at different pH setpoints – 6.5, 8.0 and 9.5. These cycles were led between May and August of 2021, months which present the highest and most similar daily solar radiation averages, thus minimizing the impact of this parameter on the obtained results. The culture was renewed before the initiation of each cycle, and NaOH or HCl solutions were added to establish the pH setpoints defined for the trial cycles (described in Table 4.3). The system was provided with an adaptation period before data acquisition, and the cycles conducted at pH 6.5 and 9.5, were separated by a month-long pH 8.0 cultivation period, to equate the starting conditions of both cycles.

Table 4.3 – Parameters and duration of the pH cycles, and their establishment procedures.

Cultivation Conditions				pH Establishment	Cycle Duration
Cultivation Cycle	pH Setpoint*	Working Volume (L)	N-Setpoint (mM)		
1	pH 8.0	800	5.0	Renewal	3rd May 2021 – 26th May 2021
2	pH 9.5	800	5.0	Renewal + NaOH to a final concentration of 0.9 mM	1st June 2021 – 14th June 2021
3	pH 6.5	800	5.0	Renewal + HCl to a final concentration of 0.1 mM	26th July 2021 – 14th August 2021

*All pH conditions were maintained by automated CO_2 injection.

4.1.6. Biomass Harvesting and Storage

The biomass produced during the pH trial cycles was harvested by centrifugation using a disc stack centrifuge. An appropriate biomass preservative[5] provided by the IFPP was added to the harvested concentrates, according to the product's specifications. The biomass concentrates were then reserved in appropriate flasks and stored in a freezer at -20ºC, for later assessment of their potential as biostimulants for seed germination (explored in section 4.2).

[5]The preservative's formulation and active ingredient was not disclosed by the company.

4.1.7. Analytical Methods

4.1.7.1. Determination of Biomass Concentration

For Liquid Culture

Microalgae biomass concentration was estimated through dry weight (DW) determinations. The samples were homogenized using a 50 mL syringe to degrade small aggregates and reduce error. A set sample volume (V) was filtered through pre-weighed (m_0) 0.7 µm pore and Ø47 mm microfiber filters, with filtration ramps and a vacuum pump (Feixing XZ-1B). The filters were afterwards dried (m_f) at 180ºC in a moisture analyser (AND MS-70 – 71 g ± 0.1 mg), and the biomass was quantified using equation (4.1:

$$\mathrm{DW}\ (\mathrm{g\ L^{-1}}) = \frac{m_f - m_0}{V} \tag{4.1}$$

Where, m_0: mass of the pre-dried filters (g); m_f: mass of the filters with the filtered biomass after drying (g); V: volume of the filtered culture sample (L).

For Microalgal Paste (or Concentrate)

The biomass concentration of the harvested microalgae paste was assessed through dry weight determination. The paste samples were homogenized, and a pea-size paste portion (≈ 0.5 g) was evenly spread onto the surface of a pre-weighed (m_0) aluminium dish (Ø90 mm), for measurement of its initial fresh weight (m_i). The dish was dried (m_f) at 105ºC in a moisture analyser, and the biomass was quantified using equation (4.2**:**

$$\mathrm{DW}\ (\%) = \frac{(m_f - m_0)}{(m_i - m_0)} \times 100 \tag{4.2}$$

Where m_0: mass of the pre-dried aluminium dishes (g); m_i: mass of the aluminium dish with the fresh paste sample (g); m_f: mass of the aluminium dish with the paste sample after drying (g).

4.1.7.2. Nitrogen Quantification

As the effluent contains N in both the form of nitrate and ammoniacal nitrogen (NH_4^+/NH_3, hereon referred to as NH_4^+-N), the determination of nitrogen concentration required two distinct spectrophotometric analyses.

Samples were prepared using the same method for both nitrate and ammoniacal nitrogen quantification. The culture was centrifuged (HERMLE Z 400) at 3500 rpm for 15 minutes, and the supernatants were collected for analysis.

Nitrate Ion Concentration

The supernatants were diluted with deionized water (DI), and HCl was added to a final concentration of 3% (v/v), to degrade compounds such as carbonate and hydroxide anions, which can interfere with the spectrophotometric reading.

Duplicates were read against DI water at 3% (v/v) HCl, in quartz cuvettes with 1 cm path length using a UV-Vis spectrophotometer (Genesys UV-Vis 10S). Readings were conducted at 220 and 275 nm wavelengths to account for dissolved organic matter present in the samples, as both nitrate and biomolecules (such as aromatic amino acids) absorb at 220 nm. Since only the biomolecules absorb at 275 nm, NO_3^- absorbance was determined by equation (4.3:

$$\text{Abs } NO_3^- = \text{Abs}(220\text{ nm}) - 2 \times \text{Abs}(275\text{ nm}) \quad (4.3)$$

The nitrate absorbance measurements were used for its quantification through a calibration curve developed for a standard potassium nitrate solution.

Ammoniacal Nitrogen Concentration

Samples were diluted using DI water and treated with a commercial ammoniacal nitrogen content determination kit (Sera). Quadruplicates were read against DI water with the kit's reagents, in 96-well plates, using a UV-Vis spectrophotometer (BMG Labtech, SPECTROstar nano) at 690 nm.

The absorption readings allowed ammoniacal nitrogen quantification, through the use of a calibration curve, developed for a standard ammonium nitrate solution.

The measurement of ammoniacal nitrogen concentration was implemented in December 2019.

4.1.7.3. Microscopic Analysis

The ecosystem's species assemblage was evaluated after each monitorization visit, with the collected samples being analysed under a microscope (Olympus BX53) at a magnification range of 100 to 800x. Cell measurements were conducted using a calibrated eye graticule, allowing microalgae to be identified to genus level based on the taxonomic descriptions of Bellinger and Sigee[53] and associated literature.

The consortium's microbial composition was estimated after observation of several lamellae preparations, following a qualitative rating approach. Both protozoan and microalgal microorganisms were rated from one to five, according to their relative abundance: 1 – present in trace amounts, 2 – rare, 3 – few, 4 – common, and 5 – abundant. The most dominant microalgae genus was distinguished, being marked with the number seven.

For data treatment purposes, the protozoans' scores were summed according to their corresponding phylum (e.g., Rotifera, Ciliophora or Amoebozoa), providing a relative measure of their populational density, inside the ecosystem, at the time of sampling.

Microorganisms' behavioural and stress indicators were noted, to allow the association between external factors and alterations in the ecosystem's ecology.

The ecosystem's microbiological assessment was only thoroughly monitored throughout 2021. Hence, the seasonal dynamics of the microalgal assemblage cannot be compared to the previous years of this experiment.

4.1.7.4. System's Behaviour and Performance Indicators

Total Biomass Produced

The total biomass production verified between monitorization visits, was determined using equation (4.4, which considers the culture volume measured at the time of sampling (V_{RWP}), and the sample's DW:

$$\text{Total Biomass Produced (g)} = (DW \times V_{RWP})_b - (DW \times V_{RWP})_a \quad (4.4)$$

Where $(DW \times V_{RWP})_b$ represents the total biomass (g) that was present in the bioreactor upon arrival on week II – cultivation day *b*; and $(DW \times V_{RWP})_a$ the total biomass, present in the bioreactor after being intervened in week I – cultivation day *a*, (schematic representation shown in Figure 4.3).

Areal Biomass Productivity

The areal biomass productivity was evaluated weekly, after applying the following equation:

$$\text{Weekly Areal Biomass Productivity } (g\,m^{-2}\,day^{-1}) = \frac{DW_b - DW_a}{b - a} \quad (4.5)$$

Where DW_a and DW_b represent the biomass concentration results derived from equation (4.1 (section 4.1.7.1), expressed in g m^{-2}, for the sample taken after intervention in week I, and the sample taken before intervention in week II – cultivation days a and b, respectively (schematic representation shown in Figure 4.3). The monthly areal productivity was later determined by the sum of the weekly productivities calculated.

Total Nitrogen Removal and Areal Nitrogen Removal Rate

To determine the total nitrogen removal, and N removal efficiency among monitorization visits, the same equations used for biomass evaluation were employed; equations (4.4 and (4.5 respectively. However, as nitrogen consumption occurs in both the form of nitrate and ammoniacal nitrogen, the sum of both nitrogen ions' quantification must be applied in place of the DW parameters included in the equations.

Radiation, Temperature and Photoperiod Data Acquisition

Local weather patterns were followed from 2019 to 2021, through *In-situ* temperature and radiation measurements were taken at 15-minute intervals, by a nearby weather probe. Monthly photoperiod data was acquired from Weather Spark.[87]

4.1.7.5. Statistical Analysis

Correlation Between Parameters

The correlation between variables was calculated using RStudio Version 4.1.2. Pearson product-moment correlations (r) were used to compare continuous variables (i.e., temperature, solar radiation, nutrients and biomass concentrations), while Spearman's rank correlation coefficients (r_s) were used for comparison between discontinuous, as well as between continuous and discontinuous variables (microorganisms' relative abundance).

For both cases, the value of r varies between negative and positive one; $|r| = 1$ represents perfectly correlated variables, while $|r| = 0$ is indicative of uncorrelated variables. Positive and negative r values, respectively imply a direct and inverse relationship between the considered variables.

To assess the existence of an association between the ecosystem's biomass productivity and N removal rates, with either the regional temperature or radiation patterns, cultivation cycles where operational problems occurred, were excluded from the dataset (e.g., cycles with equipment failure – CO_2 addition system or paddlewheel; or where culture renewal was extensively delayed, resulting in overconcentration of biomass and ultimately self-shading).

4.2. Assessment of the Biomass' Potential as an MBS for Seed Priming

To assess the potential of the microalgal biomass derived from the bioremediation of the IFPP's effluent, for the development of agronomical biostimulant products, the biomass batches derived from the trial pH cultivation cycles (described in section 4.1.5) were processed and applied as priming solutions to commercial rice seeds. The latter were evaluated for susceptibility to salinity stress (at 0, 80 and 160 mM of NaCl), when unprimed, after priming with the microalgal treatments, and with DI water. Seed germination was followed for 10 days, and the obtained seedlings were morphologically assessed on the 12th incubation day.

4.2.1. Biological Material

Rice Seeds – *Oryza sativa* L. cultivar Japonica

Commercial *Oryza sativa* L. cultivar Japonica (variety Euro) seeds were acquired from Aparroz (Figure 4.4). This variety was chosen as it belongs to the carolino rice cultivars, one of the most cultivated varieties in Portugal. The seeds used belonged to the same monovarietal lot and arrived with the fungicidal pre-treatment that is standardly applied to all the company's dried seeds, as to avoid early developmental diseases. The composition of the applied fungicidal treatment was not disclosed by the company.

Figure 4.4 – *Oryza sativa* L. cultivar. Japonica seeds.

The seed lot was visually inspected, and seeds were selected according to their size and morphology. Seeds with smaller sizes, presenting deformities or visual signs of fungal contamination were excluded.

Microalgal Extracts

The three microalgae concentrates were taken from the freezer and placed in a fridge at 4°C to thaw. Subsequently, to release the microalgae's intracellular contents and produce compositionally homogeneous extracts, the different lots were separately processed in a laboratory-scale High-Pressure Homogenizer (GEA Lab Homogenizer PandaPLUS 2000) – Figure 4.5.

Figure 4.5 – High-pressure homogenization process (GEA Lab Homogenizer PandaPLUS 2000).

The biomass concentrates had a DW concentration of 50 g L^{-1}, and the goal was to produce priming solutions with a final concentration of 50 and 25 g_{DW} L^{-1}, according to application concentrations described by Garcia-Gonzales and Sommerfeld.[61] However, the rheological properties of the concentrates were causing the homogenizer's circuit to preclude, requiring the dilution of the concentrates to a final DW concentration of 30 g L^{-1}. After 3 milling cycles at a flow rate of 150 mL min^{-1} and 60 (± 5) MPa, the extracts presented a homogeneous microscopical appearance with complete cell lysis and were therefore bottled and stored at 4°C for later use.

Microalgal Priming Solutions

The three microalgal extracts attained were tested as priming solution, at three different concentrations each – 30, 15 and 5 g_{DW} L^{-1}, being diluted with DI water just before application.

4.2.2. Experimental Design

Tree replicates were used to test the different priming treatments and incubation conditions, each being composed of a group of ten equally prepared seeds. The experimental conditions are presented in Table 4.4. A nomenclature key was attributed to each incubation condition and treatment applied – Table 4.5.

Table 4.4 – Summary table for the number of replicates used to assess the effects of each incubation condition, and priming treatments applied. Conditions used as control are marked with an asterisk.

Salinity Stress Condition – [NaCl]	Biomass Extract n°1 (g_{DW} L^{-1})			Biomass Extract n°2 (g_{DW} L^{-1})			Biomass Extract n°3 (g_{DW} L^{-1})			Hydropriming*	No Priming*
	5	**15**	**30**	**5**	**15**	**30**	**5**	**15**	**30**	–	–
0 mM*	3	3	3	3	3	3	3	3	3	3	3
80 mM	3	3	3	3	3	3	3	3	3	3	3
160 mM	3	3	3	3	3	3	3	3	3	3	3
Total Seed Count	990										

Table 4.5 – Abbreviation key used for the priming treatment and incubation conditions of the seed priming assay.

Code	Definition
B1	Biomass extract n°1.
B2	Biomass extract n°2.
B3	Biomass extract n°3.
$C_{5g/L}$	Extract concentration of 5 g_{DW} L^{-1}.
$C_{15g/L}$	Extract concentration of 15 g_{DW} L^{-1}.
$C_{30g/L}$	Extract concentration of 30 g_{DW} L^{-1}.
B1_ $C_{5g/L}$	Biomass extract n°1 at 5 g_{DW} L^{-1}.
B1_ $C_{15g/L}$	Biomass extract n°1 at 15 g_{DW} L^{-1}.
B1_ $C_{30g/L}$	Biomass extract n°1 at 30 g_{DW} L^{-1}.
B2_ $C_{5g/L}$	Biomass extract n°2 at 5 g_{DW} L^{-1}.
B2_ $C_{15g/L}$	Biomass extract n°2 at 15 g_{DW} L^{-1}.
B2_ $C_{30g/L}$	Biomass extract n°2 at 30 g_{DW} L^{-1}.
B3_ $C_{5g/L}$	Biomass extract n°3 at 5 g_{DW} L^{-1}.
B3_ $C_{15g/L}$	Biomass extract n°3 at 15 g_{DW} L^{-1}.
B3_ $C_{30g/L}$	Biomass extract n°3 at 30 g_{DW} L^{-1}.
$[NaCl]_{0mM}$	Incubation under optimal conditions, no salinity.
$[NaCl]_{80mM}$	Incubation under moderate salinity stress, at [NaCl] = 80 mM.
$[NaCl]_{160mM}$	Incubation under high salinity stress, at [NaCl] = 160 mM.

Seed-Surface Disinfection and Priming

The un-hulled seeds were manipulated in a laminar flow chamber (Teslar® Bio II Advance Plus, Class II) using either autoclaved or disinfected materials, to reduce the risk of introducing microorganisms foreign to the priming solutions at study. To achieve surface sterilization the seeds were soaked in an ethanol 70% (v/v) solution for 5 min, rinsed 5 times with autoclaved DI water and embedded in a 2%

(v/v) commercial bleach solution for an additional 5 min, which was finally removed through eight washes with autoclaved DI water.

The seeds were hand-dried with paper towels, and distributed in 24-well plates, with each well containing four seeds and 1 mL of the respective priming solution. The plates were placed in an orbital incubator at 25 (± 0.5)°C and 80 rpm in the dark for 24 hours. Following the 24-hour priming (soaking) period, the seeds were removed from the wells and separated according to the priming treatment applied. Paper towels were used to pat-off the excess biomass, and the seeds were placed in sterile Ø90 mm Petri dishes, which were placed back in the orbital incubator at 25 (± 0.5)°C and 0 rpm in the dark for a 24-hour drying period.

Incubation Conditions

The germination assay included the top-of-paper germination strategy as described by Biodiversity International.[88] Sterile Petri dishes were lined with two layers of previously cut and autoclaved 100% cellulose coffee filters, which were soaked with 3 mL of the designated autoclaved incubation solution (DI water at 0 mM; 80 mM and 160 mM of NaCl). The plates' lids were secured with two trips of 3M micropore paper tape and placed in the orbital incubator in the dark at 25 (± 0.5)°C and 0 rpm agitation.

4.2.3. Evaluation of the Seeds Germinative and Early Developmental Performance

4.2.3.1. Germination

Despite the 14-day incubation period proposed for rice germination assays[88]; due to time constraints, germination parameters were only monitored until the 10th incubation day. Plates were checked at 24-hour intervals, to assess the number of germinated seeds. Germination was considered successful once 2 mm of either the radicle or shoot had emerged, as suggested by Biodiversity International.[88]

4.2.3.2. Seedlings' Morphological Evaluation

Seedling Root and Shoot Length Measurements

On the 12th day, the plates were removed from the orbital incubator and seedlings were placed on top of a dark surface, covered with a glass slide and photographed for later measurement of the longest root and shoot lengths, using ImageJ Version 1.53n (Figure 4.6). A ruler was included in all photographs for size referencing. Measurements were taken for all seedlings.

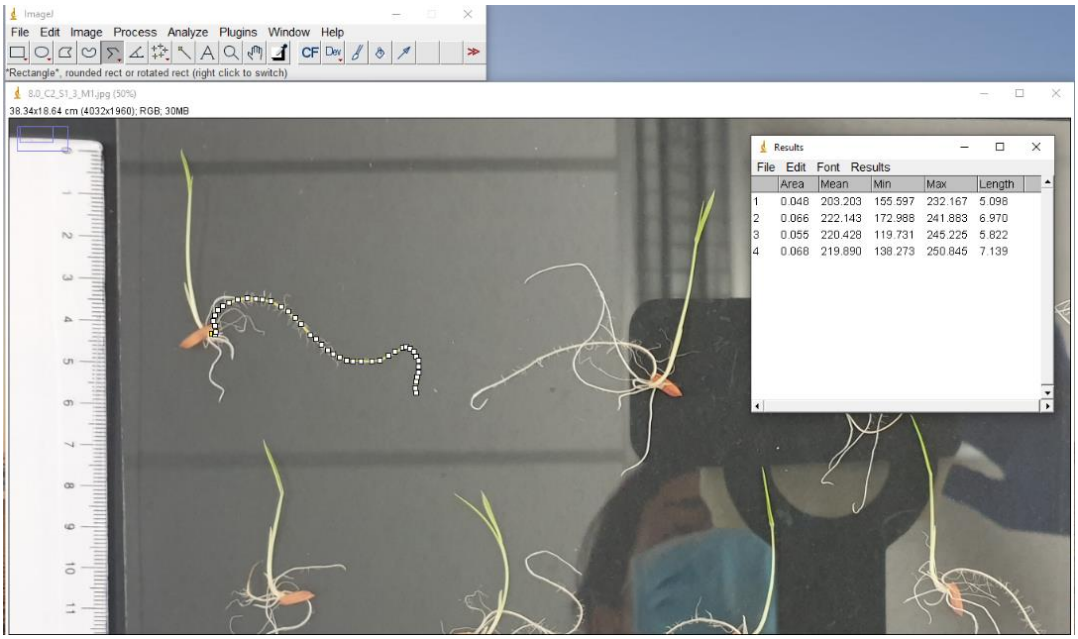

Figure 4.6 – Length measurements on ImageJ.

Regarding measurements of the shoot length, it is important to mention that in cases where the leaf blade was the only organ present above the seedling collar (Figure 4.7a); the collar was considered the upper limit for height measurements. On the other hand, when seedlings presented growth past the collar (Figure 4.7b), the highest point verified excluding the leaf blade was used as the upper limit for height measurement.

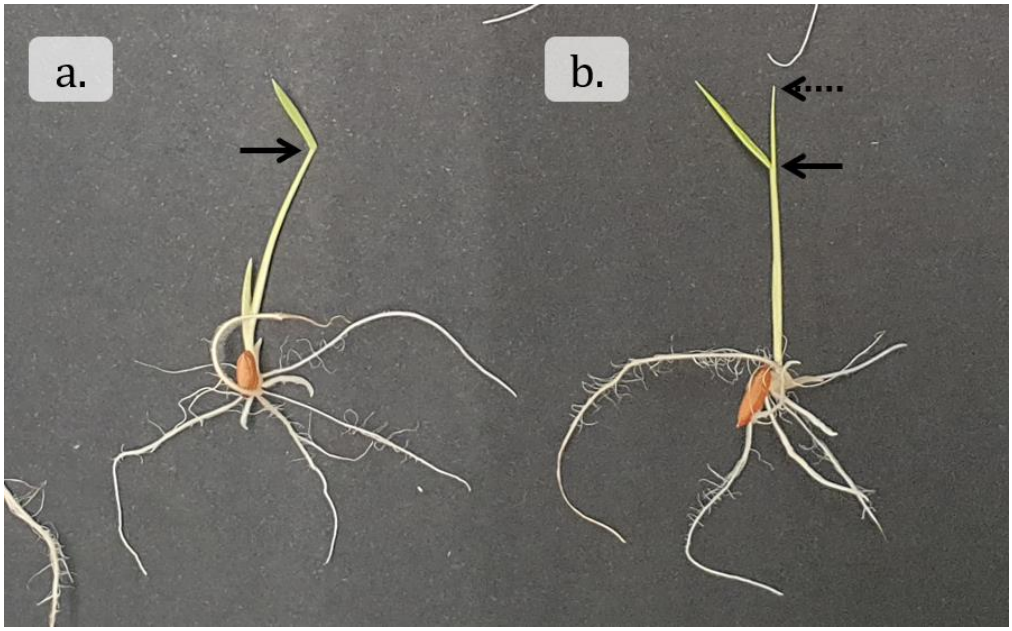

Figure 4.7 – Indication of the upper limit established for measurement of the shoot length. Where, → indicated the location of the seedling collar, where the highest measurement was taken when no growth was verified past this structure (a); ⋯→ represents the location of the highest measurement for seedlings presenting leaf growth past the collar (b).

Seedling Dry Weight Determination

For each seedling, both the root system and shoot were excised from the seed structure using a scalpel. The excised shoots and root systems of each of the replicate's seedlings were compiled and placed in separate pre-dried and weighed paper bags, for oven drying – 48 hours at 70 (± 1)ºC. After the time elapsed, the bags were placed in the desiccator until second weight measurements were taken on an analytical scale (OHAUS PIONEER, PA114C – 110.0 g ± 0.1 mg).

Seedlings whose size noticeably differed compared to the remaining seedlings of the same replicate were placed in individual paper bags for separate weighing. If the weight measurements for these seedlings were close to the average DW of its corresponding group (considering a 10% error), it was included in the replicate's weight; otherwise, these individuals were considered to be morphological outliers and were not included in the statistical analysis.

4.2.4. Analytical Methods

4.2.4.1. Germination and Early Developmental Performance Indicators

Final Germination Percentage (FGP)

Is an indication of the viability of the seed population represented by the sample tested, as well as its germinability under the incubation conditions applied.[61]

$$\mathrm{FGP}\ (\%) = \frac{\mathrm{n}}{\mathrm{N}} \times 100 \tag{4.6}$$

Where n represents the total number of seeds germinated at the end of the assay and N is the total number of seeds used.

Mean Germination Time (MGT)

Was proposed by Edmond and Drapala[89], and consists of a measurement of the mean length of time required for maximum germination of a seed lot under the experimental conditions applied.[90]

$$\mathrm{MGT}\ (\mathrm{days}) = \frac{\sum_{\mathrm{i}=1}^{\mathrm{k}} \mathrm{n_i} \times \mathrm{T}_i}{\mathrm{n}} \tag{4.7}$$

Where k is the duration of the germination assay, $\mathrm{T_i}$ is the time taken from the start of the experiment to the $\mathrm{i^{th}}$ incubation day, $\mathrm{n_i}$ is the number of newly germinated seeds on the $\mathrm{i^{th}}$ day, and n represents the total number of seeds germinated at the end of the assay.

Germination Index (GI)

The germination index proposed by Melville et al.[91], describes the relationship between germination percentage and spread. The formula attributes maximum weight to the seeds germinated on the first incubation day, and gradually decreasing importance to those germinated on subsequent days. A higher GI value denotes a higher percentage and germination rate.[90,92]

$$\mathrm{GI} = \frac{\sum_{\mathrm{i}=1}^{\mathrm{k}} [\left((\mathrm{k}+1) - \mathrm{T_i}\right) n_i]}{\mathrm{FGP}} \tag{4.8}$$

Where k is the duration of the germination assay, $\mathrm{T_i}$ is the time taken from the start of the experiment to the $\mathrm{i^{th}}$ incubation day, and $\mathrm{n_i}$ is the number of newly germinated seeds on the $\mathrm{i^{th}}$ day.

Seedling Vigour Index (SVI)

As proposed by Abdul-Baki and Anderson[93], seedling vigour provides an indication of the seedling's performance and resilience under the incubation conditions it is exposed to. Higher SVI values are indicative of more vigorous seedlings.

$$\text{SVI} = \text{Total Seedling Length} \times \text{FGP} \tag{4.9}$$

4.2.4.2. Statistical Analysis

The statistical analysis was performed using RStudio Version 4.1.2.[94] A two-way analysis of variance (ANOVA), was used to determine differences among the groups' means; followed by the *Post-Hoc* assessment for significant differences between the priming treatments and incubation conditions, via Tukey's range test (Shoot and Root's DW). Data which did not initially satisfy the ANOVA's assumptions were subjected to arcsine transformation before the analysis (GI and SVI). Those which did not meet the assumptions even after mathematical transformations were assessed via the Kruskal-Wallis evaluation of medians, with *Post-Hoc* analysis conducted through Dunn's test with Holm correction (FGP, MGT, Seedling DW, Seedling Length, Longest Root, Seedling Height). The level of significance was set at $p < 0.05$, for all the statistic tests conducted. The data is expressed by the groups' means ± standard deviation.

5. Results and Discussion

5.1. Bioremediation of a N-rich Effluent Derived from Industrial Fertilizer Production

5.1.1. Experimental Site and Environmental Variables

Impact of Seasonality on the Performance of Open Systems

In outdoor microalgae production systems, seasonal variations in radiation intensity, photoperiod, and environmental temperature, significantly impact the annual productivity and economic feasibility of large-scale operations.[13] As these parameters are unique to every location and cannot be controlled, it is important to study and recognize patterns within the geographical area of interest before the implementation of any production unit. In this sense, this section presents an analysis of the data acquired from 2019 to 2021, for the pilot-scale RWP installed in the IFPP's premises, as to assess the system's seasonal behaviour and establish a forecast of its performance.

The practical component of this thesis included the operation of the RWP from November 2020 to December 2021, however, data from the two previous years were included in this analysis to allow a more robust assessment. Three main parameters were considered in this analysis: N removal, biomass productivity and the evolution of the ecosystem's microalgal assortment.

Impacts of Environmental Temperature and Incident Radiation on the System's Productivity

Throughout the three years analysed, the system's average annual biomass productivity curve generally followed the trend of both the average environmental temperature and solar radiation curves, with greater proximity to the shape of the solar radiation (Figure 5.1). The Pearson product-moment correlations conducted for the weather data acquired in this period, corroborate this observation, showing a slightly stronger link between biomass productivity and solar radiation ($r = 0.61; p = 1.91 \times 10^{-14}$), compared to that of biomass productivity and environmental temperature ($r = 0.53; p = 5.63 \times 10^{-11}$). This was expected, not only due to the photosynthetic nature of microalgae, which greatly depends on light quality and intensity but also because the temperature data used in the correlation, corresponds to environmental temperature, rather than to culture medium temperature. Culture medium temperature increases mainly due to the absorption of heat derived from incident radiation[95], which in turn is influenced by radiation intensity and nebulosity. It is thus very different to evaluate the performance of open systems in response to each of these two temperature parameters, as the former is not necessarily a direct indication of the latter.[101] Accordingly, environmental temperature might not be the most appropriate parameter to assess the performance of these systems.

Nonetheless, despite microalgal health and ecosystem dynamics being substantially affected by culture temperature, different species present distinct sensitivities to temperature fluctuations, with some being tolerant to broader variation ranges.[96] In this case, as an open bioreactor with an ecosystem derived from spontaneous colonization of endogenous microalgae, it is expectable that seasonal variations in both environmental and culture temperatures would promote the establishment of other local species,

as the environment becomes less favourable for the microalgae species dominating at any specific time of the year (temporal ecological succession). This behaviour also supports the lesser impact of environmental temperature on biomass productivity, as the surrounding ecological environment provides the system with the ability to respond to temperature variations, thus not significantly impacting the overall biomass outputs.

Contrarily to what was verified for biomass productivity, the average N removal rate showed a stronger link with environmental temperature ($r = 0.65; p = 1.11 \times 10^{-7}$) compared to solar radiation ($r = 0.60; p = 1.16 \times 10^{-6}$). Additionally, N removal strongly correlated with biomass productivity ($r = 0.68; p = 9.59 \times 10^{-9}$), likely as a result of its constitutive role in all structural and functional proteins of cells, with its incorporation being fundamental for microalgal growth.[14]

Figure 5.1 presents a summary of the productivity results obtained during the 36 months of this assay. However, important considerations regarding this graphical representation and analysis are disclosed in section 5.1.2.

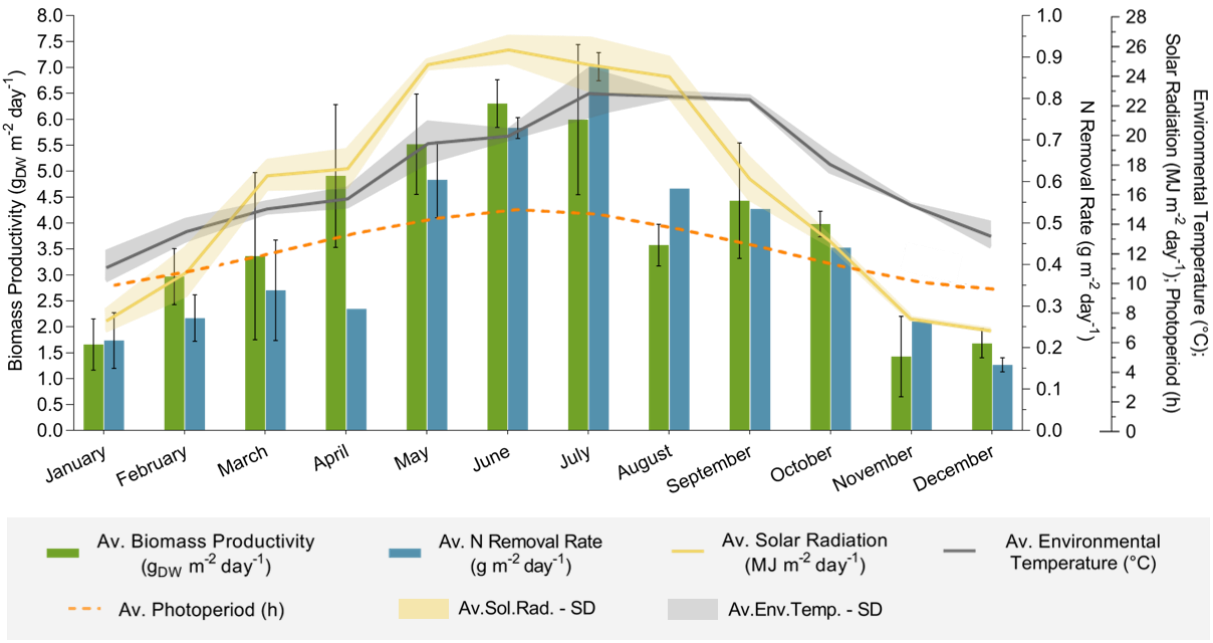

Figure 5.1 – Summary of the system's performance from January 2019 to December 2021. The error bars represent the SD for the average values verified for each parameter in the months evaluated.

5.1.2. Considerations for the Analysis of the System's Seasonal Performance

To establish an accurate representation of the system's seasonal behaviour, data attained for months where unexpected events or external conditions majorly impacted the state or performance of the ecosystem, were excluded from the dataset analysed (Figure 5.1). Hence, Figure 5.2 presents a timeline indicative of the available data, followed by a discussion about which were disregarded and why.

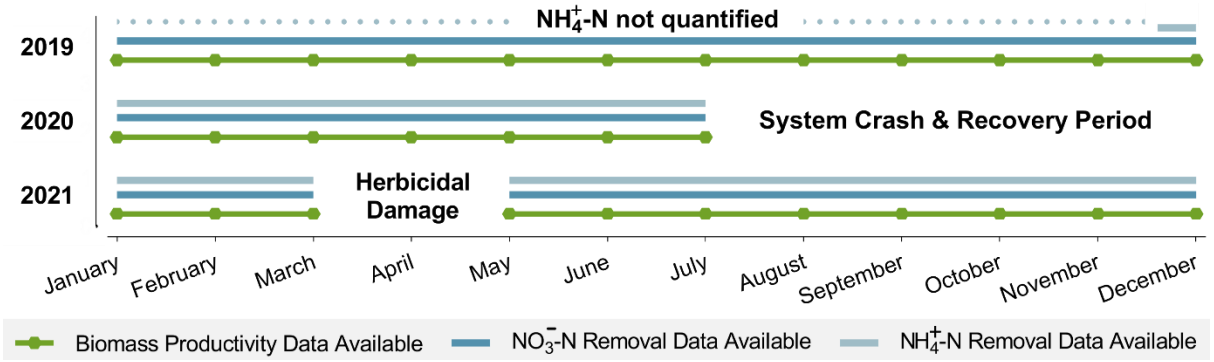

Figure 5.2 – Chronological representation of the data included in the analysis of the system's performance. Months for which data was analysed are represented by a continuous line; months for which data is unavailable are represented by an intermittent line, and months excluded from the dataset present no line. Temperature and radiation data are available for the 3 years.

Excluded Data

2019 – NH_4^+–N only started being quantified in December 2019; thereby, the total N removal rates presented in Figure 5.1, from January to March and May to July, derive from averaging the data acquired in 2020 and 2021. Conversely, April's N removal results correspond solely to the outputs of 2020; and those presented from August to November to 2021's outputs.

2020 – Precautionary measures implemented in response to the COVID-19 pandemic, restricted access to the IFPP, hindering the proper maintenance of the system and ultimately causing the culture to crash in August 2020. The bioreactor remained inoperative until November of that same year, and after reestablishment, it underwent an adaptation period of two months, during which performance was not representative of the settled ecosystem. Consequently, productivity results obtained during this period were excluded from the graphical summary and analysis.

2021 – At the beginning of April 2021, the culture suffered a gradual change in its macroscopical appearance, with a significant increase in biomass agglomeration and discolouration, resulting from the accumulation of dead cells, organic debris, and an increase in micro-grazer abundance. Simultaneously, the proportion of insects and larvae increased along the bioreactor's margins, indicating the poor state of the ecosystem. The system's biomass productivity and N removal, significantly decreased over 10 days, followed by biomass loss. The culture recovered after several interventions for the removal of biomass clusters and partial system renewals. However, since this month's results were considerably affected, these were excluded from the analysis.

It was later found that in the area surrounding the bioreactor, herbicidal applications are conducted triannually and that one of these took place in the week preceding this event. It is thus likely that the culture was contaminated and affected by the product.

Coincidently, and despite no previous report of such an event, a drastic yield reduction was verified in March 2020. If herbicidal applications take place at around the same period each year, this might have

been the cause behind the observed productivity decrease. However, as this assumption was not confirmed, the data acquired in March 2020 were included in the analysis.

5.1.2.1. Factors that Likely Contributed Towards the System's Monthly Results Variability

Despite the environmental conditions having remained similar throughout the three years of this assay, and productivity being strongly correlated with solar radiation; the system's monthly performance results present some variability (Figure 5.1). The outputs of open production systems are expected to fluctuate; however, it is important to identify and discuss inherent and extrinsic factors that might have influenced the results obtained for this particular system.

Firstly, as a significant portion of the data was excluded from the analysis (Figure 5.2), the sample size available for each parameter differed for each of the 12 months evaluated. This ultimately increased the variability of the monthly averages calculated for smaller datasets, due to the inverse mathematical relationship between sample size and variability.[97] Along with the problems listed in section 5.1.2, other aspects might have contributed towards the observed variability:

I. Placement and Conditions Surrounding the RWP

Activities led at the industrial site, have influenced the system's performance on several occasions, as the site is not always managed towards the protection of the RWP. The before mentioned herbicide applications are one example, but throughout the years, countless other activities took place at the site of this experiment. The installation of temporary fences, and placement of large construction machines and materials near the bioreactor, may have led to the temporary reduction of the photosynthetic area, inevitably causing a decrease in the culture's productivity potential (exemplified in Figure 5.3c and d).

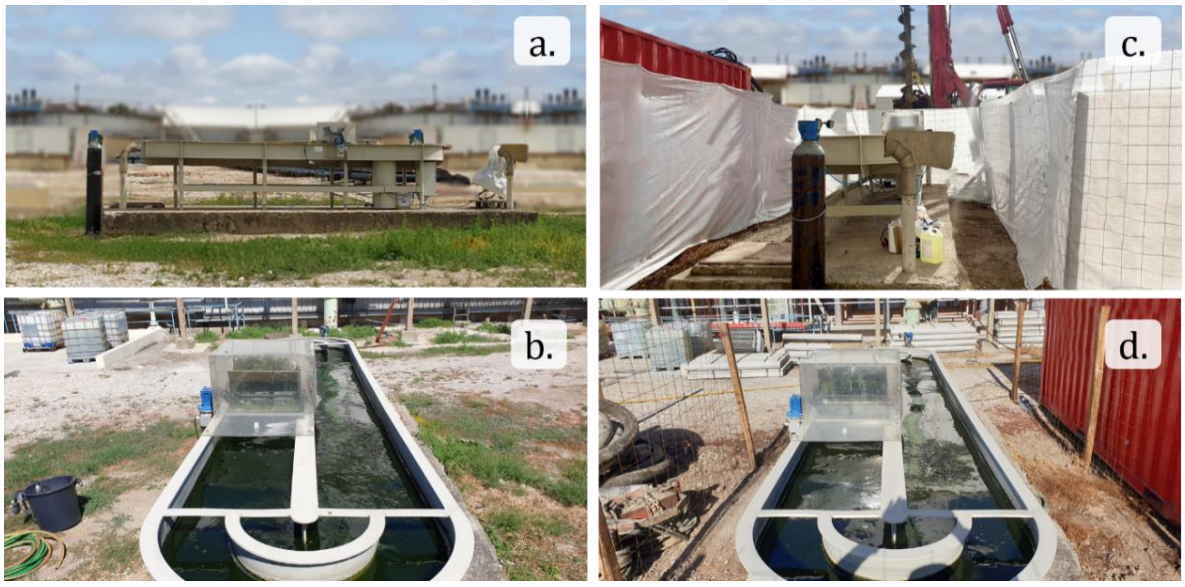

Figure 5.3 – Raceway used for this assay. Photographs a. and b. represent the typical disposition of the bioreactor in the industrial site. Photographs c. and d. were taken in September 2021, when construction work was initiated and is still ongoing.

II. Biological Factors

Open cultivation systems are susceptible to biological contamination, with organisms ranging from macroscopic insects to microscopic and unsought microalgal species, herbivorous zooplankton as well as fungi and bacteria. Grazing can greatly reduce biomass yields, cause crop loss, and in extreme cases, lead to culture crash; threatening the profitability of the production process.[38,95,98–100] As previously referred, the ecosystem's macro- and microorganisms, were mostly monitored in 2021, thus it is not possible to assess the overall impact of biological contamination on the system's productivity throughout the three years. Additionally, for 2021, no significant correlation was verified between the presence of macro- and micro-grazers and the system's performance. Although for valid conclusions to be drawn, this parameter should be followed for several years, as to unveil the influence of endogenous species; in the ecosystem's yearly ecology and performance.

III. Equipment Malfunctions

As this system was maintained by different employees throughout the years, important information regarding the state of the culture and operational problems verified, ended up getting lost; making it impossible to identify all the factors that may have influenced its performance from 2019 to 2020. However, malfunctions in the carbonation circuit were reported for several of the months that presented unusually low productivity results. These usually lead to abrupt changes to the culture's pH, disrupting the ecosystem and ultimately causing a decline in monthly productivity.

IV. Frequency of Intervention and Effluent Addition

Following the previous point, despite the system having been mostly operated according to the experimental design and setpoint parameters specified in sections 4.1.3 and 4.1.4, the frequency of intervention, and consequently of nutrient addition, varied slightly throughout the assay. Additionally, as the volume of effluent required to maintain the established N setpoint was calculated with a one-week lag period (Figure 4.3), in weeks when productivity unexpectedly increased, the system may have been deprived of N, limiting biomass productivity and N removal rate.

5.1.2.2. Nitrogen Removal Behaviour

Ammoniacal nitrogen is the preferential N source for microalgae since the metabolic cost to reduce NH_4^+–N to organic matter is lower than to reduce other N forms.[13] As the effluent contained a lower NH_4^+–N concentration compared to that of NO_3^-–N (Table 4.1), NH_4^+ was often depleted within the first days after supplementation, leaving microalgae with NO_3^- as their only nitrogen source until the following intervention. Consequently, either NO_3^-–N removal surpassed that of NH_4^+–N or both were proportionately removed. This dynamic was strongly dependent on the supplementation frequency and the N setpoint in effect. If effluent was added with enough frequency to sustain NH_4^+–N availability, amidst interventions, NH_4^+ was likely to be removed in greater amount. This was especially true during

summer months, when the N setpoint was higher, as the presence of NH_4^+ has been verified to suppress the expression of genes involved in the nitrate assimilation pathway, up until a given inferior concentration limit, which varies depending on the considered species.[101–105]

The N removal results obtained for June of both 2020 and 2021, clearly showcase the impact of supplementation frequency, on the system's N removal behaviour and selectiveness between NH_4^+ and NO_3^- (Table 5.1).

Table 5.1 – Environmental and operational conditions verified in June 2020 and 2021 with the respective productivity results obtained. Environmental parameters are represented by mean ± SD, with *n* = 30 for both years.

Environmental and Operational Conditions				
June	Average Solar Radiation (MJ m^{-2} day^{-1})	Average Environmental Temperature (°C)	Nitrogen Setpoint	N° of Interventions & Effluent Supplementation
2020	25.8 (± 4.3)	20.2 (± 1.8)	56 mg L^{-1} (4 mM)	3 (2 Production Cycles)
2021	26.5 (± 5.7)	19.9 (± 2.0)	70 mg L^{-1} (5 mM)	8 (3 Production Cycles)
Total Effluent Supplementation				
June	Added Volume (L)	N Equivalent (g)*****	NO_3^-–N Equivalent (g)*****	NH_4^+–N Equivalent (g)*****
2020	2.7	127	75	52
2021	3.0	143	85	58
Obtained Results				
June	Total N Removed (g)	NO_3^-–N Removed (g)	NH_4^+–N Removed (g)	Biomass Produced (kg)
2020	105.7 **(83.3%)**▪	76.1 **(72.0%)**□	29.6 **(28.0%)**□	0.9
2021	113.1 **(79.2%)**▪	61.0 **(53.9%)**□	52.1 **(46.1%)**□	0.9

*****Approximate theoretical values, calculated based on the effluent composition determined in 2019 (Table 4.1b), slight variations in the elements' proportions might have occurred throughout the assay. ▪Removal percentage regarding the total N supplied to the system in the respective month and year. □Removal percentage regarding the total N removed for the respective month and year.

For both years the environmental conditions were analogous: same photoperiod (≈ 14:50 hours), similar daily solar radiation average (25.8 MJ m^{-2} day^{-1} in 2020 and 26.5 MJ m^{-2} day^{-1} in 2021) and average environmental temperature (20.2°C in 2020 and 19.9°C in 2021). Additionally, the system was supplemented with approximately the same total effluent volume (2.7 L in 2020 and 3.0 L in 2021).

As a result, the total biomass produced in both years was virtually the same (896.4 g_{DW} in 2020 and 896.6 g_{DW} in 2021), as was the total N removed from the system (105.7 g in 2020 and 113.1 g in 2021). However, the uptake proportion between NH_4^+–N and NO_3^-–N significantly differed.

In June 2020, of the total N removed, 72.0% corresponded to NO_3^-, and 28.0% to NH_4^+ removal. Contrastingly, in 2021 both N forms were proportionally removed, with 53.9% corresponding to NO_3^- removal and 46.1% to the removal of NH_4^+. This was likely a result of the different supplementation frequencies practised in June of both years, with the system being intervened three times less frequently in 2020 compared to 2021 (Figure 5.4).

After the initiation of a new cultivation cycle on the 1st of June 2020, the system was intervened a total of three times, with the analysis conducted indicating that it was nearly depleted of both N sources at

the time of each supplementation (Figure 5.4a). Contrarily, in 2021, effluent supplemented was frequent enough to maintain a high NO_3^- concentration and extend NH_4^+ availability; thus, allowing microalgae to have prolonged access to their preferred N source and increasing its removal percentage.

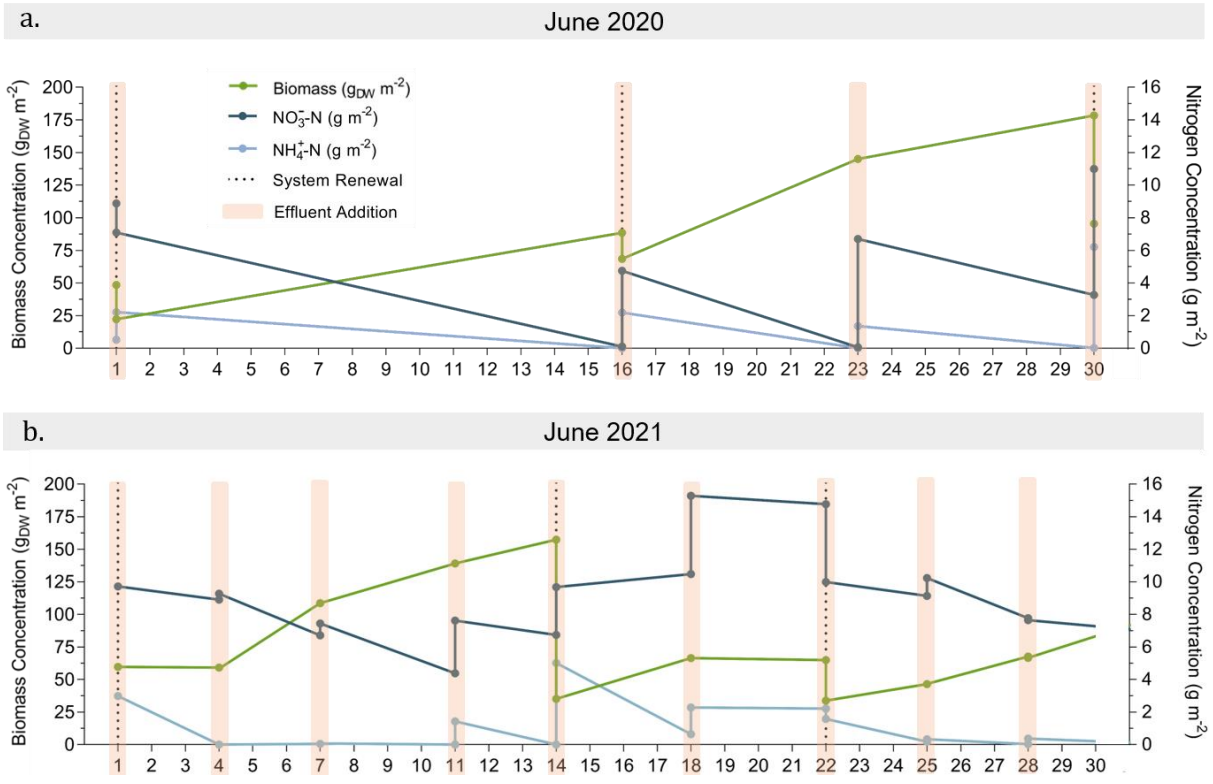

Figure 5.4 – RWP's Biomass, NO_3^-–N and NH_4^+–N profiles, throughout June of 2020 (a) and 2021 (b).

As there was only one bioreactor available for this project, it was not possible to simultaneously test different operational procedures or perform technical replicates. Since the evaluation of the impacts of supplementation frequency, on the ecosystem's N removal behaviour was not accounted for in the experimental design, only the data attained in June 2020 and 2021, was found do suit this analysis. The analysis of these results alone is insufficient to confidently determine the impacts of such operational differences, this would require additional monthly comparisons, using year-round data, ideally acquired following an assay plan previously designed for this purpose.

Nonetheless, these indicate that modifying operational procedures may cause marked differences in the removal proportion of both nitrogen forms, although not interfering with total N removal or biomass productivity. Thereby, the system will be evaluated in its total N removal efficiency.

5.1.3. System's Performance as a Function of the Daily Solar Radiation

5.1.3.1. System's Overall Performance from January 2019 to December 2021

Given the correlation found between solar radiation and biomass productivity, the system's behaviour will be further analysed in function of the daily solar radiation. Additionally, as radiation averages and productivity results were most similar between months belonging to different seasons, to simplify the results' interpretation; these were clustered into three groups, according to their daily radiation averages, with those in group 1 presenting the lowest, and in group 3 the highest average values. The monthly biomass productivity and N removal results are presented in Table I.1 (Annex I), the groups' environmental parameters are indicated in Table 5.2, and their biomass productivity and N removal rates are represented in Figure 5.5.

Table 5.2 – Groups ranked by average daily solar radiation range. The average daily radiation and environmental temperatures are presented for groups 1, 2 and 3 (mean ± SD, n = 70; n = 39; n = 79, respectively).

Group	Average Solar Radiation Range (MJ m^{-2} day^{-1})	Average Daily Solar Radiation (MJ m^{-2} day^{-1})	Included Months	Average Photoperiod (hh:mm)	Average Environmental Temperature (ºC)
1	[6.7–13.4]	9.0 (± 2.3)	January, February, October, November & December	10:14 (± 36')	14.2 (± 2.3)
2	[13.4–20.0]	17.3 (± 0.3)	March, April & September	12:34 (± 32')	17.7 (± 3.3)
3	[20.0–26.7]	24.7 (± 0.6)	May, June, July & August	14:21 (± 28')	21.1 (± 1.5)

The three groups presented considerably different productivity results, increasing from groups 1 to 3. Since group 3 simultaneously presents the highest productivity and daily solar radiation average, there is no indication that the highest radiation values reached in this geographical location, hamper biomass productivity through photoinhibition, for this bioreactor design, placement and operational conditions employed. The monthly productivity results, presented in Figure 5.1, support this observation.

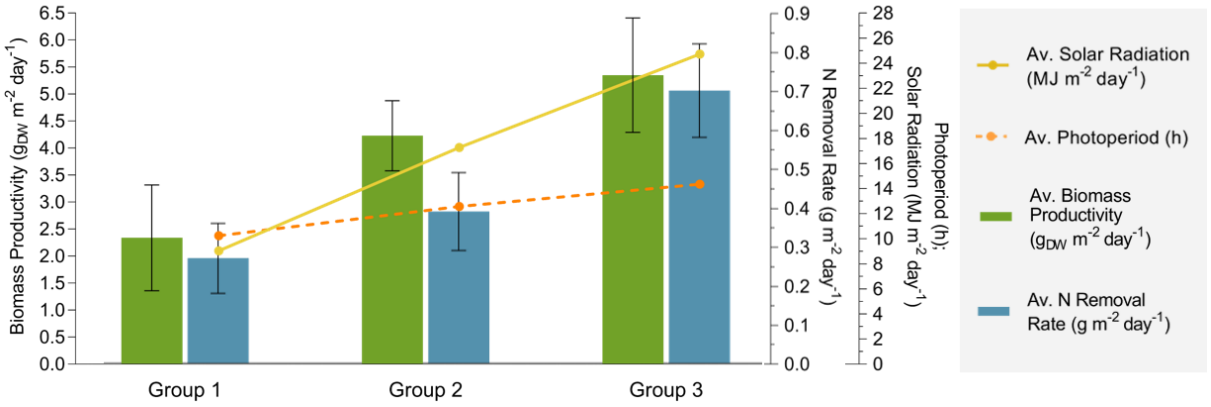

Figure 5.5 – Summary of the solar radiation groups' daily biomass productivity and N removal rates. The number of observations used to calculate the groups' mean and SD, for daily solar radiation, environmental temperature and biomass productivity was *n* = 70, *n* = 39, *n* = 79; and for N removal rate determination, *n* = 39, *n* = 21, *n* = 48 for groups 1, 2 and 3, respectively.

Despite the productivity increase verified between groups 1 and 2, and groups 2 and 3, their percentual rise was not proportional among the evaluated parameters (daily solar radiation, biomass productivity and total N removal rate).

The most significant percentual rise in daily biomass productivity was verified between groups 1 and 2, with an 81% increase from 2.34 ± 0.98 g_{DW} m^{-2} day^{-1} to 4.23 ± 0.65 g_{DW} m^{-2} day^{-1}, respectively. The increase verified between groups 2 and 3 was considerably less steep, with a 26% surge to a final biomass productivity of 5.35 ± 1.06 g_{DW} m^{-2} day^{-1}, for group 3. These results were consistent with the percentual increase verified for daily solar radiation; which rose by 91% from group 1 to group 2 and by 43% from group 2 to 3 (values indicated in Table 5.2).

Despite the percentual increase in the group's average photoperiod and environmental temperature, also being greater between groups 1 and 2, it was much more subtle; with the average photoperiod and environmental temperature having increased by 23% and 25% between groups 1 and 2; and by 14% and 20% for groups 2 and 3 (values indicated in Table 5.2).

In contrast to what was verified for biomass productivity, the percentual increase verified for N removal was less steep between groups 1 and 2, with a 44% increase from 0.27 ± 0.09 g m^{-2} day^{-1} to 0.39 ± 0.10 g m^{-2} day^{-1}. An 80% increase was observed between groups 2 and 3, to a final N removal rate of 0.70 ± 0.12 g m^{-2} day^{-1}. This agrees with the higher correlation result obtained between N removal and environmental temperature, *versus* that with solar radiation.

It is important to consider the size difference between the datasets available for N removal and biomass productivity, as it might interfere with the interpretation of results. Nonetheless, these parameters were strongly correlated, and the estimated amount of N removed per gram of biomass produced, did not greatly differ among the groups: Group 1 – 11.9%; Group 2 – 11.1%; Group 3 – 14.1%; annual weighed average – 12.5% (using the data described in Figure 5.2).

The increased N/biomass ratio obtained for group 3, may result from an increase in micro-grazer density in warmer months, as a slight positive correlation was verified between micro-grazer density and environmental temperature (Figure 5.9). This would mean that group 3's biomass productivity was higher, with microalgal growth contributing towards N removal, and with grazing causing a slight decrease in the system's total biomass, affecting the presented ratio. If this were to be true, these results would fully agree with the reported N-content of microalgal – 4 to 12% (w/w, DW basis)[13,106].

Productivity Results Within each Solar Radiation Group

Group 3 – Includes mostly summer months, presenting the highest daily irradiation average and longest photoperiod. As a result, this group presented the highest biomass productivity and N removal rate.

June showed the highest biomass productivity result, both within group 3 and compared to the remaining months. July's daily radiation average and biomass productivity results were similar to June's (June's radiation average and biomass productivity – 25.68 ± 0.73 MJ m^{-2} day^{-1} and 6.30 ± 0.46 g_{DW} m^{-2} day^{-1}; July's – 24.69 ± 1.42 MJ m^{-2} day^{-1} and 6.00 ± 1.45 g_{DW} m^{-2} day^{-1}), despite it simultaneously presenting the highest average N removal rate and environmental temperature (0.88 ± 0.03 g m^{-2} day^{-1}; 22.75 ±

1.27ºC). Nonetheless, due to the dataset's limitations (section 5.1.2), no definitive conclusion can be drawn relative to months presenting the highest N-removal potential.

August was the group's least productive month, presenting an average biomass production of 3.57 ± 0.40 g_{DW} m^{-2} day^{-1}. This month's N removal rate is only available for 2021, thus its removal average cannot be assessed.

Finally, the presented productivity results are consistent with the average irradiation and photoperiod verified for this group's months; with June presenting the highest values for both parameters, July coming as a close second, and August holding the lowest results. The same tendency was observed for environmental temperature and N removal rate, which were highest in July and lowest in May.

Groups 1 & 2 – As previously observed, the months presenting the highest photoperiod and daily irradiation averages, also showed the highest biomass productivity results. April was the most productive month within group 2, and October within group 1; showing an average biomass productivity of 4.91 ± 1.38 g_{DW} m^{-2} day^{-1} and 3.98 ± 0.25 g_{DW} m^{-2} day^{-1}, respectively.

Despite it not holding the lowest photoperiod or solar radiation averages, November showed the lowest biomass productivity out of all 12 months – 1.42 ± 0.78 g_{DW} m^{-2} day^{-1}. This month's biomass productivity average was calculated using data obtained in 2019 and 2021; and in the latter year, the culture's pH was affected by malfunctions in the carbonation circuit, causing a decrease in biomass productivity.

Considering that November's biomass productivity result may be an anomaly, it is important to determine this group's second least productive month, which was January.

January's biomass productivity result was roughly the same as December's (1.66 ± 0.49 g_{DW} m^{-2} day^{-1} *versus* December's 1.68 ± 0.28 g_{DW} m^{-2} day^{-1}); which in turn was the month presenting the lowest photoperiod and daily irradiation average, granting that these were still very similar (December's photoperiod and radiation average – 9:30 h and 6.76 ± 0.05 MJ m^{-2} day^{-1}; January's – 9:48 h and 7.42 ± 0.59 MJ m^{-2} day^{-1}).

Despite the stronger link identified between photoperiod and daily solar radiation with biomass productivity, compared to that of productivity and environmental temperature; which would justify December's biomass productivity result; January presents the lowest environmental temperature. It significantly differed from that verified for the remaining months, including from December's average value, which was 2°C higher than January's (13.12 ± 0.59°C *versus* 11.01 ± 0.80°C).

Most importantly, January's environmental temperature came very close to the lower limit of the temperature range described as suitable for microalgae species growing in temperate regions (10-25°C)[54,95]; and despite environmental temperature not being the most appropriate parameter to evaluate microalgal growth, it is an indicator of the culture medium's temperature, and in this particular case, of the observed results. Nonetheless, it is very important to emphasize that the differences highlighted in this discussion fall very close or even within the SD values associated with the calculated means; hence more data would be required to settle these observations.

5.1.3.2. System's Performance in 2021

The monthly biomass productivity verified in 2021, showed an identical performance pattern to that of previous years, either coming very close to prior results or surpassing them altogether (Figure 5.6). As a result, its annual biomass productivity was very similar to the annual average verified between 2019 and 2021 – 3.82 g_{DW} m^{-2} day^{-1} *versus* 3.92 g_{DW} m^{-2} day^{-1}.

Within 2021, April and November showed lower biomass productivity compared to previous years, the first resulting from herbicidal contamination, and the latter from malfunctions in the carbonation system. July showed the highest average daily solar radiation (26.65 MJ m^{-2} day^{-1}), biomass productivity (7.18 g_{DW} m^{-2} day^{-1}) and N removal rate (0.84 g m^{-2} day^{-1}), being the best-performing month of this year.

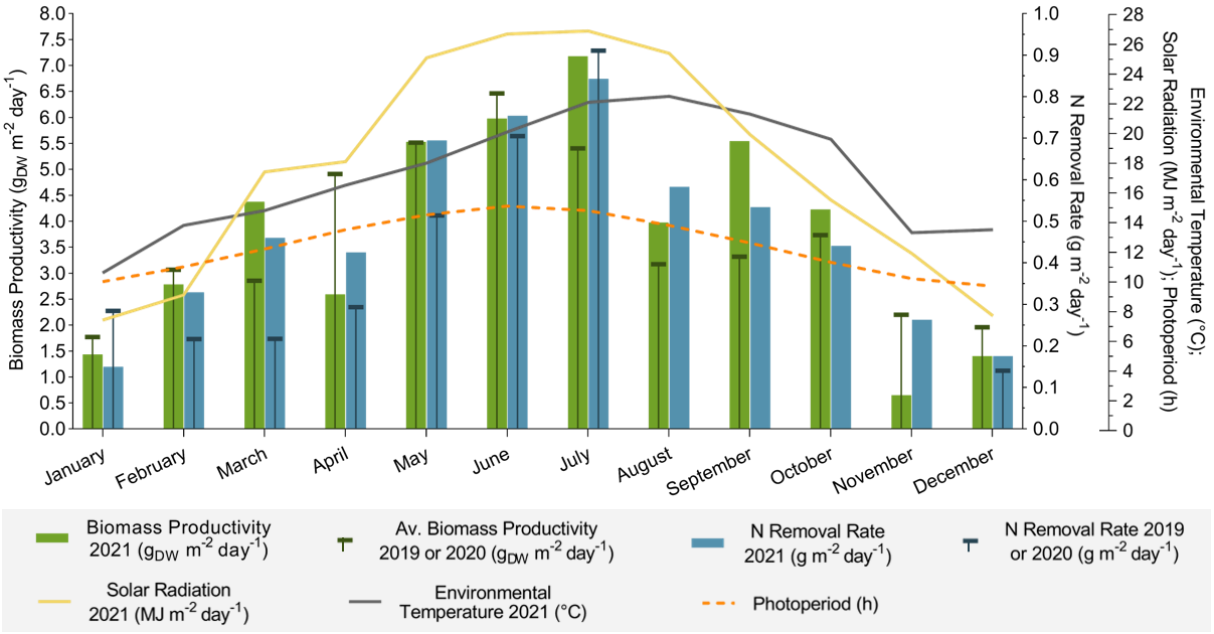

Figure 5.6 – Comparative representation of the system's performance in 2021 versus 2019 and 2020. As NH_4^+–N was not quantified up until December 2019, and data from August to December 2020 were excluded from the dataset; the graph lacks the vertical T-shaped bars for N-removal from August to December.

As this was the only year where both N forms were quantified all-year-round, and no mathematical relationship was established between biomass production and N removal (due to the system's characteristics); it is not possible to compare the bioremediation results verified in 2021, with previous years. The bioremediation outputs of 2021 are presented in Table 5.3.

Table 5.3 – Total biomass produced and N removed, in the pilot-scale RWP in 2021.

Production Time (Days)	Total NO_3^-–N Removed (g)	Total NH_4^+–N Removed (g)	Total N Removed (g)	Total Effluent Volume Treated (L)	Total Biomass Produced (kg_{DW})
365	410	452	862	18	7

This system was successful at achieving total nitrogen depletion. However, it presents the most widely reported limitation of algae-based wastewater treatment systems – significantly longer hydraulic retention time compared to bacterial-based systems.[24–26] This means that it is not a viable system if implemented exclusively for wastewater treatment purposes, as up-scaling would present high areal requirements and rising treatment costs. Therefore, assessing the value of the produced biomass is very important for the development of a cost-efficient waste valorisation strategy.

5.1.4. Composition of the Phytoplankton Community in 2021

The microalgal assemblage verified throughout 2021, mainly included species from the Chlorophyta phylum (green algae). Additionally, several morphologically different cyanobacteria (often referred to as blue-green algae, belonging to the phylum Cyanophyta), a single Xanthophyte (yellow-green algae) and a Bacillariophyta (diatom) were also identified, despite their generally reduced abundance. Most of the identified microalgae are members of a morphological group classified as non-motile Chlorococcales, which are known to be prominent in shallow and highly enriched systems; including wastewater microalgal assemblages.[49,53,107]

The most prevalent genera identified throughout this assay are shown in Figure 5.7. However, microalgae which were observed in very low relative abundance and with no reoccurrence were not included in the community composition analysis.

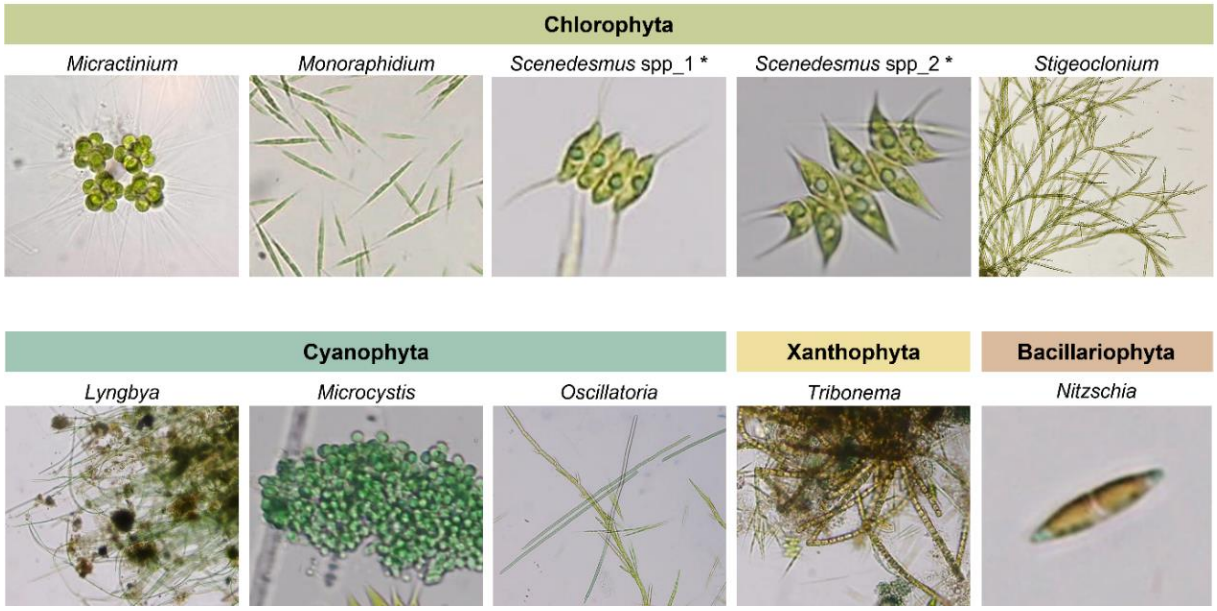

Figure 5.7 – Most prevalent microalgae phyla and genera throughout 2021. The *Scenedesmus* genus was subdivided into two groups based on general morphological traits (marked with an asterisk).

The reviewed studies describing the use of open cultivation of microalgae consortia, for the bioremediation of nutrient-rich waters, present significant differences among them and especially when compared to this work. Particularly, these studies mostly use urban effluents pre-treated to different

degrees, all presenting high levels of organic matter, which is absent in this industrial effluent. The RWPs used are often considerably larger and are usually operated in continuous mode. Additionally, these were conducted in very different geographic locations, subjecting the biological systems to distinct weather patterns. Despite the variability verified among the mentioned parameters, many similarities were identified among the studies, and between them and this assay, especially regarding the identified biota; with most microalgal genera being common to all publications.[26,45,49,50,108,109]

The total count of identified microalgae was lower than what is reported in some of the analysed studies.[45,50] However, these present microalgae identification at the species level, and such classification was not conducted due to the lack of molecular biology tools. Nonetheless, the genera identified in the RWP were described in most publications. Additionally, the species usually reported as being highly abundant have very similar morphological characteristics to the individuals identified in the RWP's microalgal assortment. It is thus likely that some of the individuals included in the genera and groups indicated in Figure 5.7 belong to different species within the identified genera, or different genera altogether, as slight morphological variations were logged throughout the assay.

Microalgal Diversity

The number of different microalgae simultaneously occurring in the pond was low, ranging from three to ten, with a median count of six. Similar results were described in other studies[45,50,107–109], and low species richness has been reported in many hypertrophic waterbodies, with numerous authors suggesting a decline in diversity adjacent to the intensification of eutrophication.[49,53]

Similarly to other analysed studies, the community was mostly dominated by a single species. However, codominance events occurred in several instances with varying duration (ranging from one week to nearly a month) and were mostly associated with changes in species dominance (turnover events[111]).[110] The length of time a given species dominated the system was variable and seemingly arbitrary, with no apparent connection to the seasonality indicators evaluated. This is noticeable in the graphical representation of microalgae relative abundance, as no single genus seems to be restricted to a specific season and all show variable relative abundance throughout 2021 – Figure 5.8.

The Spearman Rank correlation coefficients calculated, corroborate this observation, showing no evident seasonal pattern for microalgal diversity (no significant correlation ($p < 0.05$) with average daily solar radiation or environmental temperature). Diversity was also not correlated to culture pH; however, despite the low correlation value obtained, the abundance of different genera showed a negative correlation with N concentration ($r_s = -0.28,\ p = 0.03$), favouring the hypothesis of an inverse relationship between diversity and eutrophication (Figure 5.9**Erro! A origem da referência não foi encontrada.**).

A weak positive correlation was identified between microalgal diversity and micro-grazer density ($r_s = 0.27$, $p = 0.02$), despite it not correlating with micro-grazer diversity.

Regarding the system's productivity, microalgae diversity was also not significantly linked with either biomass productivity or N removal rate (in any of its available forms). Additionally, as presented by

Assemany et al. and Sutherland et al.[45,50], no significant correlation was identified between individual genera and biomass productivity or N removal; indicating that functional groups may be more important for the maintenance of the system's performance than individual species, suggesting high functional redundancy[6].

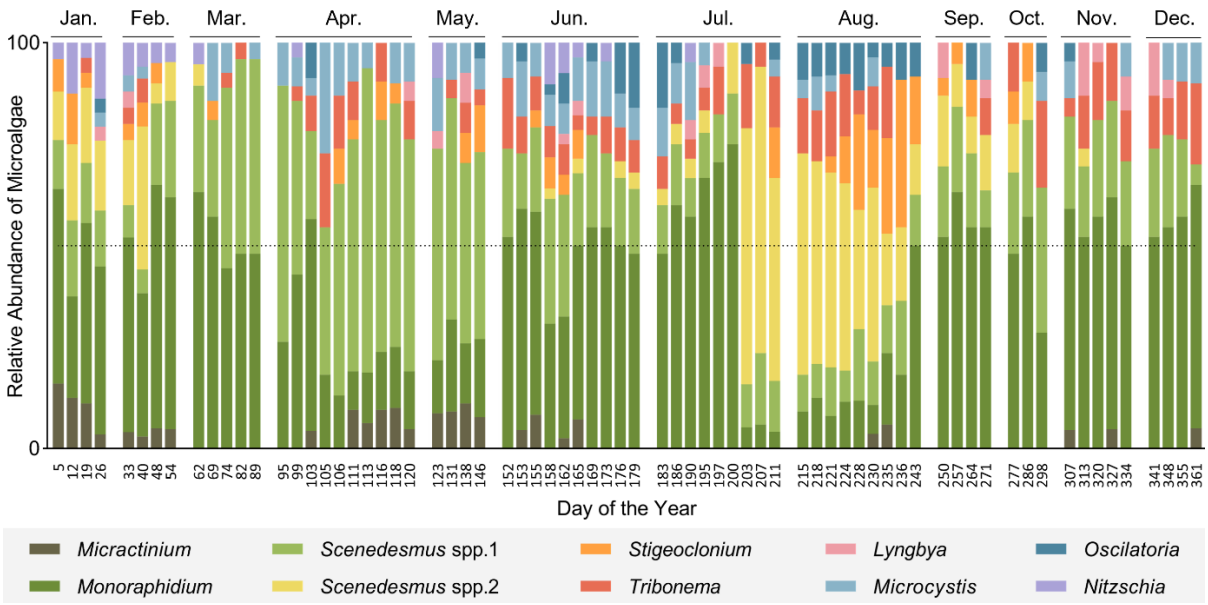

Figure 5.8 – Qualitative representation of the relative abundance of microalgae genera throughout 2021.

Contrarily to what is described in most studies, the amount of available N was found to not significantly affect biomass productivity. However, the biological systems described, are dependent on the N content of the influent (which is variable), and consistently presented a lower N concentration than what was established for this assay (averaging from 0.24 mM to 2.20 mM, with most presenting N concentrations inferior to 1.00 mM). In this system, the effluent was added to the system, in enough amount and frequency to exceed the microalgae's ability to achieve N depletion, thus not limiting microalgal growth. It is therefore understandable that no significant correlation was found between the two parameters.

In contrast with the analysed studies, zooplankton density was not significantly correlated to biomass productivity. As mentioned in section 5.1.3.1, months presenting higher daily solar radiation averages and photoperiod presented increased biomass productivity and N removal results. However, the N removal rate showed a slightly stronger correlation with environmental temperature compared to solar radiation, with the opposite being observed for biomass productivity (section 5.1.1). The fact that micro-grazers' abundance was favoured by warmer temperatures (Figure 5.9), might indicate that grazing causes some degree of biomass loss, as warmer months also were verified to present higher N removal per biomass production ratio (section 5.1.3.1). This disparity might result from the size of the available dataset.

[6]Ecological theory which defends that the environment selects for life forms that share similar roles in ecosystem functionality, rather than specific taxa.[125]

Dominant Microalgae and Turnover Events

The success of a microalgal assemblage is influenced by the comparative performance of each of its species under the prevailing environmental and biotic conditions. Changes in these conditions, such as competition for resources and selective predation by zooplankton grazers, can lead to the temporal succession of both the assemblage population and its dominant microalgal species.[49] The system's most prevalent microalgae showed distinct correlation results to the bioreactor's physicochemical and biotic parameters, as represented in Figure 5.9**Erro! A origem da referência não foi encontrada.**. These were mostly consistent with the concepts described in the bibliography.

Most studies describe seasonality and grazing pressure as being important contributors towards the occurrence of species' turnover events while recognizing that these events are most often triggered by the interaction between several factors, including operational constrains and changes in the influent's composition. The acquired data, suggests that seasonality did not drastically contribute towards the turnover of species, since these occurred with equivalent frequency throughout the year. Sutherland et al.[45] also verified that these events were not set off by seasonal changes. On the other hand, most turnover events coincided with culture renewal interventions and planned or inadvertent changes to the culture's pH, with the herbicidal contamination incident (described in section 5.1.2) having triggered one of these events (Figure 5.10). Thus, these seem to have been important triggers of these events, likely by collectively exerting selective pressure and influencing the zoo- and phytoplankton species which were able to readily recolonize the system.

Despite zooplankton grazing not having individually caused any of the turnover events verified, their presence was related to the maintenance of reduced abundance of the microalgal species these were reported to feed on, and seem to have contributed, in interaction with the indicated factors, to the success of species turnover. Namely, rotifers with similar morphology to those consistently observed in this system, have been reported to graze on *Monoraphidium*, but not on *Scenedesmus*, due to their structural characteristics.[99,109] Accordingly, *Monoraphidium* shows a low negative correlation with rotifers' abundance, and no correlation was found between *Scenedesmus* and rotifers. Some ciliates are known to be *Scenedesmus* predators[99,109]; however, throughout the year some were noticeably unable to graze on *S.* spp. 2, despite their ability to ingest *S.* spp. 1. The Spearman's correlations conducted, corroborate this observation, with a strong negative correlation between ciliates and *S.* spp. 1 and strong positive correlation with *S.* spp. 2 (Figure 5.9). Additionally, when the two *Scenedesmus* groups occurred simultaneously, only one of them showed high relative abundance, likely due to the grazing pressure exerted by these protozoans. These dynamics are apparent in the qualitative representation of microalgae genera and their respective predators' abundance (Figure 5.10).

Adding to the fact that most turnover events seemingly coincided with changes in culture pH, among all the environmental parameters evaluated, pH was the one which correlated significantly with the highest number of identified genera. As it has been widely described as an important factor affecting the development of microalgae.[13,54,96]

	Monoraphidium	*Scenedesmus* spp. 1	*Scenedesmus* spp. 2	Ciliates	Rotifers	Micro-grazer Density	Microalgal Diversity
Scenedesmus spp.1	-						
Scenedesmus spp.2	-	-0.67**					
Ciliates	-	-0.60**	0.62**				
Rotifers	-0.24*	-	-	-			
Micro-grazer Density	-0.30*	-0.43**	0.49**	0.69**	0.24*		
Microalgal Diversity	-	-	0.42**	0.32**	0.31**	0.27*	
Biomass Productivity	-	-	-	-	-	-	-
N Removal Rate	-	-	-	-	0.35**	-	-
Culture Medium initial [N]	-	-	-0.29*	-0.33**	0.32**	-	-0.28*
Medium pH	0.39**	0.42**	-0.41**	-0.27*	-	-0.37**	-
Av. Environmental Temperature	-0.27*	-0.38**	0.37**	-	0.27*	0.28*	-
Av. Solar Radiation	-	-	-	-	0.43**	-	-

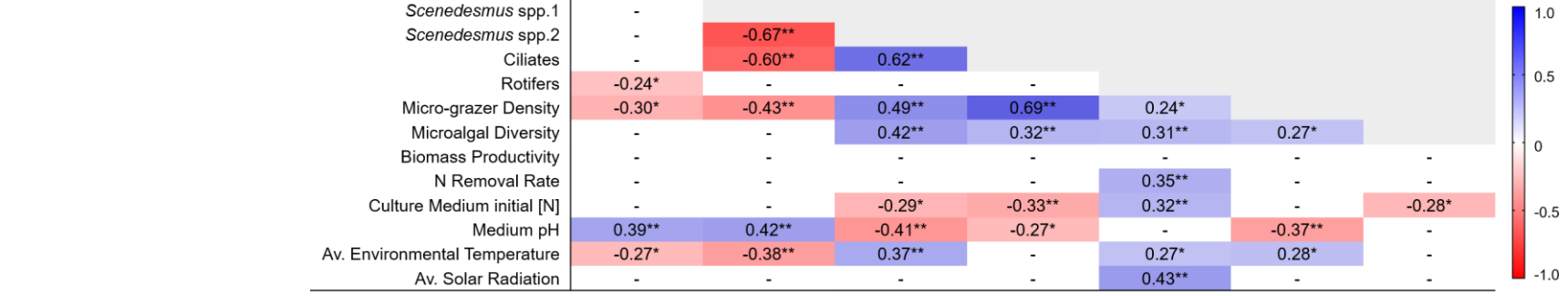

Figure 5.9 – Representation of the significant Spearman Rank coefficient results between the most prevalent microalgae, environmental and biological variables. Correlations were calculated using the data acquired from each culture sample acquired within 2021 (n = 71). **$p \leq 0.01$ – high statistical significance, *$0.01 < p < 0.05$ – moderate statistical significance.

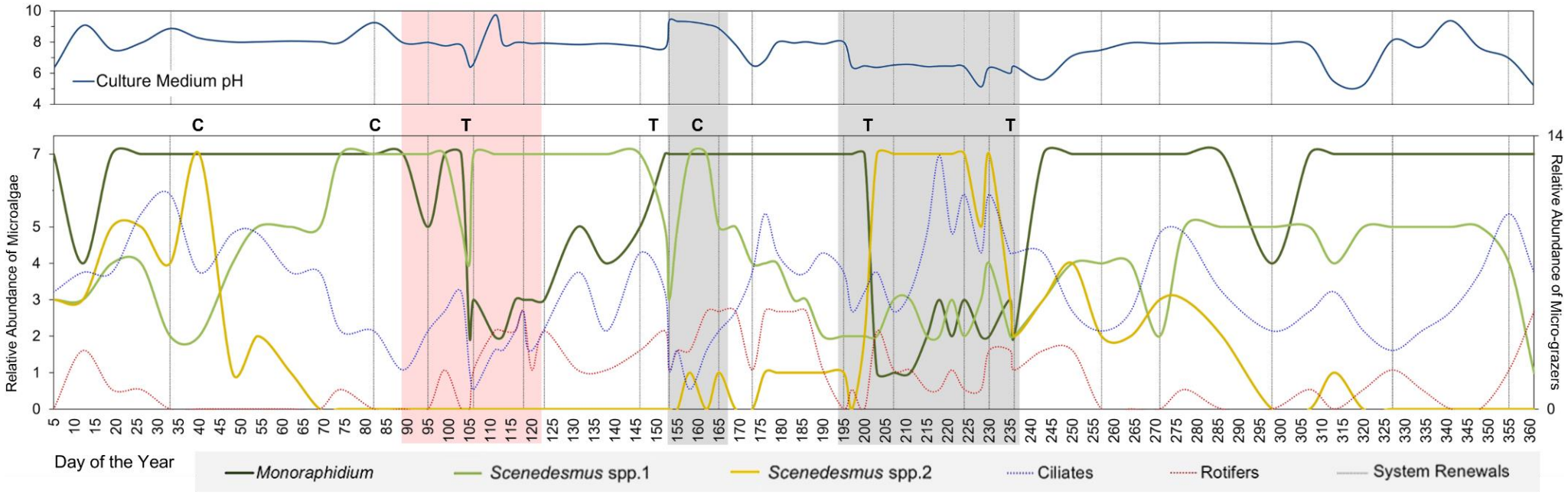

Figure 5.10 – Qualitative representation of relative abundance of the most prevalent microalgal species and respective zooplanktonic predators, verified at each intervention. The letters indicate species codominance (C) and turnover events (T). The section marked with red indicates the period where the system was contaminated with herbicide; the first grey section indicates the period when the bioreactor was operated at pH 9.5 and the second when the pH setpoint was altered to 6.5. The pH trend line was constructed using the pH values verified at peak radiation hours, between interventions.

5.1.4.1. System's Performance Under Different pH values

In 2021, during the months of greatest productivity and closest daily radiation averages (Table 5.2, group 3), the system's pH was separately altered to 9.5 and 6.5, as to explore this parameter's impacts on biomass productivity, total N removal rate, and microalgal assemblage composition. The experiment was designed to include a two-week production cycle for the two pH values tested, interleaved with a cultivation cycle at pH 8.0, to equate the starting point for both trial cycles.

The cycles performed under standard pH conditions, from 2019 to 2021 within May and August, for which no significant operational problems had been reported, and both NO_3^-–N and NH_4^+–N had been quantified (Figure 5.2) were used for comparative analysis. Five pH 8.0 cycles were selected, three conducted in 2020 and two in 2021. Their average results were lower than those acquired from both pH trial cycles, with an average biomass productivity and N removal rate of 6.29 ± 0.90 g_{DW} m^{-2} day^{-1} and 0.79 ± 0.20 g m^{-2} day^{-1}, respectively. Only one of the standard cycles (conducted in June 2020) presented a biomass productivity equivalent to that of the pH trial cycles – 7.86 g_{DW} m^{-2} day^{-1} *versus* the 7.54 and 7.90 g_{DW} m^{-2} day^{-1}, verified for the 9.5 and 6.5 pH cycles. The results of both the standard and test cycles conducted in 2021 are represented in Figure 5.11.

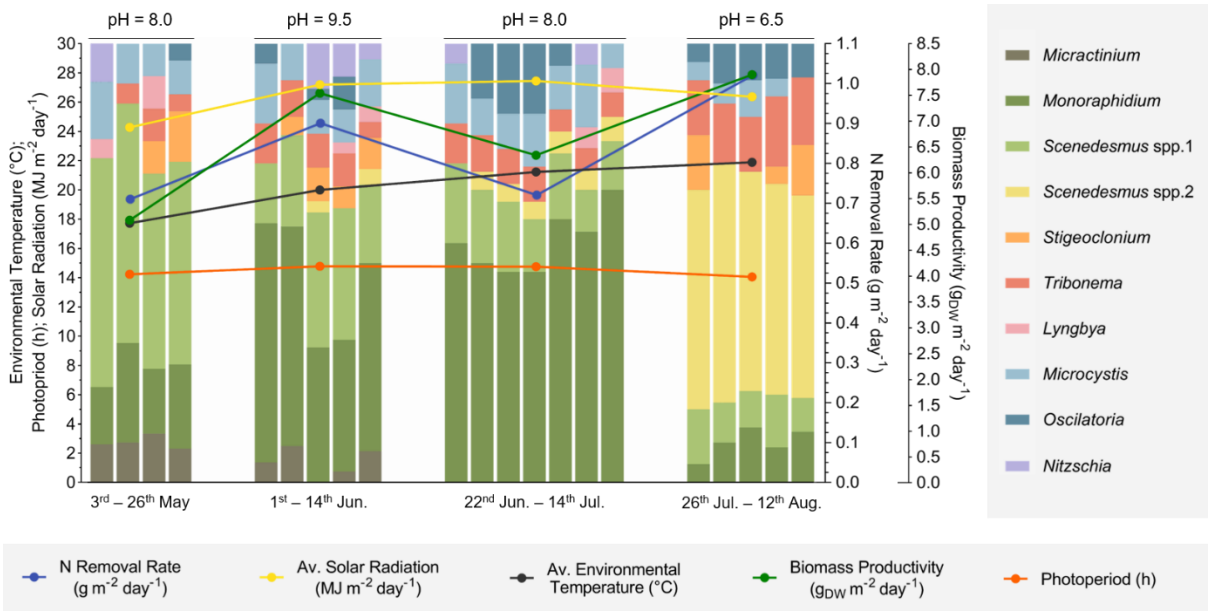

Figure 5.11 – Biomass productivity, N removal rates, and relative abundance of the microalgal genera present throughout the trial and standard cycles, performed from May to August of 2021. The results correspond to production cycles completed upon stabilization of the system, under the new pH setpoint established.

Due to the short time frame imposed by seasonality, the trial cycles were not repeated, preventing the identification of the most appropriate pH value, to maximize this system's performance. Nonetheless, both trial cycles showed greater biomass productivity and N removal rates compared to the considered standard cycles. Additionally, the system seems to perform better under lower pH, since the pH 6.5 cycle was the best performing while being subjected to a shorter photoperiod and lower solar radiation average, compared to both the pH 9.5 and 2nd standard cycles. It would therefore be interesting to repeat

this assay for a prolonged period, as to acquire more information on the ecosystem's behaviour under the tested conditions.

Both pH alterations caused the dominant microalgal genera to shift (Figure 5.10). However, the assemblage suffered the most drastic change under pH 6.5 (Figure 5.11), with *Scenedesmus* spp. 2 presenting itself as the dominant species for the entirety of the cycle and the longest period within the whole year.

The biomass produced during the 1st 8.0 pH cycle of 2021, and both the 6.5 and 9.5 trial cycles was harvested, producing three distinct batches which were evaluated for their potential as seed biostimulant treatments.

Composition of the Biomass Batches Produced During the pH Trial-Cycles

The three biomass batches presented different microalgal genera compositions (Figure 5.12), likely providing them with distinct biochemical properties. Each biomass batch was processed using a pressure homogenizer to produce cellular extracts which were used as seed priming treatments to assess their potential benefits as biostimulant treatments (section 5.2).

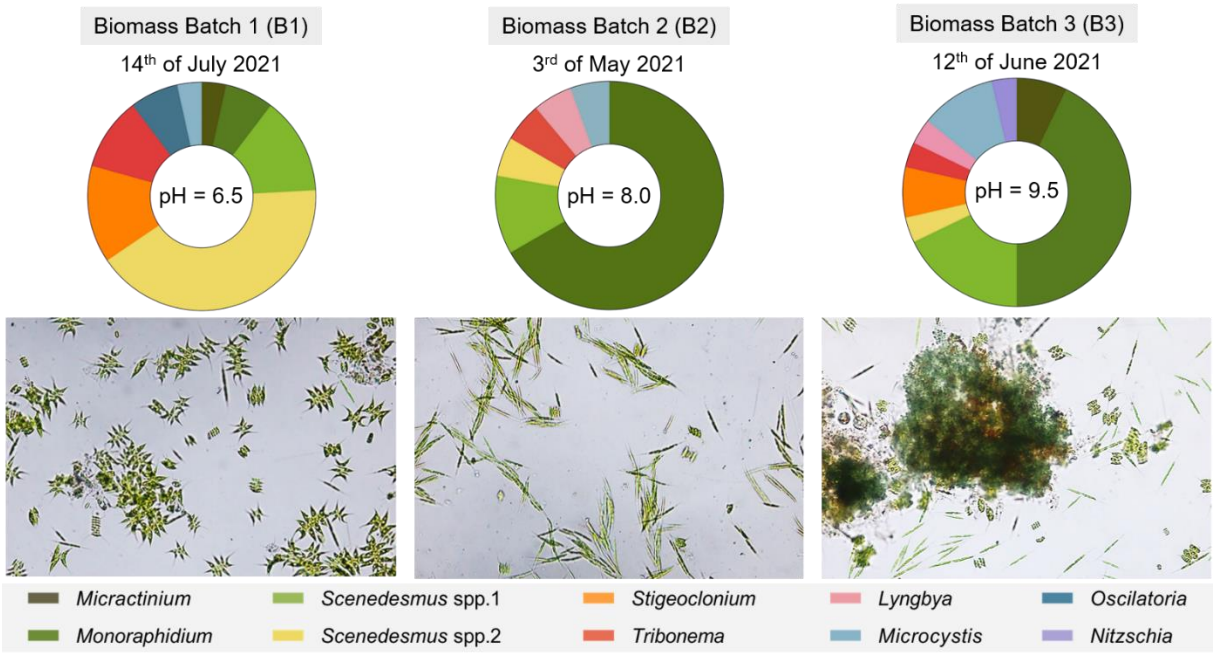

Figure 5.12 – Microalgal genera composition of the biomass batches derived from the pH trial-cycles conducted from May to August 2021. At the top of each pie-chart, is the batch's harvest date; in their centre is the production pH setpoint, and at the bottom is a photograph of the culture before harvest (200x amplification).

5.2. Assessment of the Biomass' Potential as an MBS for Seed Priming

Several studies have explored the potential of using microalgae as plant biofertilizers and biostimulants, with some applying the microalgal genera identified as predominant in the harvested biomass batches; all stating positive effects.[40,61,63] This study aims to preliminarily assess the potential of the harvested biomass to be transformed into agronomical biostimulant products. Particularly, to understand its potential to improve plants' performance under salinity stress conditions, given the worldwide increase in soil salination, including in some areas of Portugal.[111] Rice was the plant chosen for this germination assay, due to its global importance as a food crop, and its susceptibility and increased risk of exposure to salinity stress. In this sense, the three microalgae cellular extracts produced were applied as seed biostimulant treatments, at different concentrations, providing information regarding the suitable application dosage for the plant species selected.

5.2.1. Biostimulant Effects of the Microalgal Extracts in Rice Germination and Early Development

In this assay, salt exposure significantly affected all the developmental parameters evaluated ($p < 0.05$), with only some being influenced by priming. Despite seed-groups primed with microalgal extracts and water, having generally shown greater germination and early development results compared to their unprimed counterparts, for most parameters hydropriming did not cause these differences to be statistically significant. This likely resulted from the reduced number of replicates used in the study, as hydropriming has been widely reported to benefit rice germination.[79,112,113] Repeating this assay would likely help consolidate the obtained results and unravel additional interactions that were not detectable due to the observed variability.

The assay's results are summarized in Tables Table 5.4 and Table 5.5, and graphically represented in Figure II.1, Figure II.2 and Figure II.3, located in Annex II. The key to all the abbreviations attributed to the different priming treatments and incubation conditions applied is summarized in Table 4.5 (section 4.2.2).

5.2.1.1. Germinative Performance

Seed germination was initiated after two incubation days, independently of the priming treatments and incubation conditions applied. Several studies describe the final germination percentage (FGP), of different rice varieties, to be significantly impacted upon exposure to low NaCl concentrations (20-50 mM).[74,78,114] However, in this assay, only the seed-groups incubated under high salinity – $[NaCl]_{160mM}$, suffered a slight impact on FGP – 93.4 ± 7.8%, *versus* the 97.3 ± 5.7% verified for seeds incubated under no salinity – $[NaCl]_{0mM}$, and 96.1 ± 5.0% for those incubated under moderate salinity – $[NaCl]_{80mM}$ (Figure 5.13). This is not only indicative of the high viability of the seed population used, which presented a global FGP of 95.7 ± 6.4%; but also, of the individuals' resilience to salinity stress during germination.

Seed priming did not significantly affect FGP, under any of the incubation conditions tested (results in Table 5.4, and graphical representation in Figure II.1a, Annex II).

Despite FGP not having been affected by priming, and salinity only causing a significant impact at $[NaCl]_{160mM}$; the time taken for maximum germination percentage to be achieved (mean germination time – MGT) was inversely correlated with salinity, and significantly reduced by priming, under both control and salinity stress conditions; agreeing with what is reported in other rice germination studies.[74,78,114–116]

Upon $[NaCl]_{0mM}$ incubation, only the seeds primed with B1_$C_{5g/L}$, experienced a significant reduction in MGT compared to unprimed seeds, with hydropriming not significantly improving this parameter. Seed-groups grown under $[NaCl]_{80mM}$, were equivalently benefitted by hydropriming and most microalgal-extract solutions. However, under $[NaCl]_{160mM}$ incubation, all priming treatments significantly decreased MGT, with B2_$C_{5g/L}$ causing a significant reduction compared to both the positive and negative treatment control groups (hydropriming and no priming). Most notably, seeds primed with B2_$C_{5g/L}$ and incubated under $[NaCl]_{160mM}$, presented an MGT equivalent to that of unprimed seeds incubated under $[NaCl]_{0mM}$ – 3.2 ± 0.3 *versus* 3.3 ± 0.2 days, respectively (Figure 5.13, Table 5.4 and Figure II.1b, Annex II).

The germination index (GI) formula applied, considers both the FGP and germination spread, providing a comprehensive measure of the seeds' germinative fitness, and complementing the information provided by MGT (Table 5.4 and Figure II.1c, Annex II). It revealed extract-priming to also benefit germination under $[NaCl]_{0mM}$, with the seed-groups primed with B1_$C_{5g/L}$ and B1_$C_{30g/L}$, showing the best germinative performances compared to both treatment control groups. It also reinforced the direct correlation between priming-benefit and salinity concentration, with the most impactful solutions having increased the seeds' GI by 16.5%, 26.0% and 85.5%, compared to the unprimed group, under $[NaCl]_{0mM}$, $[NaCl]_{80mM}$ and $[NaCl]_{160mM}$, respectively.

As was verified for MGT, under $[NaCl]_{80mM}$ incubation, no statistically significant difference was verified between the GI results of hydro- and extract-priming treatments, despite both exceeding that of the negative treatment control group. Likewise, all priming solutions improved the GI of seeds incubated under $[NaCl]_{160mM}$, with B2_$C_{15g/L}$ priming having increased GI by 27.3% and 85.5%, compared to hydropriming and no priming respectively.

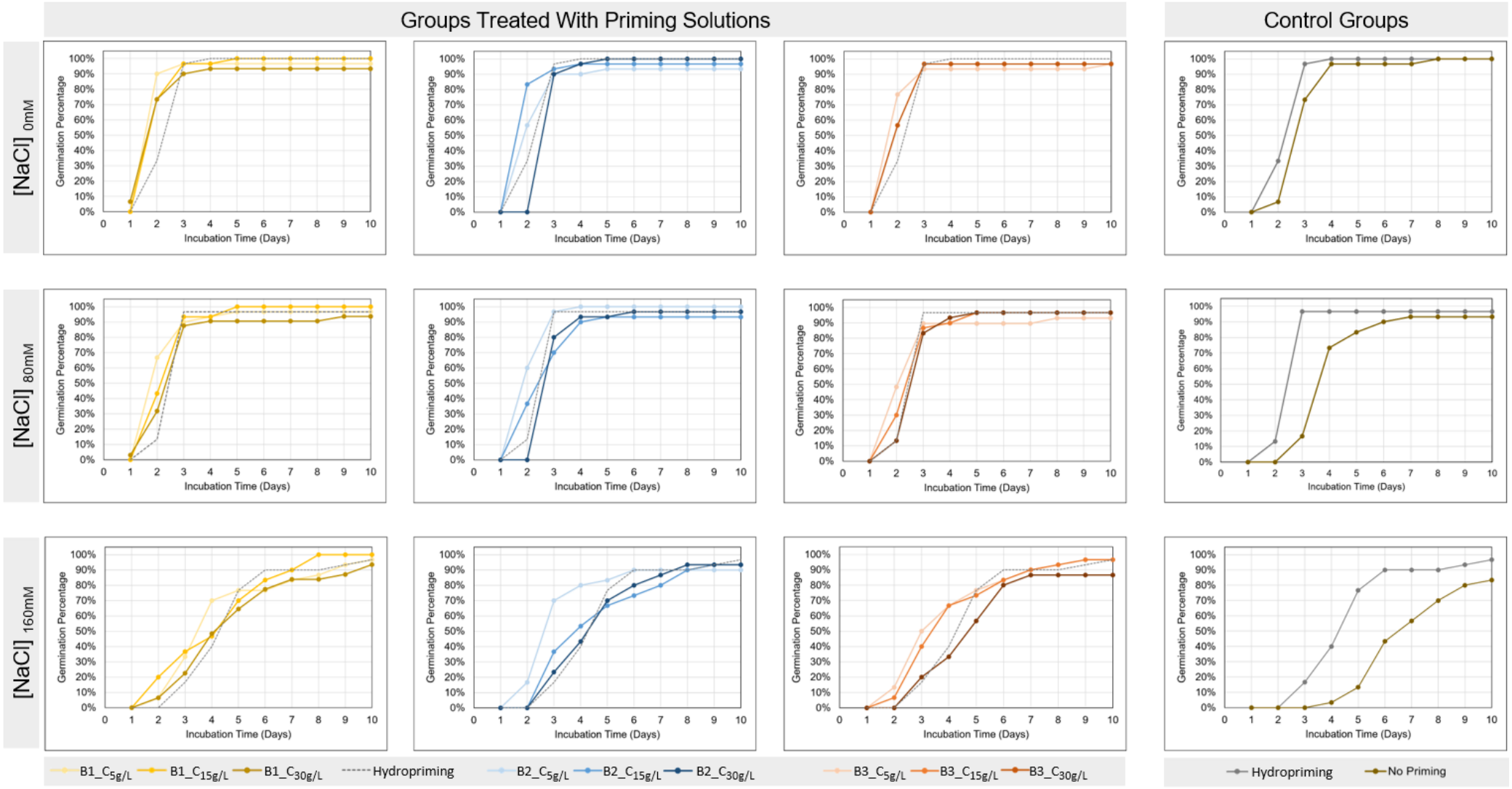

Figure 5.13 – Germinative behaviour of all priming treatments and salinity incubation groups. Each point derives from the average germination percentage verified with *n* = 3. No SD bars were included, due to the small variance verified between replicates.

Table 5.4 – Summary of the parameters used for evaluation of germinative performance. Values represent mean ± SD, with $n = 3$ for each treatment group. Results marked with the letter a. differ significantly from the positive control (hydropriming), while those marked with b. are significantly different from the negative control (no priming), considering the same incubation conditions. The last row summarizes the influence of salinity upon each evaluated parameter ($p < 0.05$).

Priming Treatment	FGP (%)	MGT (Days)	GI	SVI
No Salinity – $[NaCl]_{0mM}$				
B1_$C_{5g/L}$	96.7 (± 5.8)	2.1 (± 0.1)**b**	89.3 (± 1.2)**a,b**	8.8 (± 2.3)
B1_$C_{15g/L}$	100.0 (± 0.0)	2.3 (± 0.3)	86.7 (± 2.5)**b**	8.9 (± 0.4)
B1_$C_{30g/L}$	93.3 (± 11.5)	2.2 (± 0.3)	88.3 (± 2.9)**a,b**	9.0 (± 0.9)
B2_$C_{5g/L}$	93.3 (± 11.5)	2.5 (± 0.2)	85.3 (± 1.6)	8.6 (± 2.4)
B2_$C_{15g/L}$	96.7 (± 5.8)	2.2 (± 0.2)	88.3 (± 1.5)**b**	8.8 (± 1.1)
B2_$C_{30g/L}$	100.0 (± 0.0)	3.1 (± 0.2)	78.7 (± 1.5)	8.3 (± 0.5)
B3_$C_{5g/L}$	96.7 (± 5.8)	2.4 (± 0.5)	85.6 (± 4.9)**b**	9.0 (± 0.4)
B3_$C_{15g/L}$	96.7 (± 5.8)	2.6 (± 0.1)	84.4 (± 1.4)	9.8 (± 0.7)
B3_$C_{30g/L}$	96.7 (± 5.8)	2.4 (± 0.2)	85.9 (± 0.8)	8.6 (± 0.6)
Hydropriming	100.0 (± 0.0)	2.7 (± 0.2)	83.0 (± 1.7)	9.2 (± 1.3)
No Priming	100.0 (± 0.0)	3.3 (± 0.2)	76.7 (± 1.9)	8.0 (± 0.5)
Moderate Salinity – $[NaCl]_{80mM}$				
B1_$C_{5g/L}$	96.7 (± 5.8)	2.4 (± 0.2)**b**	85.9 (± 1.6)**b**	8.8 (± 1.0)
B1_$C_{15g/L}$	100.0 (± 0.0)	2.7 (± 0.1)**b**	83.0 (± 1.0)**b**	9.8 (± 0.1)
B1_$C_{30g/L}$	93.6 (± 5.5)	2.9 (± 0.2)**b**	84.0 (± 2.5)**b**	9.6 (± 0.4)
B2_$C_{5g/L}$	100.0 (± 0.0)	2.4 (± 0.2)**b**	85.7 (± 1.5)**b**	11.0 (± 0.5)**b**
B2_$C_{15g/L}$	93.3 (± 5.8)	2.9 (± 0.3)**b**	81.1 (± 2.9)**b**	9.6 (± 0.8)
B2_$C_{30g/L}$	96.7 (± 5.8)	3.3 (± 0.3)	77.5 (± 2.8)	9.7 (± 1.4)
B3_$C_{5g/L}$	93.0 (± 6.1)	2.7 (± 0.6)**b**	80.5 (± 4.9)**b**	8.5 (± 1.3)
B3_$C_{15g/L}$	96.7 (± 5.8)	2.9 (± 0.3)**b**	81.3 (± 3.1)**b**	9.1 (± 1.2)
B3_$C_{30g/L}$	96.7 (± 5.8)	3.0 (± 0.3)	79.7 (± 2.6)	10.6 (± 0.4)**b**
Hydropriming	96.7 (± 5.8)	2.9 (± 0.1)**b**	81.4 (± 0.7)**b**	9.0 (± 1.3)
No Priming	93.3 (± 5.8)	4.1 (± 0.3)	68.2 (± 3.4)	7.6 (± 0.5)
High Salinity – $[NaCl]_{160mM}$				
B1_$C_{5g/L}$	93.6 (± 5.5)	4.6 (± 0.5)**b**	66.7 (± 9.1)**b**	4.7 (± 1.1)
B1_$C_{15g/L}$	100.0 (± 0.0)	4.5 (± 0.7)**b**	64.7 (± 6.7)**b**	5.8 (± 0.1)
B1_$C_{30g/L}$	96.7 (± 5.8)	4.9 (± 0.3)**b**	60.8 (± 3.3)**b**	5.6 (± 1.8)
B2_$C_{5g/L}$	90.0 (± 10.0)	3.2 (± 0.3)**a,b**	77.8 (± 3.0)**a,b**	6.3 (± 0.9)
B2_$C_{15g/L}$	93.3 (± 5.8)	4.7 (± 0.3)**b**	63.0 (± 2.6)**b**	5.5 (± 1.1)
B2_$C_{30g/L}$	93.3 (± 5.8)	4.8 (± 0.9)**b**	62.3 (± 8.7)**b**	6.2 (± 1.8)
B3_$C_{5g/L}$	96.7 (± 5.8)	4.1 (± 0.5)**b**	69.1 (± 5.4)**b**	4.8 (± 1.1)
B3_$C_{15g/L}$	96.7 (± 5.8)	4.3 (± 0.3)**b**	66.9 (± 2.6)**b**	5.6 (± 0.6)
B3_$C_{30g/L}$	86.7 (± 5.8)	4.8 (± 0.6)**b**	61.9 (± 5.6)**b**	5.1 (± 0.4)
Hydropriming	96.7 (± 5.8)	4.9 (± 0.7)**b**	61.1 (± 6.8)**b**	6.3 (± 0.7)
No Priming	83.3 (± 15.3)	6.8 (± 0.2)	42.0 (± 1.7)	3.3 (± 1.1)
Salinity's Impact	0mM>160mM=80mM	160mM>80mM>0mM	0mM>80mM>160mM	80mM>0mM>160mM

5.2.1.2. Seedling Early Development and Morphology

Salinity was the most impactful factor regarding the seedlings' morphology, having affected all the morphological criteria assessed. Contrarily to what was observed for most germination parameters, seedling morphology was not extensively impacted by seed priming, with only some of the microalgal extract solutions benefiting early development, and hydropriming causing no significant benefit.

Salinity stress has been reported to cause greater impacts to shoot, compared to root growth.[68,117] Although the mechanisms behind this effect are not fully understood, it may stem from the plant's need to reduce water loss, and conserve surrounding soils' moisture, reducing its contribution towards salinity increase.[68] Despite the assay's results revealing unprimed seedlings' shoot and root system DW and length to be equally affected by salinity exposure; this was not verified for primed seedlings. The reduction in shoot length associated with salinity exposure, was not as severe for some of the extract-primed groups, as it was for control groups. Additionally, contrary to the effect verified for the control treatment groups, some extract-priming solutions caused an increase in biomass accumulation in the seedlings' root systems. Interestingly, despite increased root system DW being associated with an increase in suberization and salinity tolerance[118]; the seedlings presenting the greatest root system DW, were not the same which presented longer shoots, as a result of extract-priming (Table 5.5, Figure II.2 and Figure II.3, Annex II). This likely resulted from differences in the extracts' biochemical compositions and their impacts on early seedling development.

Most analyzed studies report rice to present an inversely proportional relationship between salinity exposure and both root and shoot DW and length, starting at low salt concentrations (20-40 mM).[71,74,77,78,114,115] Biomass accumulation was inversely correlated with salinity (Table 5.5 and Figure II.3, Annex II). Yet, the same was not verified for length parameters, with no significant differences being verified between seedling groups incubated under $[NaCl]_{0mM}$ and $[NaCl]_{80mM}$. Additionally, root, and consequently, total seedling length was higher for seeds incubated under $[NaCl]_{80mM}$ than for those incubated at $[NaCl]_{0mM}$; and $[NaCl]_{160mM}$ incubation caused a significant length reduction to both sections. This observation favors the hypothesis of decreased salt susceptibility of the seeds used in this assay.

In *Arabidopsis* and tomato, both dicotyledonous plants, primary and lateral root growth is inhibited under salinity stress exposure.[119,120] In rice, rye, and maize, monocotyledonous plants, inhibition of root length has been observed under high salinity.[119] Despite the lack of studies indicating the inhibition of root hair and secondary-root development in rice grown under saline environments, in this experiment, seedlings consistently showed decreased root system complexity, upon exposure to increasing salinity concentration; regardless of the priming treatment applied (Figure 5.14).

Considering the three incubation conditions applied, priming with B1 acted exclusively on DW accumulation, B2 on the seedlings' overall length, and B3 influenced both parameters. Under $[NaCl]_{0mM}$, $B3\_C_{15g/L}$ was the only impactful treatment, causing the seedlings' shoots to be longer compared with unprimed seedlings. Under $[NaCl]_{80mM}$ and $[NaCl]_{160mM}$, however, several of the priming treatments significantly impacted the evaluated parameters (Table 5.5, Figure II.2 and Figure II.3, Annex II).

Table 5.5 – Summary of the measurements taken of 12-day-old seedlings. Values represent mean ± SD, with n = 3 for each treatment group. Results marked with the letter a. differ significantly from the positive control (hydropriming), while those marked with b. are significantly different from the negative control (no priming), considering the same incubation conditions. The last row summarizes the influence of salinity upon each evaluated parameter ($p < 0.05$).

Priming Treatment	Length of the Longest Root (cm)	Seedling Height (cm)	Total Seedling Length (cm)	Dry Weight of the Root System (mg)	Dry Weight of the Shoot (mg)	Total Seedling Dry Weight (mg)
No Salinity – $[NaCl]_{0mM}$						
B1_$C_{5g/L}$	5.98 (± 1.66)	3.09 (± 0.34)	9.07 (± 1.97)	5.30 (± 0.29)	5.34 (± 0.64)	10.63 (± 0.89)
B1_$C_{15g/L}$	5.95 (± 0.25)	2.94 (± 0.14)	8.89 (± 0.39)	5.86 (± 0.30)	4.25 (± 0.37)	10.11 (± 0.09)
B1_$C_{30g/L}$	6.23 (± 0.52)	3.43 (± 0.21)	9.66 (± 0.30)	5.58 (± 0.82)	4.52 (± 0.13)	10.10 (± 0.69)
B2_$C_{5g/L}$	5.64 (± 1.04)	3.48 (± 0.58)	9.12 (± 1.62)	5.37 (± 0.81)	5.06 (± 0.86)	10.44 (± 1.64)
B2_$C_{15g/L}$	5.53 (± 0.46)	3.52 (± 0.48)	9.05 (± 0.81)	4.62 (± 0.24)	4.64 (± 0.38)	9.26 (± 0.33)
B2_$C_{30g/L}$	4.90 (± 0.61)	3.42 (± 0.27)	8.32 (± 0.50)	4.52 (± 0.23)	4.68 (± 0.32)	9.20 (± 0.17)
B3_$C_{5g/L}$	5.91 (± 0.37)	3.42 (± 0.25)	9.32 (± 0.62)	4.43 (± 0.57)	4.44 (± 0.32)	8.87 (± 0.76)
B3_$C_{15g/L}$	6.39 (± 0.44)	3.75 (± 0.22)**b**	10.14 (± 0.24)	4.37 (± 0.22)	4.24 (± 0.28)	8.62 (± 0.50)
B3_$C_{30g/L}$	5.79 (± 0.49)	3.12 (± 0.16)	8.91 (± 0.35)	4.53 (± 0.38)	4.52 (± 0.56)	9.05 (± 0.94)
Hydropriming	6.25 (± 0.85)	2.93 (± 0.54)	9.18 (± 1.30)	4.78 (± 1.04)	4.10 (± 0.36)	8.88 (± 1.36)
No Priming	5.58 (± 0.39)	2.47 (± 0.13)	8.05 (± 0.50)	4.40 (± 0.18)	3.82 (± 0.04)	8.22 (± 0.18)
Moderate Salinity – $[NaCl]_{80mM}$						
B1_$C_{5g/L}$	6.21 (± 0.56)	2.86 (± 0.16)	9.07 (± 0.62)	5.90 (± 0.96)**a,b**	4.29 (± 0.29)	10.19 (± 0.67)
B1_$C_{15g/L}$	6.48 (± 0.31)	3.35 (± 0.17)	9.83 (± 0.14)	6.35 (± 0.22)**a,b**	4.61 (± 0.58)	10.96 (± 0.76)
B1_$C_{30g/L}$	6.98 (± 0.44)	3.33 (± 0.31)	10.32 (± 0.74)	4.84 (± 0.33)	4.71 (± 0.58)	9.55 (± 0.84)
B2_$C_{5g/L}$	7.09 (± 0.43)	3.86 (± 0.03)**a,b**	10.95 (± 0.46)	3.89 (± 0.22)	4.13 (± 0.82)	8.02 (± 1.02)
B2_$C_{15g/L}$	6.57 (± 0.49)	3.71 (± 0.29)**b**	10.28 (± 0.23)	3.81 (± 0.54)	4.28 (± 0.12)	8.09 (± 0.49)
B2_$C_{30g/L}$	6.43 (± 0.59)	3.58 (± 0.32)**b**	10.01 (± 0.90)	4.25 (± 0.46)	3.41 (± 0.82)	7.69 (± 0.36)
B3_$C_{5g/L}$	5.83 (± 0.65)	3.31 (± 0.48)	9.157 (± 1.00)	4.29 (± 0.34)	3.90 (± 0.22)	8.19 (± 0.43)
B3_$C_{15g/L}$	6.37 (± 0.76)	3.03 (± 0.31)	9.41 (± 1.01)	3.96 (± 0.94)	3.97 (± 0.39)	7.93 (± 1.33)
B3_$C_{30g/L}$	7.24 (± 0.26)	3.72 (± 0.55)**b**	10.96 (± 0.63)	4.06 (± 0.59)	4.28 (± 0.74)	8.34 (± 1.14)
Hydropriming	6.65 (± 0.78)	2.67 (± 0.31)	9.32 (± 0.89)	3.54 (± 0.59)	4.22 (± 0.44)	7.75 (± 0.52)
No Priming	5.84 (± 0.09)	2.32 (± 0.07)	8.16 (± 0.05)	4.01 (± 0.30)	3.77 (± 0.60)	7.77 (± 0.90)
High Salinity – $[NaCl]_{160mM}$						
B1_$C_{5g/L}$	3.27 (± 0.74)	1.71 (± 0.37)	4.98 (± 1.10)	4.79 (± 1.15)**a,b**	3.43 (± 0.50)	8.22 (± 1.53)
B1_$C_{15g/L}$	3.98 (± 0.21)	1.82 (± 0.13)	5.81 (± 0.08)	4.85 (± 0.55)**a,b**	3.24 (± 0.32)	8.10 (± 0.40)
B1_$C_{30g/L}$	4.01 (± 1.57)	1.79 (± 0.18)	5.80 (± 1.71)	4.28 (± 1.27)	3.62 (± 1.12)**b**	7.90 (± 2.14)
B2_$C_{5g/L}$	4.77 (± 0.43)	2.25 (± 0.18)**b**	7.02 (± 0.60)	3.46 (± 0.97)	3.18 (± 0.42)	6.64 (± 1.38)
B2_$C_{15g/L}$	4.00 (± 0.83)	1.86 (± 0.13)	5.86 (± 0.92)	3.29 (± 0.30)	3.30 (± 0.57)	6.58 (± 0.85)
B2_$C_{30g/L}$	4.75 (± 1.38)	1.89 (± 0.39)	6.63 (± 1.77)	3.25 (± 0.62)	3.32 (± 0.62)	6.56 (± 0.22)
B3_$C_{5g/L}$	3.10 (± 1.23)	1.90 (± 0.29)	5.00 (± 1.49)	3.20 (± 0.73)	3.61 (± 1.62)**b**	6.81 (± 2.36)
B3_$C_{15g/L}$	3.86 (± 0.18)	1.98 (± 0.29)	5.83 (± 0.41)	3.41 (± 0.72)	3.10 (± 0.33)	6.51 (± 0.69)
B3_$C_{30g/L}$	3.83 (± 0.08)	2.01 (± 0.22)	5.84 (± 0.15)	3.14 (± 0.26)	3.22 (± 0.62)	6.36 (± 0.88)
Hydropriming	4.62 (± 0.32)	1.87 (± 0.16)	6.48 (± 0.38)	2.76 (± 0.16)	2.43 (± 0.29)	5.19 (± 0.19)
No Priming	2.99 (± 0.58)	0.97 (± 0.10)	3.96 (± 0.67)	2.49 (± 0.26)	1.97 (± 0.24)	4.45 (± 0.48)
Salinity's Impact	80mM>0mM> 160mM	0mM=80mM> 160mM	80mM>0mM> 160mM	0mM>80mM> 160mM	0mM>80mM> 160mM	0mM>80mM> 160mM

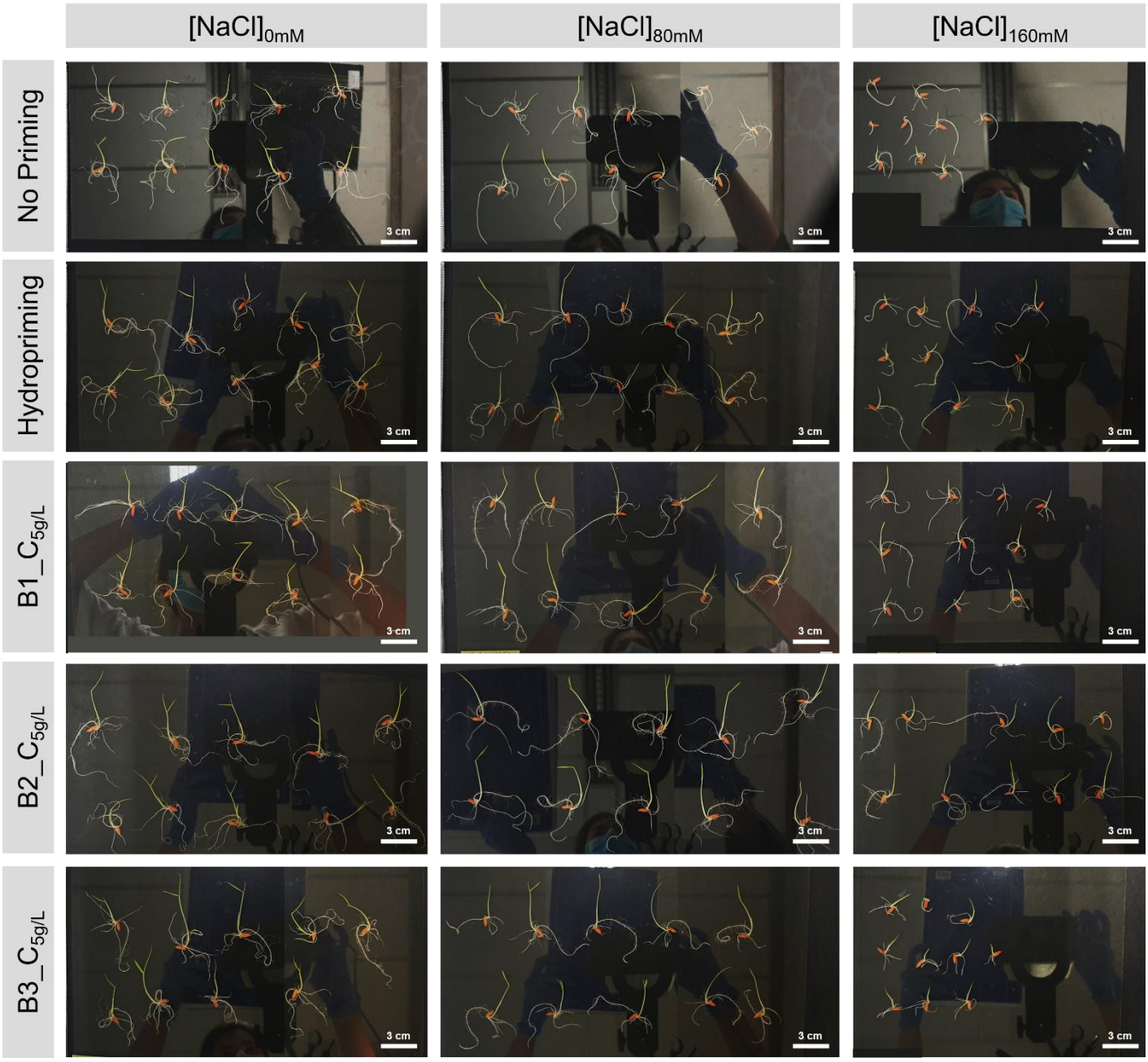

Figure 5.14 – Morphological appearance of the 12-day-old seedlings subjected to no priming, hydropriming, primed with B1, B2 and B3 at 5 g_{DW} L^{-1}; incubated under all salinity conditions.

Seedling Length

Priming with B2 benefited the seedlings' shoot length under both salinity conditions. The shoot length of seedlings incubated under $[NaCl]_{80mM}$, was also benefited by B3_$C_{30g/L}$ priming, compared to the negative control group; however, the group primed with B2_$C_{5g/L}$, presented longer shoots compared to both treatment control groups. The latter was the single significantly beneficial treatment solution, under $[NaCl]_{160mM}$ incubation, having benefited both shoot and total seedling length.

Seed groups grown under $[NaCl]_{80mM}$ and primed with B3_$C_{30g/L}$ and B2_$C_{5g/L}$, presented a significantly higher vigour index (SVI, Table 5.4), compared to the unprimed seed group. The B2_$C_{5g/L}$ primed seed group, simultaneously presented the highest SVI, MGT and GI, under $[NaCl]_{80mM}$ incubation. Most notably, however, when grown under $[NaCl]_{160mM}$, it presented the best MGT and GI results, which significantly differed from both treatment control groups, and exceeded those obtained by unprimed seeds grown under no salinity.

Seedling Dry Weight Accumulation

Seedling DW accumulation was less affected by seed priming, with no significant effects being detected under optimal incubation conditions. However, under $[NaCl]_{80mM}$ and $[NaCl]_{160mM}$, priming with B1_$C_{5g/L}$ and B1_$C_{15g/L}$, significantly increased DW accumulation to the seedlings' root systems, compared to both control treatment groups, despite this increase not transpiring into the total seedling DW results. The results verified for the seed groups primed with B1_$C_{5g/L}$ and B1_$C_{15g/L}$, under $[NaCl]_{160mM}$ incubation, were equivalent to the verified for unprimed seeds incubated at $[NaCl]_{0mM}$.

Even though B1_$C_{5g/L}$ and B1_$C_{15g/L}$ priming only benefited root DW accumulation, these still improved the seedlings' MGT and GI, under all incubation conditions; with B1_$C_{5g/L}$ presenting virtually the same result as B2_$C_{5g/L}$ priming under $[NaCl]_{80mM}$.

Seedlings incubated under $[NaCl]_{160mM}$ and primed with B1_$C_{30g/L}$ and B3_$C_{30g/L}$, presented greater shoot DW accumulation relative to the negative control treatment. However, the high variability verified among the replicates of both groups, questions these results' certainty.

Considering the results presented in other studies[71,74,77,78,114–119], and the fact that Japonica rice has been described as being susceptible to moderate salinity exposure[116,121], it came as a surprise that most parameters were not heavily penalized after exposure to $[NaCl]_{80mM}$. However, upon further investigation, it was found that the acquired seeds derive from rice plants cultivated in Alcácer do Sal – Vale do Sado, Portugal, in soils presenting salinity; thus giving rise to seeds described as being resistant to some degree of salinity stress.[122]

Overall, none of the microalgal extracts was found to cause inhibitory effects on seed germination or early seedling development, regardless of the applied concentrations. However, extract priming seems to have been most beneficial at lower application dosage, and as is often reported in similar studies, mainly for seeds exposed to salinity stress.

Extracts B1 and B2_$C_{5g/L}$ positively influenced several of the germinative performance and early seedling development parameters evaluated. These groups' results were significantly improved compared to those of both treatment control groups. Seedling shoot growth is reportedly more susceptible to salinity stress compared to root growth, and increased root biomass accumulation is associated with higher salinity tolerance. Despite B1 and B2 having acted on only one of these parameters, both improved the seeds' MGT and GI, with B1's effects being more pronounced under no salinity, and B2_$C_{5g/L}$ under high salinity. Seeds primed with B1_$C_{5g/L}$ and B2_$C_{5g/L}$ showed equivalent results when grown under moderate salinity stress conditions (Table 5.4Table 5.5, Figure II.1,Figure II.2 and Figure II.3, Annex II).

Despite extract-priming having provided greater benefit to seeds grown under salinity stress, their improved germinative performance might be uncorrelated with salinity tolerance later in the plant's life cycle.[115] Also, these extracts would probably cause significantly different effects if applied using other methods or at different plant developmental stages; likely depending on the environmental conditions verified during cultivation and/or incubation. Different outcomes would presumably be verified for this same seed lot, If this assay were to be developed using hydroponics or soil, in a growth chamber, greenhouse or open-field cultivation. Further, the fact that these extracts improved the germinative performance of this seed lot, does not imply that the same results would be obtained for other seed populations of the same species, despite providing a good indication of the method's potential.

Additionally, due to the method used for biomass production, the biochemical composition of the extracts derived from the effluent bioremediation process, would likely suffer substantial compositional fluctuations, even if operational procedures remained unaltered.

It would be interesting to repeat this assay, as to strengthen the obtained results and to further explore the potential of the microalgal biomass derived from this bioremediation process. The biochemical characterization of the extracts would likely reveal some of the causes behind their priming effects. Other application methods could also be explored, such as foliar spray application; through soil incorporation and application at different phases of development or areas of the plant – e.g., during the seedling or flowering stage; on leaves or roots.

It would be important to duplicate this test using different plant species, to assess the extracts' impacts on the development of various plant groups; particularly on horticultural as an alternative to cereal species. The microalgal biomass could also be transformed into different agronomical products, to further unveil its prospective applications (e.g., aqueous solution or liquid-soluble powder form for soil application).

6. Conclusions and Future Prospects

Socio-economic development, populational growth and industrial expansion are coupled with increased reliance on natural resources. Aquatic ecosystems have been seriously compromised by decades of overexploitation, poor ecosystem management and pollution. A circular economy model is fundamental for correcting this pattern, as it promotes the preservation of the available natural resources by extending the lifespan of the materials in current circulation, reintegrating by-products and waste streams into the value chain, thus contributing to sustainable development.

This study presents an evaluation of the performance of an endogenous microalgal assemblage, cultivated in a pilot-scale open raceway pond for the bioremediation of a nitrogen-rich effluent derived from the industrial production of chemical fertilizers. The work was performed at the location being considered for the implementation of a waste management unit. It considers the impacts of year-round environmental variations on biomass productivity, nitrogen removal efficiency and the ecosystem's microalgae genera. Additionally, it preliminarily assesses the potential of the produced microalgal biomass to be transformed into a seed biostimulant for rice incubated under salinity stress conditions.

The assay's results were congruent with the behaviour expected for this system. Biomass productivity and N removal generally followed the tendency of environmental parameters, increasing in months of greater solar radiation and photoperiod whilst showing some level of variation throughout the three years. External parameters, including operational constraints, are thought to have significantly impacted performance. However, parameters such as solar radiation, turbidity (which may lead to microalgal self-shading), N concentration, and renewal frequency have been the most consistently determinative. Additionally, no significant correlation was found between productivity and the different pH values tested.

Nitrogen removal rate showed a slightly stronger positive correlation with environmental temperature compared to solar radiation, with the opposite being observed for biomass productivity. Nitrogen is one of the most important elements regarding microalgal growth, with microalgal biomass reportedly presenting a 4 to 12% nitrogen content (w/w, DW basis). The analysis of the 2019 to 2021 results, showed the biomass produced in most months to be in check with this range, except for summer months, which presented a slightly increased N removal to biomass production proportion – 14.1%. Despite this difference not being very pronounced, the microbiological data acquired in 2021, revealed micro-grazer abundance to be favoured by warmer temperatures ($p < 0.05$). Although no significant correlation was found between these parameters, this might indicate some degree of crop loss due to grazing, with microalgal growth causing N to be removed and grazers feeding on the growing algae, removing them from the system.

The microalgal genera observed in the raceway's naturally established ecosystem are ubiquitously prevalent in eutrophic environments. Throughout 2021, the relative abundance of different microalgae suffered great variation, begging the question of whether or not the system's species composition affected its productivity and bioremediation performance. It was verified that biomass productivity and

N removal efficiencies remained unchanged regardless of the prevalent microalgal genera; supporting the hypothesis that in consortium cultivation, microalgal functional groups are more impactful towards RWP performance, rather than individual species.

The RWP's microalgal assortment was mostly dominated by a single genus, and codominance events were mostly associated with the shift in the dominating species (turnover events). These occurred with equivalent frequency throughout the year and were not triggered by seasonal variations, having mostly coincided with culture renewal interventions and changes to the culture's pH. The latter has caused the most drastic compositional variations in the community.

This effect may be significant towards the valorisation of the biomass derived from the bioremediation process since the cultivation conditions can be adapted to promote the establishment of species with biochemical properties desirable for their final application objective.

As a proof-of-concept, the system was operated under three pH setpoint values (6.5, 8.0 and 9.5); with the biomass produced under each condition (B1, B2 and B3) having been harvested, processed and used as seed biostimulant for rice germination under salinity stress incubation conditions (80 and 160 mM). Seeds were primed with microalgal extracts at different concentrations ($C_{5g/L}$, $C_{15g/L}$ and $C_{30g/L}$), with unprimed and hydro-primed seeds being used as control.

None of the microalgal extracts was found to inhibit seed germination or early seedling development, regardless of the applied concentrations. However, extract priming seems to have been most beneficial at lower application dosages and for seeds incubated under salinity stress.

The acquired rice seeds (*Oryza sativa* L. cultivar Japonica) presented high viability, as their germination percentage was only slightly reduced when under high salinity stress, with priming not significantly affecting FGP. Nonetheless, the seeds' germinative performance, determined by the germination index which considers both the germination spread and FGP, was improved by priming, showing a direct correlation between priming benefit and salinity concentration. The most impactful solutions increased the seeds' GI by 17%, 26% and 86%, compared to the unprimed group, under $[NaCl]_{0mM}$, $[NaCl]_{80mM}$ and $[NaCl]_{160mM}$, respectively. The seeds' GI was also significantly benefited by hydropriming under salinity conditions (80 mM and 160 mM), although extract-priming conferred better average results and a significantly greater advantage under both optimal and $[NaCl]_{160mM}$ incubation.

The morphology of the 12-day-old seedlings benefited from some of the microalgal extract solutions, with hydropriming causing no significant impact. Priming with B1 acted exclusively on DW accumulation, B2 on the seedlings' overall length, and B3 influenced both parameters independently. Extracts B1 and $B2\_C_{5g/L}$ positively influenced several of the germinative performance and early seedling development parameters. These groups' results were significantly improved compared to both treatment control groups. Seedling shoot growth is reportedly more susceptible to salinity stress compared to root growth, and increased root biomass accumulation is associated with higher suberization and salinity tolerance. Despite B1 and B2 having acted on only one of these parameters, both improved the seeds' MGT and GI, with B1's effects being more pronounced under no salinity, and $B2\_C_{5g/L}$ under high salinity stress. Seeds primed with $B1\_C_{5g/L}$ and $B2\_C_{5g/L}$ showed equivalent results when grown under moderate salinity stress conditions.

Despite this preliminary evaluation suggesting that this strategy may not be viable if implemented exclusively for wastewater treatment purposes, it revealed the ability of the same bioremediation system to produce microalgae biomass batches with different species compositions, and distinct bio-stimulatory effects on rice seed germination. This may potentially support the development of a cost-efficient waste valorization strategy, integrating a circular economy model.

As the extracts successfully diminished the detrimental effects of salinity exposure during germination and early development of rice, it would be interesting to repeat this assay, using different plant species, to assess the extracts' effects on the development of various plant groups; e.g., horticultural as an alternative to cereal species. Other application methods could also be explored, such as foliar spray application; through soil incorporation and application at different phases of development or areas of the plant – e.g., during the seedling or flowering stage; on leaves or roots. Biomass batches used in future assays should be biochemically characterized, as to reveal the likely causes behind their priming effects.

Additionally, considering the performance of this bioremediation system, several optimization steps should be considered. As solar radiation was the most determinant parameter for biomass productivity, and biomass concentration impacts the medium's turbidity, substantially affecting the amount of light available to the system, it would be beneficial to increase the frequency of monitorization visits and renewal procedures. This is especially important during summer months, when productivity is more likely to decrease as a result of self-shading within a week, directly impacting the system's bioremediation potential (N removal efficiency).

Carbon availability is often the most significantly constraining factor for microalgal performance in open systems; and although this assay includes CO_2 supplementation, off-gassing is still a frequent problem in these systems. Raceway ponds with carbonation sumps present greater CO_2 transfer efficiency, resulting in higher carbon availability to the microalgae and increasing process efficiency. This can however incur in increased operation and maintenance costs, which should be contemplated when establishing the future objectives of this project.

Ultimately, the water extracted during biomass harvesting should be recovered for further utilization, whether through reintroduction into the cultivation system or intermediate steps inherent to the operation and production process.

This bioremediation assay has endless improvement opportunities, whether related to the optimization of the cultivation parameters, the assays' operational design, or development of different biomass valorisation strategies and products. All of these should be considered in the development and planning of this project's next steps.

7. References

[1] United Nations. *The Sustainable Development Goals Report 2022*; 2022. https://unstats.un.org/sdgs/report/2022. (accessed Mar 04, 2022).

[2] Malone, T. C.; Newton, A. The Globalization of Cultural Eutrophication in the Coastal Ocean: Causes and Consequences. *Front Mar Sci*, **2020**, *7*, 1–30. https://doi.org/10.3389/fmars.2020.00670.

[3] Steffen, W.; Richardson, K.; Rockström, J.; Cornell, S. E.; Fetzer, I.; Bennett, E. M.; Biggs, R.; Carpenter, S. R.; de Vries, W.; de Wit, C. A.; et al. Planetary Boundaries: Guiding Human Development on a Changing Planet. *Science*, **2015**, *347*(6223). https://doi.org/10.1126/science.1259855.

[4] United Nations Human Settlements Programme. *Annual Report 2021 – UN-Habitat*; 2021. https://unhabitat.org/annual-report-2021. (accessed Feb 18, 2022).

[5] European Environment Agency. *Beyond Water Quality: Sewage Treatment in a Circular Economy*; Publications Office of the European Union, 2022. https://doi.org/10.2800/897113

[6] Robles, Á.; Aguado, D.; Barat, R.; Borrás, L.; Bouzas, A.; Giménez, J. B.; Martí, N.; Ribes, J.; Ruano, M. V.; Serralta, J.; et al. New Frontiers from Removal to Recycling of Nitrogen and Phosphorus from Wastewater in the Circular Economy. *Bioresour. Technol.* **2020**, *300*. https://doi.org/10.1016/j.biortech.2019.122673.

[7] Cutter, S.; Osman-Elasha, B.; Campbell, J.; Cheong, S. M.; McCormick, S.; Pulwarty, R.; Supratid, S.; Ziervogel, G.; Calvo, E.; Mutabazi, K.; et al. Managing the Risks from Climate Extremes at the Local Level. *Managing the Risks of Extreme Events and Disasters to Advance Climate Change Adaptation*, Cambridge University Press: Cambridge, UK, 2012, pp 291–338. https://doi.org/10.1017/cbo9781139177245.008.

[8] Rockström, J.; Steffen, W.; Noone, K.; Persson, Å.; Chapin, F. S.; Lambin, E. F.; Lenton, T. M.; Scheffer, M.; Folke, C.; Schellnhuber, H. J.; et al. A Safe Operating Space for Humanity. *Nature,* **2009,** *461*, 472–475. https://doi.org/10.1038/461472a.

[9] Rockström, J.; Steffen, W. L.; Noone, K.; Persson, Å.; Stuart, F. III C.; Rockstrom, J.; Steffen, W.; Noone, K.; Persson, A.; et al. Planetary Boundaries: Exploring the Safe Operating Space for Humanity. *Ecol. Soc.* **2009**, *14*(2).

[10] Persson, L.; Carney Almroth, B. M.; Collins, C. D.; Cornell, S.; de Wit, C. A.; Diamond, M. L.; Fantke, P.; Hassellöv, M.; MacLeod, M.; Ryberg, M. W.; et al. Outside the Safe Operating Space of the Planetary Boundary for Novel Entities. *Environ. Sci. Technol*. **2022**, *56*(3), 1510–1521. https://doi.org/10.1021/acs.est.1c04158.

[11] Li, M.; Dong, J.; Zhang, Y.; Yang, H.; van Zwieten, L.; Lu, H.; Alshameri, A.; Zhan, Z.; Chen, X.; Jiang, X.; et al. A Critical Review of Methods for Analyzing Freshwater Eutrophication. *Water*, **2021**, *13*. https://doi.org/10.3390/w13020225.

[12] le Moal, M.; Gascuel-Odoux, C.; Ménesguen, A.; Souchon, Y.; Étrillard, C.; Levain, A.; Moatar, F.; Pannard, A.; Souchu, P.; Lefebvre, A.; et al. Eutrophication: A New Wine in an Old Bottle? *Sci. Total Environ.* **2019**, *651*, 1–11. https://doi.org/10.1016/j.scitotenv.2018.09.139.

[13] Amos, R.; Qiang, H. *Handbook of Microalgal Culture: Applied Phycology and Biotechnology*, 2nd Edition; John Wiley & Sons, 2013. https://doi.org/10.1002/9781118567166.

[14] Beusen, A. H. W.; Bouwman, A. F.; van Beek, L. P. H.; Mogollón, J. M.; Middelburg, J. J. Global Riverine N and P Transport to Ocean Increased During the 20th Century Despite Increased Retention Along the Aquatic Continuum. *Biogeosciences*, **2016**, *13*(8), 2441–2451. https://doi.org/10.5194/bg-13-2441-2016.

[15] Paerl, H. W. Assessing and Managing Nutrient-Enhanced Eutrophication in Estuarine and Coastal Waters: Interactive Effects of Human and Climatic Perturbations. *Ecol. Eng*. **2006**, *26*(1), 40–54. https://doi.org/10.1016/j.ecoleng.2005.09.006.

[16] European Environment Agency. *Environmental Signals 2000 – Evironmental Assessment Report No 6*; 2016. https://www.eea.europa.eu/publications/92-9167-205-X/page014.html. (accessed Jan 07, 2022).

[17] Bouwman, A. F.; van Drecht, G.; van der Hoek, K. W. Global and Regional Surface Nitrogen Balances in Intensive Agricultural Production Systems for the Period 1970-2030. *Pedosphere*, **2005**, *15*(2), 137–155.

[18] Hoff, H.; Häyhä, S. C.; Lucas, P. *Discussion Brief: Bringing EU Policy into Line with The Planetary Boundaries*; Netherlands Environmental Assessment Agency and Stockholm Resilience Centre, 2017.

[19] Gerba, C. P.; Pepper, I. L. Municipal Wastewater Treatment. *Environmental and Pollution Science,* 3rd Edition; Elsevier, 2019; pp 393–418. https://doi.org/10.1016/B978-0-12-814719-1.00022-7.

[20] Directorate-General for Communication (European Commission). *A New Circular Economy Action Plan for a Cleaner and More Competitive Europe*; 2020. https://op.europa.eu/en/publication-detail/-/publication/45cc30f6-cd57-11ea-adf7-01aa75ed71a1

[21] Ellen MacArthur Foundation. What is a Circular Economy? https://ellenmacarthurfoundation.org/topics/circular-economy-introduction/overview (accessed Jun 13, 2022).

[22] Geissdoerfer, M.; Savaget, P.; Bocken, N. M. P.; Hultink, E. J. The Circular Economy – A New Sustainability Paradigm? *J. Clean Prod.* **2017**, *143*, 757–768. https://doi.org/10.1016/j.jclepro.2016.12.048.

[23] Ellen MacArthur Foundation. Urban Biocycles https://ellenmacarthurfoundation.org/cities-urban-biocycles (accessed Sep 13, 2022).

[24] C. P. Leslie Grady, Jr.; Glen T. Daigger; Nancy G. Love; Carlos D. M. Filipe. *Biological Wastewater Treatment*, 3rd Edition; CRC Press, 2011. https://doi.org/https://doi.org/10.1201/b13775.

[25] Muralikrishna, I. V.; Manickam, V. Wastewater Treatment Technologies. *Environmental Management*; Elsevier, 2017; pp 249–293. https://doi.org/10.1016/B978-0-12-811989-1.00012-9.

[26] Abdel-Raouf, N.; Al-Homaidan, A. A.; Ibraheem, I. B. M. Microalgae and Wastewater Treatment. *Saudi J. Biol. Sci*. **2012**, *19*(3), 257–275. https://doi.org/10.1016/j.sjbs.2012.04.005.

[27] Banayan Esfahani, E.; Asadi Zeidabadi, F.; Bazargan, A.; McKay, G. The Modified Bardenpho Process. *Handbook of Environmental Materials Management*; Springer International Publishing, 2018; pp 1–43. https://doi.org/10.1007/978-3-319-58538-3_87-2.

[28] Carvalho, V. C. F.; Kessler, M.; Fradinho, J. C.; Oehmen, A.; Reis, M. A. M. Achieving Nitrogen and Phosphorus Removal at Low C/N Ratios Without Aeration Through a Novel Phototrophic Process. *Sci. Total Environ*. **2021**, *793*. https://doi.org/10.1016/j.scitotenv.2021.148501.

[29] Plappally, A. K.; Lienhard V, J. H. Energy Requirements for Water Production, Treatment, End Use, Reclamation, and Disposal. *Renewable Sust. Energ. Rev.* **2012**, *16*(7), 4818–4848. https://doi.org/10.1016/j.rser.2012.05.022.

[30] Chae, K. J.; Kang, J. Estimating the Energy Independence of a Municipal Wastewater Treatment Plant Incorporating Green Energy Resources. *Energy Convers. Manag.* **2013**, *75*, 664–672. https://doi.org/10.1016/j.enconman.2013.08.028.

[31] Rosso, D.; Larson, L. E.; Stenstrom, M. K. Aeration of Large-Scale Municipal Wastewater Treatment Plants: State of the Art. *Water Sci. Technol.*, **2008**, *57*(7), 973–978. https://doi.org/10.2166/wst.2008.218.

[32] Mohsenpour, S. F.; Hennige, S.; Willoughby, N.; Adeloye, A.; Gutierrez, T. Integrating Microalgae into Wastewater Treatment: A Review. *Sci. Total Environ.* **2021**, *752*. https://doi.org/10.1016/j.scitotenv.2020.142168.

[33] Toledo-Cervantes, A.; Posadas, E.; Bertol, I.; Turiel, S.; Alcoceba, A.; Muñoz, R. Assessing the Influence of the Hydraulic Retention Time and Carbon/Nitrogen Ratio on Urban Wastewater Treatment in a New Anoxic-Aerobic Algal-Bacterial Photobioreactor Configuration. *Algal Res*. **2019**, *44*. https://doi.org/10.1016/j.algal.2019.101672.

[34] Muñoz, R.; Guieysse, B. Algal-Bacterial Processes for the Treatment of Hazardous Contaminants: A Review. *Water Res*. **2006**, *40*(15), 2799–2815. https://doi.org/10.1016/j.watres.2006.06.011.

[35] Gonçalves, A. L.; Pires, J. C. M.; Simões, M. A Review on the Use of Microalgal Consortia for Wastewater Treatment. *Algal Res*. **2017**, 24(B), 403–415. https://doi.org/10.1016/j.algal.2016.11.008.

[36] Liu, L.; Fan, H.; Liu, Y.; Liu, C.; Huang, X. Development of Algae-Bacteria Granular Consortia in Photo-Sequencing Batch Reactor. *Bioresour. Technol*. **2017**, *232*, 64–71. https://doi.org/10.1016/j.biortech.2017.02.025.

[37] Muñoz, R.; Jacinto, M.; Guieysse, B.; Mattiasson, B. Combined Carbon and Nitrogen Removal from Acetonitrile Using Algal-Bacterial Bioreactors. *Appl. Microbiol. Biotechnol.* **2005**, *67*, 699–707. https://doi.org/10.1007/s00253-004-1811-3.

[38] Sutherland, D. L.; Ralph, P. J. 15 Years of Research on Wastewater Treatment High-Rate Algal Ponds in New Zealand: Discoveries and Future Directions. *N. Z. J. Bot*. **2020**, *58*(4), 334–357. https://doi.org/10.1080/0028825X.2020.1756860.

[39] Bulgari, R.; Franzoni, G.; Ferrante, A. Biostimulants Application in Horticultural Crops Under Abiotic Stress Conditions*. J. Agron.* **2019**, *9*(6). https://doi.org/10.3390/agronomy9060306.

[40] Ronga, D.; Biazzi, E.; Parati, K.; Carminati, D.; Carminati, E.; Tava, A. Microalgal Biostimulants and Biofertilisers in Crop Productions*. J. Agron.* **2019**, *9*(4). https://doi.org/10.3390/agronomy9040192.

[41] Whitton, R.; Ometto, F.; Pidou, M.; Jarvis, P.; Villa, R.; Jefferson, B. Microalgae for Municipal Wastewater Nutrient Remediation: Mechanisms, Reactors and Outlook for Tertiary Treatment. *Environ. Technol. Rev.* **2015**, *4*(1), 133–148. https://doi.org/10.1080/21622515.2015.1105308.

[42] Costa, J. A. V.; Freitas, B. C. B.; Santos, T. D.; Mitchell, B. G.; Morais, M. G. Open Pond Systems for Microalgal Culture. *Biofuels from Algae*; 3rd Edition. Elsevier, 2019; pp 199–223. https://doi.org/10.1016/B978-0-444-64192-2.00009-3.

[43] Park, J. B. K.; Craggs, R. J.; Shilton, A. N. Wastewater Treatment High-Rate Algal Ponds for Biofuel Production. *Bioresour. Technol*. **2011**, *102*(1), 35–42. https://doi.org/10.1016/j.biortech.2010.06.158.

[44] Unnithan, V. V.; Unc, A.; Smith, G. B. Mini-Review: A Priori Considerations for Bacteria-Algae Interactions in Algal Biofuel Systems Receiving Municipal Wastewaters. *Algal Res*. **2014**, *4*(1), 35–40. https://doi.org/10.1016/j.algal.2013.11.009.

[45] Sutherland, D. L.; Turnbull, M. H.; Craggs, R. J. Environmental Drivers That Influence Microalgal Species in Full-Scale Wastewater Treatment High-Rate Algal Ponds. *Water Res*. **2017**, *124*, 504–512. https://doi.org/10.1016/j.watres.2017.08.012.

[46] Young, P.; Taylor, M.; Fallowfield, H. J. Mini-Review: High-Rate Algal Ponds, Flexible Systems for Sustainable Wastewater Treatment. *World J. Microbiol. Biotechnol*. **2017**, *33*(6). https://doi.org/10.1007/s11274-017-2282-x.

[47] Gupta, P. L.; Lee, S.-M.; Choi, H.-J. A Mini Review: Photobioreactors for Large Scale Algal Cultivation. *World J. Microbiol. Biotechnol*. **2015**, *31*(9), 1409–1417. https://doi.org/10.1007/S11274-015-1892-4.

[48] Flynn, K. J. Enhancing Microalgal Production: Constructing Decision Support Tools Using System Dynamics Modelling. 2021. https://doi.org/10.5281/zenodo.5036605.

[49] Reynolds, C. S. Environmental Requirements and Habitat Preferences of Phytoplankton: Chance and Certainty in Species Selection. *Bot. Mar.* **2012**, *55*(1), 1–17. https://doi.org/10.1515/bot.2011.121.

[50] Assemany, P. P.; Calijuri, M. L.; de Aguiar do Couto, E.; Batalha de Souza, M. H.; Silva, N. C.; da Fonseca Santiago, A.; de Siqueira Castro, J. Algae/Bacteria Consortium in High-Rate Ponds: Influence of Solar Radiation on the Phytoplankton Community. *Ecol. Eng.* **2015**, *77*, 154–162. https://doi.org/10.1016/j.ecoleng.2015.01.026.

[51] Guiry, M. D. How Many Species of Algae Are There? *J. Phycol.* **2012**, *48*(5), 1057–1063. https://doi.org/10.1111/j.1529-8817.2012.01222.x.

[52] Smith, A. G.; Tredici, M. R.; Boussiba, S.; Verdelho, V.; Cadoret, J.-P.; Davey, M. P.; Huete-Ortega, M.; Acien, F. G.; Schmid-Staiger, U.; Rodriguez, H.; et al. EABA Position Paper – What Are Algae? **2021**. https://doi.org/10.13140/rg.2.2.31633.35688.

[53] Bellinger, E. G.; Sigee, D. C. *Freshwater Algae: Identification and Use as Bioindicators*, 2nd Edition; John Wiley & Sons, 2015. https://doi.org/10.1002/9780470689554.

[54] Barsanti, L.; Gualtieri, P. *Algae Anatomy, Biochemistry, and Biotechnology*, 2nd Edition; Taylor & Francis Group, 2015. https://doi.org/10.1201/b16544-10.

[55] Kosek, K.; Polkowska, Z.; Zyszka, B.; Lipok, J. Phytoplankton Communities of Polar Regions-Diversity Depending on Environmental Conditions and Chemical Anthropopressure. *J. Environ. Manage*. **2016**, *171*, 243–259. https://doi.org/10.1016/j.jenvman.2016.01.026.

[56] Blankenship, R. E. *Molecular Mechanisms of Photosynthesis*, 2nd Edition; John Wiley & Sons, 2014. https://doi.org/10.1002/9780470758472.

[57] Johnson, M. P. Photosynthesis. *Essays Biochem*. **2016**, *60*(3), 255–273. https://doi.org/10.1042/ebc20160016.

[58] Harper, J. L. *Population Biology of Plants*, The Blackburn Press, 1977.

[59] Tyrrell, T. Redfield Ratio. *Encyclopedia of Ocean Sciences*; Elsevier, 2001; pp 2377–2387. https://doi.org/10.1006/rwos.2001.0271.

[60] Grobbelaar, J. U. Inorganic Algal Nutrition. *Handbook of Microalgal Culture: Applied Phycology and Biotechnology*, 2nd Edition; John Wiley & Sons, 2013, pp 123–133. https://doi.org/10.1002/9781118567166.ch8.

[61] Garcia-Gonzalez, J.; Sommerfeld, M. Biofertilizer and Biostimulant Properties of the Microalga *Acutodesmus dimorphus*. *J. Appl. Phycol*. **2016**, *28*, 1051–1061. https://doi.org/10.1007/s10811-015-0625-2.

[62] Colla, G.; Rouphael, Y. Microalgae: New Source of Plant Biostimulants. *J. Agron.* **2020**, *10*(9), 1–4. https://doi.org/10.3390/agronomy10091240.

[63] Dineshkumar, R.; Kumaravel, R.; Gopalsamy, J.; Sikder, M. N. A.; Sampathkumar, P. Microalgae as Bio-Fertilizers for Rice Growth and Seed Yield Productivity. *Waste Biomass Valorization*, **2018**, *9*(5), 793–800. https://doi.org/10.1007/S12649-017-9873-5.

[64] Chiaiese, P.; Corrado, G.; Colla, G.; Kyriacou, M. C.; Rouphael, Y. Renewable Sources of Plant Biostimulation: Microalgae as a Sustainable Means to Improve Crop Performance. *Front. Plant Sci*. **2018**, *9*. https://doi.org/10.3389/fpls.2018.01782.

[65] Barone, V.; Baglieri, A.; Stevanato, P.; Broccanello, C.; Bertoldo, G.; Bertaggia, M.; Cagnin, M.; Pizzeghello, D.; Moliterni, V. M. C.; Mandolino, G.; et al. Root Morphological and Molecular Responses Induced by Microalgae Extracts in Sugar Beet (*Beta vulgaris* L.). *J. Appl. Phycol*. **2018**, *30*(2), 1061–1071. https://doi.org/10.1007/s10811-017-1283-3.

[66] Ashraf, M. A.; Akbar, A.; Askari, S. H.; Iqbal, M.; Rasheed, R.; Hussain, I. Recent Advances in Abiotic Stress Tolerance of Plants Through Chemical Priming: An Overview. *Advances in Seed Priming*; Springer, 2018; pp 51–79. https://doi.org/10.1007/978-981-13-0032-5_4.

[67] Hanin, M.; Ebel, C.; Ngom, M.; Laplaze, L.; Masmoudi, K. New Insights on Plant Salt Tolerance Mechanisms and Their Potential Use for Breeding. *Front. Plant. Sci*. **2016**, *7*. https://doi.org/10.3389/fpls.2016.01787.

[68] Munns, R.; Tester, M. Mechanisms of Salinity Tolerance. *Annu. Rev. Plant. Biol.* **2008**, *59*, 651–681. https://doi.org/10.1146/annurev.arplant.59.032607.092911.

[69] Munns, R.; Gilliham, M. Salinity Tolerance of Crops – What Is the Cost? *New Phytol.* **2015**, *208*(3), 668–673. https://doi.org/10.1111/nph.13519.

[70] Shahid, S. A.; Zaman, M.; Heng, L. Introduction to Soil Salinity, Sodicity and Diagnostics Techniques. *Guideline for Salinity Assessment, Mitigation and Adaptation Using Nuclear and Related Techniques*; Springer, 2018; pp 1–42. https://doi.org/10.1007/978-3-319-96190-3_1.

[71] Puvanitha, S.; Mahendran, S. Effect of Salinity on Plant Height, Shoot and Root Dry Weight of Selected Rice Cultivars. *Scholars J. Agric. Vet. Sci.* **2017**, *4*(4), 126–131. https://doi.org/10.13140/rg.2.2.10540.72322.

[72] Wassmann, R.; Jagadish, S. V. K.; Sumfleth, K.; Pathak, H.; Howell, G.; Ismail, A.; Serraj, R.; Redona, E.; Singh, R. K.; Heuer, S. Regional Vulnerability of Climate Change Impacts on Asian Rice Production and Scope for Adaptation. *Advances in Agronomy*; Academic Press, 2009; Vol. 102, pp 91–133. https://doi.org/10.1016/s0065-2113(09)01003-7.

[73] Alexandre, C.; Borralho, T.; Durão, A. Evaluation of Salinization and Sodification in Irrigated Areas with Limited Soil Data: Case Study in Southern Portugal. *Span. J. Soil Sci.* **2018**, *8*(1), 102–120. https://doi.org/10.3232/sjss.2018.v8.n1.07.

[74] Hakim, M. A.; Juraimi, A. S.; Begum, M.; Hanafi, M. M.; Ismail, M. R.; Selamat, A. Effect of Salt Stress on Germination and Early Seedling of Rice (*Oryza sativa* L.). *Afr. J. Biotechnol.* **2010**, *9*(13), 1911–1918. https://doi.org/10.5897/ajb09.1526.

[75] Qin, H.; Li, Y.; Huang, R. Advances and Challenges in the Breeding of Salt-Tolerant Rice. *Int. J. Mol. Sci.* **2020**, *21*. https://doi.org/10.3390/ijms21218385.

[76] Frouin, J.; Languillaume, A.; Mas, J.; Mieulet, D.; Boisnard, A.; Labeyrie, A.; Bettembourg, M.; Bureau, C.; Lorenzini, E.; Portefaix, M.; et al. Tolerance to Mild Salinity Stress in Japonica

Rice: A Genome-Wide Association Mapping Study Highlights Calcium Signalling and Metabolism Genes. *PLoS One*, **2018**, *13*(1). https://doi.org/10.1371/journal.pone.0190964.

[77] Vibhuti, C. S.; Bargali, K.; Bargali, S. S. Seed Germination and Seedling Growth Parameters of Rice (*Oryza sativa* L.) Varieties as Affected by Salt and Water Stress. *Indian J. Agric. Sci.* **2015**, *85*(1), 102–108.

[78] Kazemi, K.; Eskandari, H. Effects of Salt Stress on Germination and Early Seedling Growth of Rice (*Oryza Sativa*) Cultivars in Iran. *Afr. J. Biotechnol.* **2011**, *10*(77), 17789–17792. https://doi.org/ 10.5897/ajb11.2219.

[79] Paparella, S.; Araújo, S. S.; Rossi, G.; Wijayasinghe, M.; Carbonera, D.; Balestrazzi, A. Seed Priming: State of the Art and New Perspectives. *Plant Cell Rep.* **2015**, *34*(8), 1281–1293. https://doi.org/10.1007/s00299-015-1784-y.

[80] Lutts, S.; Benincasa, P.; Wojtyla, L.; Kubala S., S.; Pace, R.; Lechowska, K.; Quinet, M.; Garnczarska, M. Seed Priming: New Comprehensive Approaches for an Old Empirical Technique. *New Challenges in Seed Biology*; InTech, 2016; Vol. 32, pp 137–144. https://doi.org/ 10.5772/64420.

[81] Jisha, K. C.; Vijayakumari, K.; Puthur, J. T. Seed Priming for Abiotic Stress Tolerance: An Overview. *Acta Physiol. Plant.* **2013**, *35*, 1381–1396. https://doi.org/10.1007/s11738-012-1186-5.

[82] Petersen, R. Influence of Copper and Zinc on the Growth of a Freshwater Alga, *Scenedesmus quadricauda*: The Significance of Chemical Speciation. *Environ. Sci. Technol.* **2002**, *16*(8), 443–447. https://doi.org/10.1021/es00102a003.

[83] Omar, H. H. Bioremoval of Zinc Ions by *Scenedesmus obliquus* and *Scenedesmus quadricauda* and Its Effect on Growth and Metabolism. *Int. Biodeterior. Biodegradation*, **2002**, *50*(2), 95–100. https://doi.org/10.1016/s0964-8305(02)00048-3.

[84] Fargašová, A. Interactive Effect of Manganese, Molybdenum, Nickel, Copper I and II, and Vanadium on the Freshwater Alga *Scenedesmus quadricauda*. *Bull. Environ. Contam. Toxicol.* **2001**, *67*(5), 688–695. https://doi.org 10.1007/s001280178.

[85] Lombardi, A. T.; dos Reis Hidalgo, T. M.; Henriques Vieira, A. A.; Sartori, A. L. Toxicity of Ionic Copper to the Freshwater Microalga *Scenedesmus acuminatus* (Chlorophyceae, Chlorococcales). *Phycologia*, **2007**, *46*(1), 74–78. https://doi.org/10.2216/06-40.1.

[86] Bux, F.; Chisti, Y. Large-Scale Production of Algal Biomass: Raceway Ponds. *Algae Biotechnology;* Springer, 2016. https://doi.org/10.1007/978-3-319-12334-9.

[87] Weather Spark. Clima, Condições Meteorológicas e Temperatura Média por Mês de Lisboa (Portugal) https://pt.weatherspark.com/y/32022/Clima-caracter%C3%ADstico-em-Lisboa-Portugal-durante-o-ano (accessed Apr 9, 2022).

[88] Rao, N. K.; Hanson, J.; Dulloo, M. E.; Ghosh, K.; Nowell, D.; Larinde, M. Manual of Seed Handling in Genebanks. *Handbooks for Genebanks No. 8*; Biodiversity International; Rome, 2006.

[89] J. B. Edmond; W. J. Drapala. The Effects of Temperature, Sand and Soil, and Acetone on Germination of Okra Seeds. *J. Am. Soc. Hortic. Sci.* **1958**, *71*(1), 428–434.

[90] Ranal, M. A.; de Santana, D. G. How and Why to Measure the Germination Process? *Braz. J. Bot.* **2006**, *29*(1), 1–11. https://doi.org/10.1590/s0100-84042006000100002.

[91] Melville, A.; Galletta, G.; Draper, A. Seed Germination and Early Seedling Vigor in Progenies of Inbred Strawberry Selections. *Am. Soc. Hortic. Sci.* **1980**, *15*(6), 749–750. https://doi.org/10.21273/hortsci.15.6.749.

[92] M. A. Kader. A Comparison of Seed Germination Calculation Formulae and the Associated Interpretation of Resulting Data. *J. Proc. R. Soc. N. S. W.* **2005**, *138*, 65–75.

[93] Abdul-Baki, A. A.; Anderson, J. D. Vigor Determination in Soybean Seed by Multiple Criteria. *Crop Sci*. **1973**, *13*(6), 630–633. https://doi.org/10.2135/cropsci1973.0011183x001300060013x.

[94] R Core Team. R: A Language and Environment for Statistical Computing. R Foundation for Statistical Computing; Vienna, Austria 2021.

[95] Gonzalez-Fernandez, C.; Muñoz, R. *Microalgae-Based Biofuels and Bioproducts*; Elseiver, 2017.

[96] Padisák, J.; Naselli-Flores, L. Phytoplankton in Extreme Environments: Importance and Consequences of Habitat Permanency. *Hydrobiologia*, **2021**, *848*(1), 157–176. https://doi.org/10.1007/s10750-020-04353-4.

[97] Illowsky, B.; Dean, S. Introductory Statistics; Open Access Textbooks, 2018.

[98] Lam, T. P.; Lee, T.-M.; Chen, C.-Y.; Chang, J.-S. Strategies to Control Biological Contaminants During Microalgal Cultivation in Open Ponds. *Bioresour. Technol*. **2018**, *252*, 180–187. https://doi.org/10.1016/j.biortech.2017.12.088.

[99] Day, J. G.; Gong, Y.; Hu, Q. Microzooplanktonic Grazers – A Potentially Devastating Threat to the Commercial Success of Microalgal Mass Culture. *Algal Res*. **2017**, *27*, 356–365. https://doi.org/10.1016/j.algal.2017.08.024.

[100] Molina, D.; de Carvalho, J. C.; Júnior, A. I. M.; Faulds, C.; Bertrand, E.; Soccol, C. R. Biological Contamination and Its Chemical Control in Microalgal Mass Cultures. *Appl. Microbiol. Biotechnol*. **2019**, *103*, 9345–9358. https://doi.org/10.1007/s00253-019-10193-7.

[101] Sanz-Luque, E.; Chamizo-Ampudia, A.; Llamas, A.; Galvan, A.; Fernandez, E. Understanding Nitrate Assimilation and Its Regulation in Microalgae. *Front. Plant Sci*. **2015**, *6*. https://doi.org/10.3389/fpls.2015.00899.

[102] Fallahi, A.; Rezvani, F.; Asgharnejad, H.; Khorshidi, E.; Hajinajaf, N.; Higgins, B. Interactions of Microalgae-Bacteria Consortia for Nutrient Removal from Wastewater: A Review. *Chemosphere*, **2021**, *272*. https://doi.org/10.1016/j.chemosphere.2021.129878.

[103] Dortch, Q. The Interaction Between Ammonium and Nitrate Uptake in Phytoplankton. *Mar. Ecol. Prog. Ser*. **1990**, *61*, 183–201. https://doi.org/10.3354/meps061183.

[104] Chen, H.; Wang, Q. Microalgae-Based Nitrogen Bioremediation. *Algal Res*. **2020**, *46*. https://doi.org/10.1016/j.algal.2019.101775.

[105] Hii, Y.; Chuah, T.-S.; Ambak, M. A.; Bolong Abol-Munafi, A. Interactive Effect of Ammonia and Nitrate on the Nitrogen Uptake by *Nannochloropsis* sp. *J. Sustain. Sci. Manag*. **2011**, *6*(1), 60–68.

[106] Tibbetts, S. M.; Milley, J. E.; Lall, S. P. Chemical Composition and Nutritional Properties of Freshwater and Marine Microalgal Biomass Cultured in Photobioreactors. *J. Appl. Phycol*. **2015**, *27*(3), 1109–1119. https://doi.org/10.1007/s10811-014-0428-x.

[107] Sutherland, D. L.; Howard-Williams, C.; Turnbull, M. H.; Broady, P. A.; Craggs, R. J. Seasonal Variation in Light Utilisation, Biomass Production and Nutrient Removal by Wastewater Microalgae in a Full-Scale High-Rate Algal Pond. *J Appl Phycol*, **2014**, *26*(3), 1317–1329. https://doi.org/10.1007/s10811-013-0142-0.

[108] Dae-Hyun, C.; Rishiram, R.; Jina, H.; Zion, K.; Byung-Hyuk, K.; Chi-Yong, A.; Hee-Mock, O.; Hee-Sik, K. Organic Carbon, Influent Microbial Diversity and Temperature Strongly Influence Algal Diversity and Biomass in Raceway Ponds Treating Raw Municipal. *Bioresour. Technol*. **2015**, *191*, 481–487. https://doi.org/10.1016/j.biortech.2015.02.013.

[109] Montemezzani, V.; Duggan, I. C.; Hogg, I. D.; Craggs, R. J. Zooplankton Community Influence on Seasonal Performance and Microalgal Dominance in Wastewater Treatment High-Rate Algal Ponds. *Algal Res*. **2016**, *17*, 168–184. https://doi.org/10.1016/j.algal.2016.04.014.

[110] Naselli-Flores, L.; Padisák, J.; Dokulil, M. T.; Chorus, I. Equilibrium/Steady-State Concept in Phytoplankton Ecology. *Hydrobiologia,* **2003,** *502*, 395–403. https://doi.org/10.1023/b:hydr.0000004297.52645.59.

[111] Gonçalves, M.; Martins, J.; Ramos, T. A Salinização Do Solo Em Portugal. Causas, Extensão e Soluções. *Rev. Cienc. Agrar.* **2015**, *38*(4), 574–586. https://doi.org/10.19084/rca15140.

[112] Farooq, M.; Basra, S. M. A.; Hafeez, K. Seed Invigoration by Osmohardening in Coarse and Fine Rice. *Seed Sci. Technol.* **2006**, *34*(1), 181–187. https://doi.org/10.15258/sst.2006.34.1.19.

[113] Subedi, R.; Maharjan, B.; Adhikari, R. Effect of Different Priming Methods in Rice (*Oryza sativa*). *J. Agric. Environ.* **2015**, *16*, 152–160. https://doi.org/10.3126/aej.v16i0.19848.

[114] Ologundudu, A. F.; Adelusi, A. A.; Akinwale, R. O. Effect of Salt Stress on Germination and Growth Parameters of Rice (*Oryza sativa* L.). *Not. Sci. Biol*. **2014**, *6*(2), 237–243. https://doi.org/10.15835/nsb629163.

[115] Pires, I. S.; Negrão, S.; Oliveira, M. M.; Purugganan, M. D. Comprehensive Phenotypic Analysis of Rice (*Oryza sativa*) Response to Salinity Stress. *Physiol. Plant*. **2015**, *155*(1), 43–54. https://doi.org/10.1111/ppl.12356.

[116] Lee, K. S.; Choi, W. Y.; Ko, J. C.; Kim, T. S.; Gregorio, G. B. Salinity Tolerance of Japonica and Indica Rice (*Oryza sativa* L.) at the Seedling Stage. *Planta*, **2003**, *216*(6), 1043–1046. https://doi.org/10.1007/S00425-002-0958-3.

[117] Negrão, S.; Courtois, B.; Ahmadi, N.; Abreu, I.; Saibo, N.; Oliveira, M. M. Recent Updates on Salinity Stress in Rice: From Physiological to Molecular Responses. *Crit. Rev. Plant Sci.* **2011**, *30*(4), 329–377. https://doi.org/10.1080/07352689.2011.587725.

[118] Horie, T.; Karahara, I.; Katsuhara, M. Salinity Tolerance Mechanisms in Glycophytes: An Overview with the Central Focus on Rice Plants. *Rice*, **2012**, *5*(1), 1–18. https://doi.org/10.1186/1939-8433-5-11.

[119] Koevoets, I. T.; Venema, J. H.; Elzenga, J. T. M.; Testerink, C. Roots Withstanding Their Environment: Exploiting Root System Architecture Responses to Abiotic Stress to Improve Crop Tolerance. *Front. Plant Sci*. **2016**, *7*. https://doi.org/10.3389/fpls.2016.01335.

[120] Deak, K. I.; Malamy, J. Osmotic Regulation of Root System Architecture. *Plant J*. **2005**, *43*(1), 17–28. https://doi.org/10.1111/j.1365-313x.2005.02425.x.

[121] Batayeva, D.; Labaco, B.; Ye, C.; Li, X.; Usenbekov, B.; Rysbekova, A.; Dyuskalieva, G.; Vergara, G.; Reinke, R.; Leung, H. Genome-Wide Association Study of Seedling Stage Salinity Tolerance in Temperate Japonica Rice Germplasm. *BMC Genet*. **2018**, *19*. https://doi.org/10.1186/s12863-017-0590-7.

[122] Agência Lusa. Seca: Produtores de Arroz Do Vale Do Sado Estimam Quebra de 20 a 25% Da Área de Cultivo. *Diário de Notícias*. Mar, 2019.

[123] Chapra, S. C.; Camacho, L. A.; McBride, G. B. Impact of Global Warming on Dissolved Oxygen and Bod Assimilative Capacity of the World's Rivers: Modelling Analysis. *Water*, **2021**, *13*(17). https://doi.org/10.3390/w13172408.

[124] European Green Deal - Consilium https://www.consilium.europa.eu/en/policies/green-deal/ (accessed Sep 5, 2022).

[125] Hubbell, S. P. Neutral Theory in Community Ecology and the Hypothesis of Functional Equivalence. *Funct. Ecol*. **2005**, *19*(1), 166–172. https://doi.org/10.1111/j.0269-8463.2005.00965.x.

Annex I. Bioremediation of a N-rich Effluent Derived from Industrial Fertilizer Production

Table I.1 – Monthly productivity results and environmental parameters verified for the pilot-scale bioreactor used in the assay (mean ± SD).

Radiation Group	Month	Average Biomass Productivity (g_{DW} m^{-2} day^{-1})	Average N Removal Rate (g m^{-2} day^{-1})	Average Photoperiod (hh:mm)	Average Daily Solar Radiation (MJ m^{-2} day^{-1})	Average Environmental Temperature (ºC)
1	January	1.66 (± 0.49)	0.22 (± 0.07)	09:48	7.42 (± 0.59)	11.01 (± 0.80)
1	February	2.97 (± 0.54)	0.27 (± 0.06)	10:48	10.70 (± 1.32)	13.45 (± 0.58)
2	March	3.36 (± 1.61)	0.34 (± 0.12)	12:00	17.20 (± 0.77)	14.97 (± 0.31)
2	April	4.91 (± 1.38)	0.29*****	13:18	17.67 (± 1.03)	15.63 (± 0.52)
3	May	5.52 (± 0.97)	0.60 (± 0.09)	14:18	24.69 (± 0.25)	19.37 (± 1.10)
3	June	6.30 (± 0.46)	0.73 (± 0.02)	14:54	25.68 (± 0.73)	19.88 (± 0.27)
3	July	6.00 (± 1.45)	0.88 (± 0.03)	14:36	24.69 (± 1.42)	22.75 (± 1.27)
3	August	3.57 (± 0.40)	0.58******	13:36	23.88 (± 1.06)	22.55 (± 0.17)
2	September	4.43 (± 1.11)	0.53******	12:24	16.98 (± 0.97)	22.34 (± 0.10)
1	October	3.98 (± 0.25)	0.44******	11:06	12.78 (± 0.20)	17.97 (± 0.44)
1	November	1.42 (± 0.78)	0.26******	10:00	7.54 (± 0.06)	15.23 (± 0.01)
1	December	1.68 (± 0.28)	0.16 (± 0.02)	09:30	6.76 (± 0.05)	13.12 (± 0.59)

*Average attained solely in 2020; ******Average obtained solely in 2021.

Annex II. Assessment of the Biomass' Potential as a MBS for Seed Priming

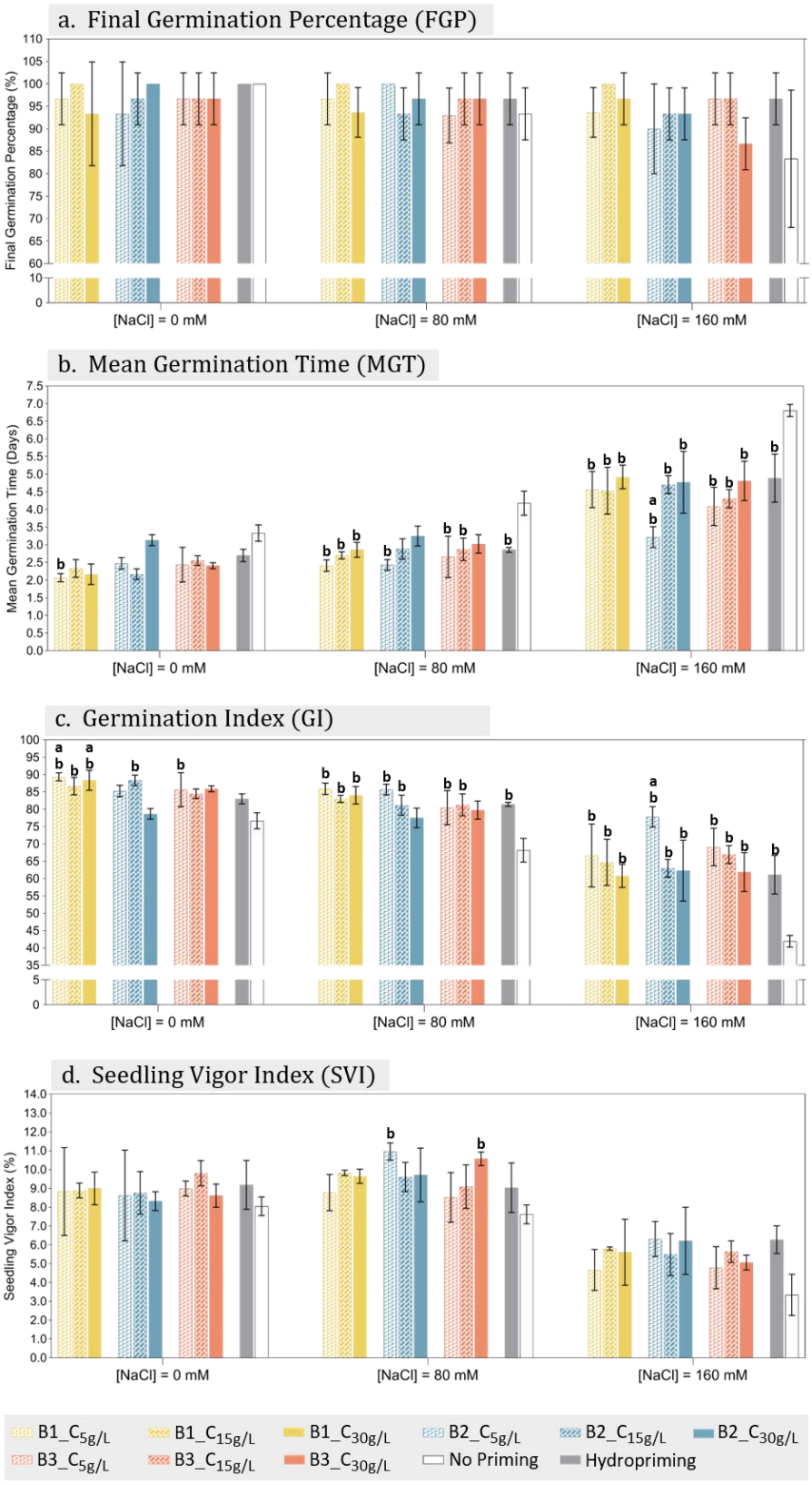

Figure II.1 – Graphical representation of the results obtained for the germination evaluation parameters, of the different priming and incubation groups. Values represent mean ± SD, with n = 3 for each priming group. Results marked with the letter a. differ significantly ($p < 0.05$) from the positive control (hydropriming), while those marked with b. are significantly different from the negative control (no priming treatment), considering the same incubation conditions.

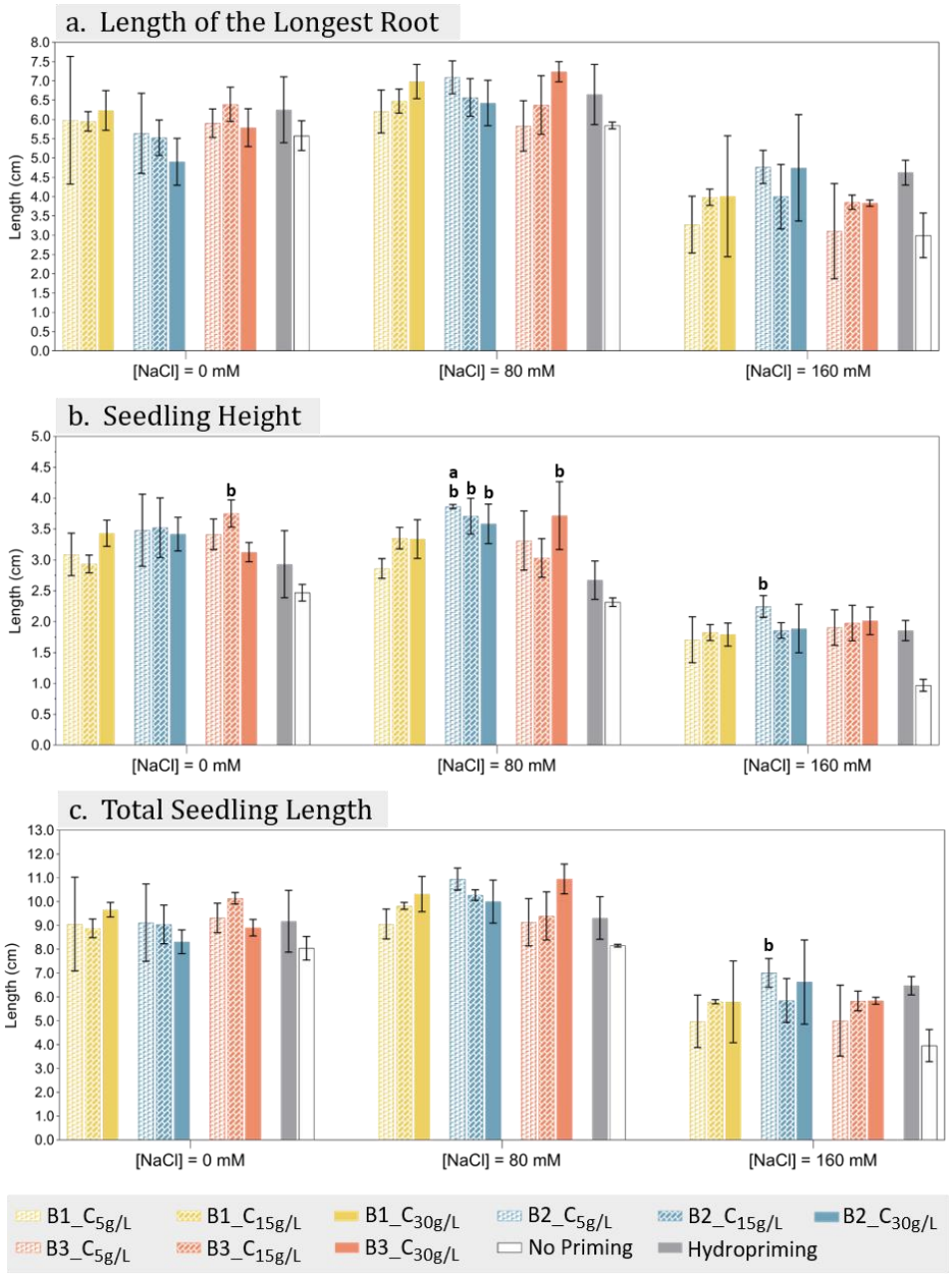

Figure II.2 – Graphical representation of the length measurements taken of the 12-day-old seedling. Values represent mean ± SD, with n = 3 for each priming group. Results marked with the letter a. differ significantly (p < 0.05) from the positive control (hydropriming), while those marked with b. are significantly different from the negative control (no priming treatment), considering the same incubation conditions.

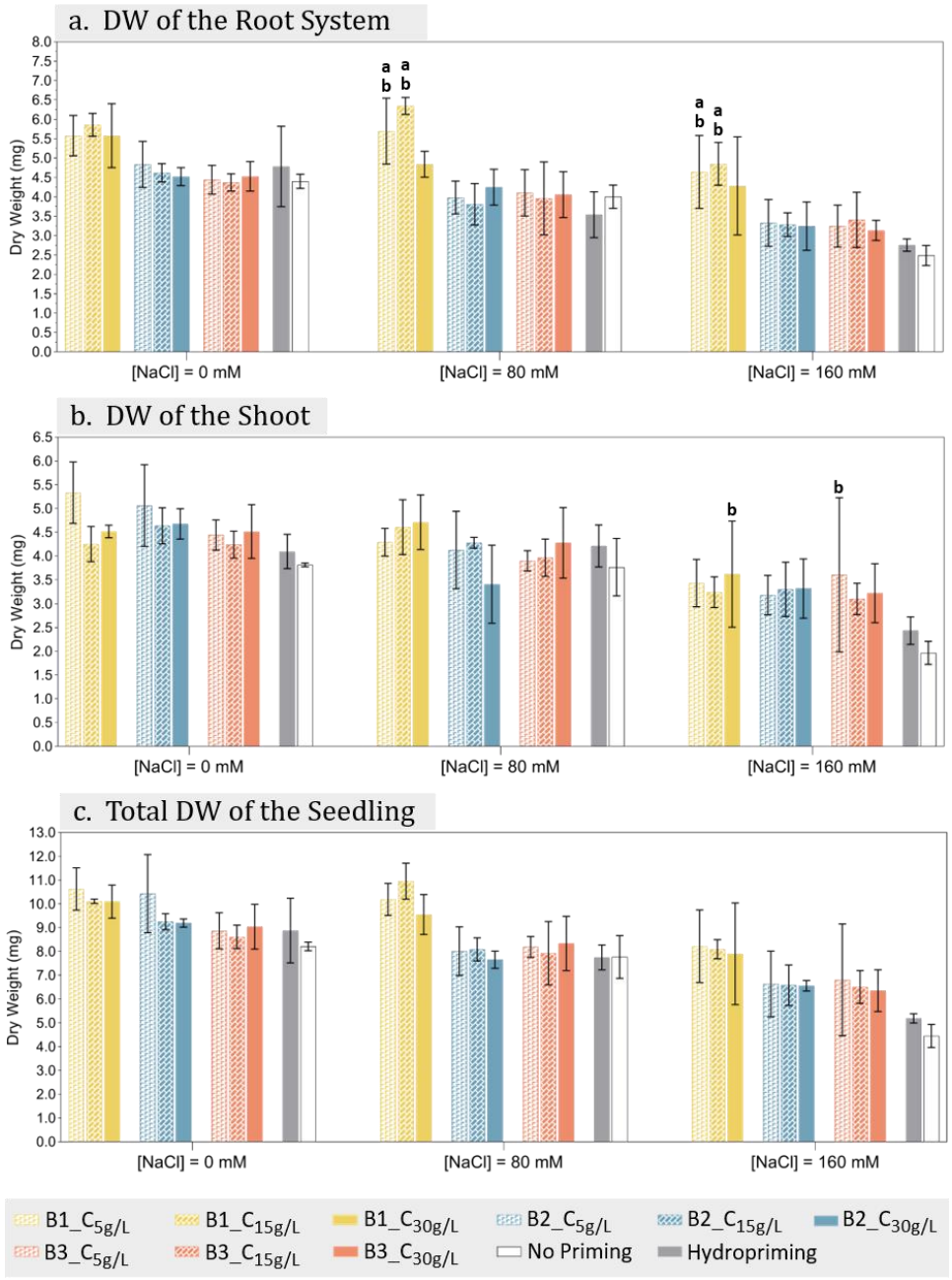

Figure II.3 – Graphical representation of the dry weight measurements taken of the 12-day-old. Values represent mean ± SD, with n = 3 for each priming group. Results marked with the letter a. differ significantly ($p < 0.05$) from the positive control (hydropriming), while those marked with b. are significantly different from the negative control (no priming treatment), considering the same incubation conditions.